ADDIS ABABA UNIVERSITY

SCHOOL OF GRADUATE STUDIES

SCHOOL OF EARTH SCIENCES

Petrogenesis of Tana area Volcanic Rocks: Implications to Magmatic Evolution of Tana Basin

By: Ayenachew Alemayhou Desta

Advisor: Asfawossen Asrat (Prof.)

A thesis submitted to the School of Graduate Studies of Addis Ababa University in partial fulfillment of the requirements for the degree of Master of Science in Earth Sciences (Petrology)

May, 2018

Addis Ababa, Ethiopia

ADDIS ABABA UNIVERSITY

SCHOOL OF GRADUATE STUDIES

SCHOOL OF EARTH SCIENCES

Petrogenesis of Tana area Volcanic Rocks: Implications to Magmatic Evolution of Tana Basin

By: Ayenachew Alemayhou Desta

Advisor: Asfawossen Asrat (Prof.)

A thesis submitted to the School of Graduate Studies of Addis Ababa University in partial fulfillment of the requirements for the degree of Master of Science in Earth Sciences (Petrology)

May, 2018

Addis Ababa, Ethiopia

Declaration of Originality

I hereby declare that the thesis titled "**Petrogenesis of Tana area Volcanic Rocks: Implications to Magmatic Evolution of Tana Basin**" is my original master's degree work under the supervision of Prof. Asfawossen Asrat, School of Earth Sciences, Addis Ababa University during the year 2018. I further declare that this work has not been presented or submitted to any other university or institution for the award of any degree or diploma. All sources and materials used for the thesis have been duly acknowledged.

Ayenachew Alemayhou Desta ________________ ___________________

Signature Date

This is to certify that the above declaration made by the candidate is correct to the best of my knowledge.

Prof. Asfawossen Asrat (Advisor) Asfawossen Asrat 30/05/2018

Signature Date

ADDIS ABABA UNIVERSITY

SCHOOL OF GRADUATE STUDIES

SCHOOL OF EARTH SCIENCES

Petrogenesis of Tana area Volcanic Rocks: Implications to Magmatic Evolution of Tana Basin

By: Ayenachew Alemayhou Desta

Dr. Balemwal Atnafu ____________________ __________________

Head, School of Earth Sciences Signature Date

Prof. Asfawossen Asrat (Advisor) Asfawossen Asrat 30/05/2018

Signature Date

Prof. Gezehagne Yirgu (Examiner) ___________________ ___________________

Signature Date

Prof. Dreje Ayalew (Examiner) ___________________ ___________________

Signature Date

Abstract

Lake Tana basin is a major part of the North Western Ethiopian plateau with numerous geologic formations and structures. The Lake occupies the center of a large circular basin of at least 100–120 km in diameter. It is situated within a faulted depression between erosional escarpment to the west overseeing the Sudan plains and tectonic escarpment overseeing the Afar depression to the east. Most of the previous works regarding petrology and Geochemistry on the Ethiopian plateau are regional. Due to its complex geology Lake Tana area has been skipped for detail works. The objective of this research is to study the Tana volcanics form part of the volcanic succession of the regional flood basalts using a combined geological mapping, petrological and geochemical characterization to understand their petrogenesis. The methodologies employed to achieve the objectives includes fieldwork for mapping and sampling, petrographic investigations, major and trace element geochemical analysis by ICP-MS and ICP-AES methods respectively. Analysis and interpretation of data have been achieved using different software packages. The major lithological units identified in the studied area includes: recent lacustrine sediments, Quaternary volcanics, Pliocene to Miocene ash tuff and associated basalt, Oligocene rhyolite and basalt. Basanite intrusions and scoria cones are also discussed under the Quaternary volcanics. The Lake Tana area bimodal volcanic rocks have been classified as alkaline and some transitional to tholeiitic mafic and sub-alkaline felsic magma series. The same age groups of rocks are co-genetic and related to each other by fractional crystallization process starting from mantle-derived basaltic magma with minimal crustal material involvement. In general, the trace element geochemistry representing all rocks is formed in an intra-continental (within plate) tectonic setting. Oligocene basalts are categorized under LT plateau basalt and also the Oligocene rhyolites are comparable with plateau felsite.

Key words: Lake Tana basin, Quaternary volcanics, Oligocene basalt, petrological and geochemical characterization, intra-continental

Acknowledgment

I would like to thank many people and organizations, who so generously contributed to the work presented in this thesis.

Firstly, I would like to extend my grateful thanks to Bahir Dar University School of Earth Sciences for giving me a chance to study my master‘s degree and funding the research project. Besides, special mention to the instructors and mentors in Addis Ababa University School of Earth Sciences for their endless academic support during my classes, they nurtured my enthusiasm for Geological Sciences.

Foremost, I would like to express my sincere gratitude and respect to my enthusiastic advisor Prof. Asfawossen Asrat for his constructive comment, valuable suggestion, encouragement and remarkable support of my thesis work.

I am also hugely appreciative to Dr. Minyahl Teferi for having valuable technical discussion with him and guidance; it‘s really meant a lot to me. He has been truly dedicated to share his expertise so willingly.

I wish to express my sincere appreciation to my friends, colleagues and Zeolite research team of Bahir Dar University. I am particularly indebted to Melese Getenet and Ibsa Abdulerahman for their continued support.

Finally, but by no means least, thanks go to my family (Asef, Mita and Buzi) for almost unbelievable support. They are the most important people in my world and I dedicate this thesis to them.

Table of Contents

List of Figures and Tables

List of Acronyms

ALS- Australian Laboratory Service

ANS- Arabian Nubian Shield

CFB- Continental Flood Basalt

DEM- Digital Elevation Model

ELIP- Ethiopian Large Igneous Provinces

HFSE- High field strength element

ICP-AES- Inductively Coupled Plasma Atomic Emission Spectrometry

ICP-MS- Inductively Coupled Plasma Mass Spectrometry

m- Meter

masl- mean above sea level

Ma. – Millions of Years

MB- Mozambique Belt

mm- millimeter

MORB- Mid-Oceanic Ridge Basalt

NE- North East

NNE- North North East

NW- North West

OIB- Oceanic Island Basalt

PPL- Plane Polarized

ppm- parts per million

REE- Rare Earth Element

SSW- South South West

SW- South West

UTM- Universal Transverse Mercator

XPL- Crossed Polarized

Chapter One

1. Introduction

1.1. Background

Petrogenetic studies of volcanic rocks encompass characterization of the source region of magma, the condition of partial melting, crystallization, and differentiation of primary mantle-derived magmas in magma chambers (Gill, 2010; Wilson, 2007). Accordingly, there are several petrogenesis models that have been recommended to explain the origin of magmas. The North-western Ethiopian Plateau, with a mean elevation of 2500 amsl, is located on the western flank of the tectonically active Main Ethiopian Rift and the Afar Depression (Fig.1). The plateau was uplifted due to the combined effects of the rising Afar mantle plume and flank uplift of the Main Ethiopian Rift with the Afar Depression (Collet et al., 2000; Sengör, 2001; Beyene and Abdelsalam, 2005).

Although, the Tana Basin geology has been the subject of several studies (e.g. Jepsen & Athearn, 1961, Abate et al., 1998, Chorowicz et al., 1998, Hautot et al., 2006, Kieffer et al., 2004 and Prave et al., 2016) there are still unclear scenarios. The present study focuses on bimodal volcanic rocks of the northwestern Ethiopian plateau, which consist mainly of Oligocene, Miocene to Pliocene forming a thick sequence overlaying the flood basalts and Quaternary volcanic dominantly outpoured on the southern regions of Lake Tana. In general, the volcanic exposures around Lake Tana area have been skipped on most of the regional works. Therefore, a systematic mapping of Tana basin and its volcanic stratigraphy is needed for an understanding of broader Ethiopian plateau evolution (Chorowicz et al., 1998).

Extensive basaltic flows (500-2000 m thick) erupted at 30 Ma over a short period of time (nearly 1 Ma) gap (Hofmann et al., 1997). This eruption, covering an area of >500,000 km^2, is inferred to mark the appearance of the Afar mantle plume (Mohr and Zanettin, 1988; Hofmann et al., 1997; Kieffer et al., 2004). This event was followed by shield volcano episodes, which gave rise to the development of the Semien, Choke, Guguftu and Guna volcanoes (Fig.1) in the North-western Ethiopian Plateau (Kieffer et al., 2004). The geochemistry of the Ethiopian continental flood magmas reflects a complex interplay of source heterogeneity, variable extents of melting and evolution of magmas prior to eruption (Meshesha and Shinjo, 2007).

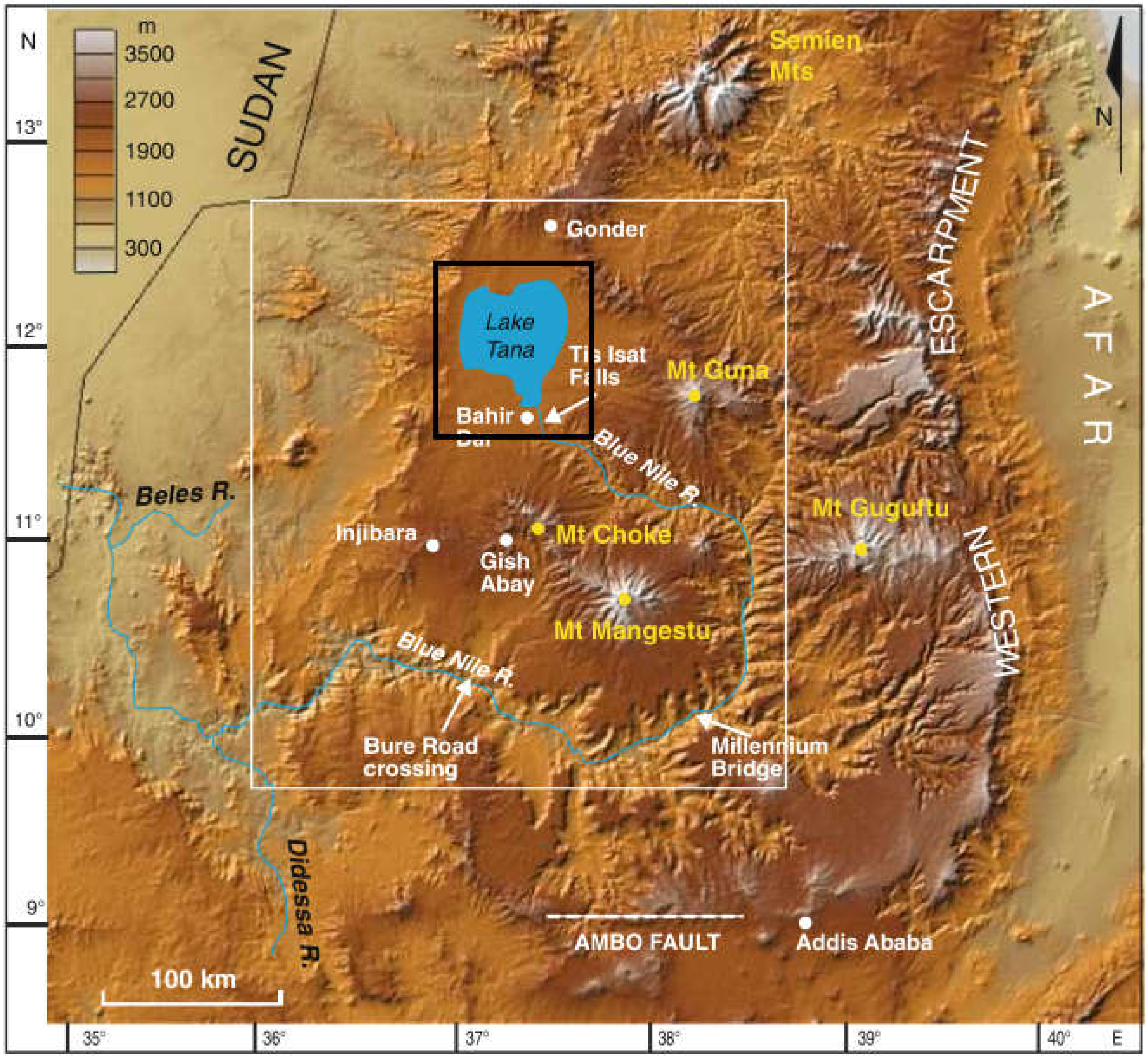

Figure 1.1: Digital elevation model showing the Northwestern Ethiopian plateau

1.2. Geographic setting of the Study Area

1.2.1. Location and Accessibility

This research project is conducted (Fig.1) in the northwestern Ethiopian plateau more specifically in Tana Basin (around Lake Tana). The study area is about 570km far from Addis Ababa to Bahir Dar (the capital city of the Amhara Regional state where the largest lake of the country, Lake Tana, found) in the North West direction. In UTM (Universal Transverse Mercator) the area is bounded by a grid of Easting from 270000to 360000 m and Northing of 1265000 to1370000 m.

The Lake Tana is bounded by the North Gondar, South Gonder, and West Gojam administrative districts. The study area has coverage of approximately 8880 Km^2. About 3625 km^2 of the study area is covered by water (Lake Tana). Accessibility of the study area was very complicated because it is far from main roads. The study area is accessed through partly asphalted and partly all-weather main roads. In addition foot trails by local people and some gravel roads are used that constructed for raw material transportation from quarries of construction materials like scoria and other masonry stones.

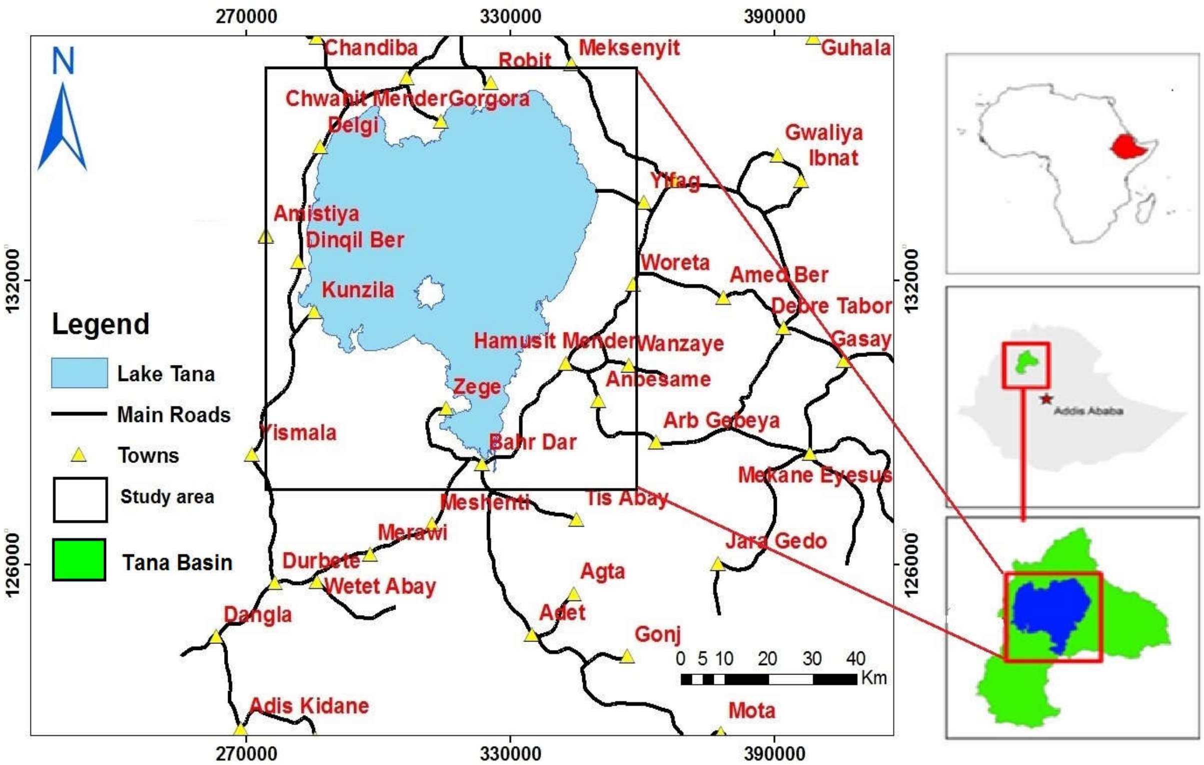

Figure 1.2: Location map of the study area

1.2.2. Physiography and Drainage of Tana Basin

Ethiopia can be divided into four major physiographic regions; the northwestern plateau, the southeastern plateau, the Main Ethiopian Rift and the Afar depression (Asrat et al., 2012). The lowest elevation in Africa is located in the Afar depression, Dallol (-126m below sea level), while the highest elevation is, Ras Dashen (4620 masl). The study area is found in the northwestern part of Ethiopian plateau, which is one of the four spectacular physiographic features comprising of a number of raised volcanic peaks in the region.

In general, the studied area could be regarded as undulating and some flat landforms. Plugs and domes form numerous discontinuous prominent volcanic ridges with very sharp peaks. Topographic slope mostly decreases towards the Tana Lake from whole sides. The minimum and maximum elevations are 1670 and 3027 m, respectively. Lake Tana is typically surrounded by floodplains and wetlands; Fogera and Dembia floodplains are good examples.

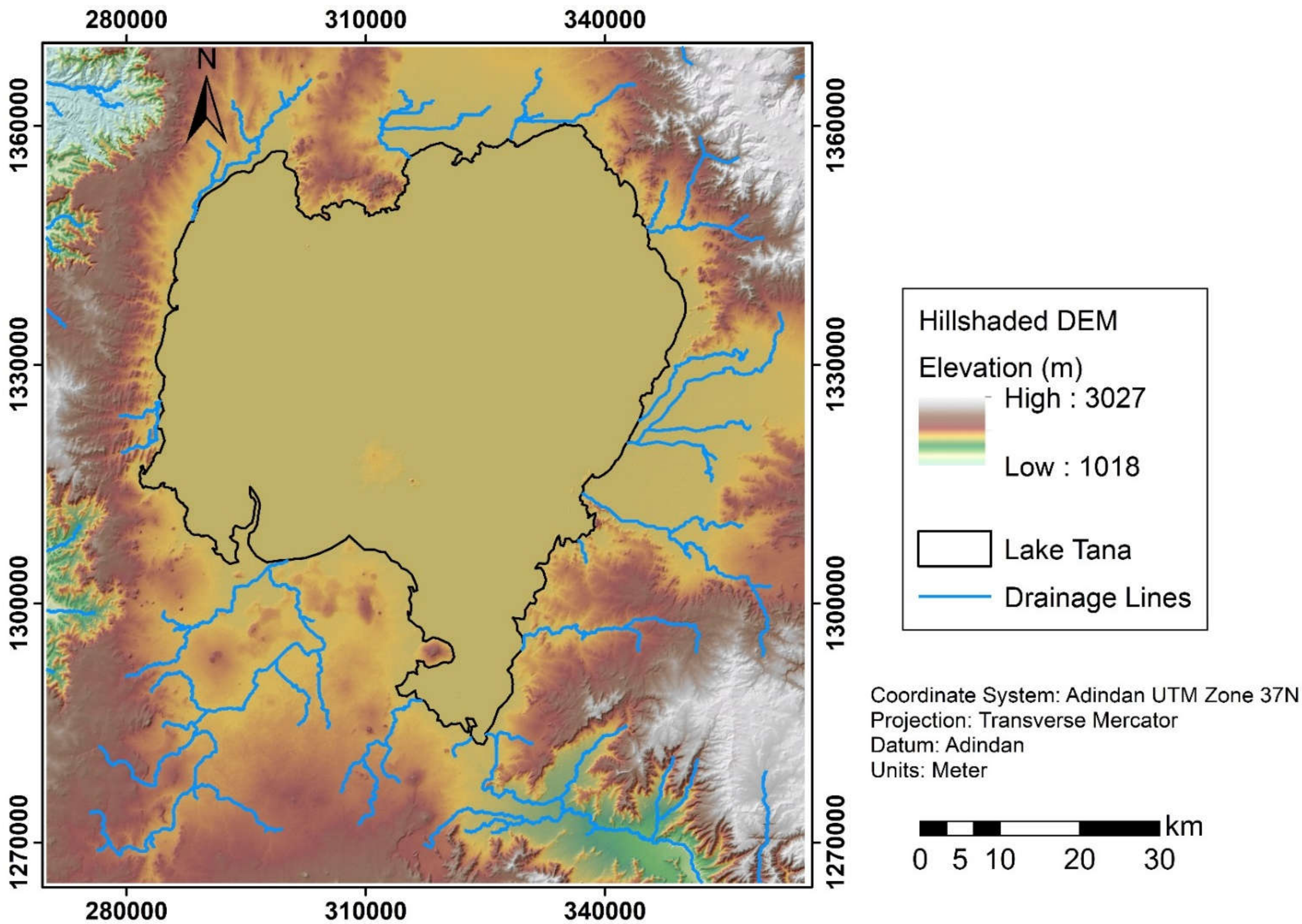

Figure 1.3: Physiography and Drainage pattern map of Lake Tana surrounding area

Lake Tana is fed by over 40 rivers and streams flowing from the surrounding areas. It has a meandering and dendritic drainage pattern with a number of perennial and seasonal streams and rivers. GilgelAbay, Rib, Gumara and Megech rivers are the main tributaries that flow to Lake Tana basin. All streams and rivers flow into the lake. Surficially water outflow from the Lake Tana only through the Blue Nile River and Belese hydropower and irrigation project outlet.

1.2.3. Climate condition and Vegetation of the study area

The climate around the study area classified as Subtropical highland. The climatic condition of the area is mainly expressed by average temperature and average precipitation. The daily average high temperature is 29.6°C measured during March while the low temperature is 8.4 °C during January (see on Fig-1). The average annual precipitation becomes high during the July (428 mm) and low during February (2 mm). Generally, the climatic condition around the study area is very hot during the daytime and become frosty and windy during the evening.

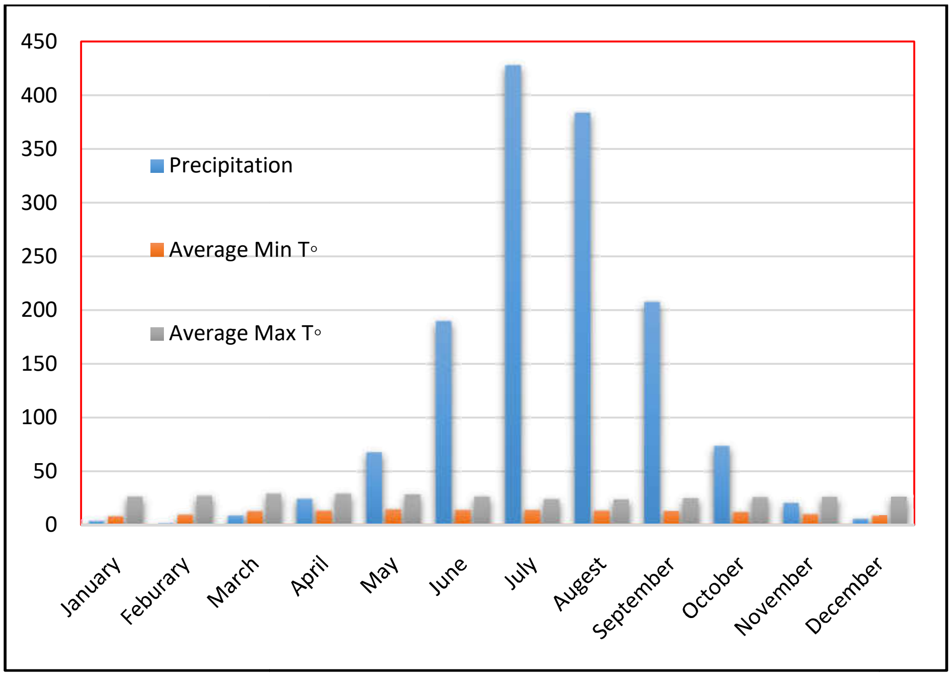

Figure 1.4: A bar chart that shows the climate condition of the area around Bahir Dar

The vegetation distribution is mainly dependent on the climatic condition of the area. As explained in the above paragraph, the climate is characterized as Subtropical highland. In Bahir Dar city down a road lined with fragrant Jacaranda plants and flamboyant Flame trees. The luxuriant vegetation found on the islands and small rainforest patches provides excellent habitat for wildlife in and around Lake Tana. The stunning red coffee grows wild in the dense forest of the Zege and Dek Peninsulas. In general Shrubs, Acacia (Grar) and Eucalyptus (Bahirzaf) plants are dominant. Teff, rice, corn, sorghum, cotton, and sesame are important cash crops for the local farmers around Lake Tana.

Figure 1.5: Vegetation covers of the study area

1.3. Objectives of the Study

1.3.1. General objective

The main objective of this research is to study the petrogenetic differences between regional Oligocene flood basalt and Quaternary volcanic rocks exposed around Lake Tana using a combined geological mapping (scale of 1:250,000) and correlation, as well as petrological and geochemical characterization.

1.3.2. Specific objectives

- To make petrographic characterization of the Tana volcanics for detail descriptions and systematic classification in Tana basin and its surroundings.
- To evaluate major and trace element signatures of Tana volcanic rocks in the study area to determine their petrogenesis.

1.4. Statement of the Problem

The northwestern Ethiopian continental food basalt has been studied by many scholars and a lot of papers are published in different scientific journals. All studies are done based on different scientific scenarios. As stated by Ayalew et al., (2002) most studies of the Ethiopian plateau have focused on basalts, and very little is known about the felsic volcanism. The geochemistry and petrography of mafic and felsic rocks around Lake Tana has been studied by Abate et al., (1998). Miocene-Pliocene volcanic rocks including Choke (22.4 Ma), Guna (10.7 Ma), and Quaternary volcanic rocks that cover the Lake Tana area have been identified by Peccerillo, (1997); Pik et al., (1998, 1999) and later by Kieffer et al., (2004). From the recent studies the geology and geochronology of Tana basin described by Prave et al., (2016). Even so, these studies are more provincial.

According to Prave et al., (2016), Tana basin is a huge caldera which resulted from supereruptions (volcano). In contrary, according to (Mohr, 1971 and Kazmin, 1975) the Tana basin results from recent volcanic activity in relation to north-south faults called Lake Tana rift. The rocks in the Tana basin have been described as Quaternary alkaline olivine basalt and trachyte (Merla, 1973) plateau basalt (Tefera et al., 1996) and the Lake Tana fissural basalt province on the plateau areas as a typical example for Quaternary age (Peccerillo et al., 2003). Despite a relatively large chemical database for the southern and western Ethiopian plateau volcanic (Kabeto et al., 2010) there are still many parts of the plateau magmatism that are not studied well, thus Lake Tana area is the one.

The previous studies indicate that there is still unfiled gaps and arguments about the nature of the Tana volcanic with an interesting question. Whether is it a caldera resulted from super volcano (Prave et al., 2016) or a structurally bounded rift (Chorowicz et al., 1998)? It is known that calderas could be identified by the juxtaposition of a topographic depression with proximal volcanic products and peripheral extensive outflow sheets or fans. Also, understanding how magma is emplaced into the shallow crust, differentiated, and erupted with the aid of petrology and geochemistry may help us to understand the magmatic and structural development of calderas. During an explosive caldera-forming eruption, the region surrounding the caldera is covered by an extensive ejecta blanket.

Moreover, lack of a detailed geological map of any particular section of the Ethiopian flood basalt province makes it difficult to correlate much of the existing high quality geochemical data from various parts of the Ethiopian flood basalt province. Therefore, as an alternative the Lake Tana area Quaternary volcanic rocks should be studied in terms of detailed mapping, petrography, and geochemistry to understand its magmatic evolution to test the previous hypothesis and to fill the existing scientific gaps. By having this concept the present study will give some information regarding the petrogenesis of Tana volcanic rocks. In the meantime, it will help us to compare and contrast the felsic rocks locally as well as regionally by using their geochemical signatures.

1.5. Data and Methods

The whole activities of this research work are mainly divided into three phases; pre-fieldwork, fieldwork, and post-fieldwork. Two types of data are collected for the research; secondary and primary data.

1.5.1. Pre-fieldwork

On the initial stage, all desk works were accomplished in the office a week before going to the field. In the pre-fieldwork assessment of literature about the methods that would be applied and about accessibility and scope of the study area are done. In addition, a logistic plan is made, and major geological structures are delineated and different lithologies are differentiated by using ArcGIS and ENVI software with satellite imagery and DEM. The preliminary geological base map has been compiled from four different geological map sheets which are prepared by geological survey of Ethiopia. Those sheets are Bahir Dar sheet, Yifag sheet, Western Gonder sheet and Debretabor sheet.

1.5.2. Fieldwork and Sampling techniques

A two days reconnaissance survey and observation were done in order to assess the cost of the fieldwork, to obtain the necessary permission from the relevant authorities to carry out the work, as well as accumulating the basic field equipment. A total of 25 days field works were conducted by following traverse lines in order to achieve the objective of this study. Throughout fieldwork, the necessary primary data such as structural data and representative rock samples were collected from each encountered variety of lithologies with field observations.

Ten traverses lines were selected to collect input data for compilation of geological maps. All traverse lines are rounds to Lake Tana from all sides and also Dek and Tana Kirkos islands are considered .Moreover, a collection of standard and representative rock samples are done. 57 samples are collected directly from the outcrops. 30 samples are mafic and the rest 27 are felsic. Those collected samples are relatively fresh and properly labeled.

Such input data includes structural measurements, lithological unit descriptions, lithological contacts, taking field photographs and also several sketches are done by hand during the field work. Structural data are collected during the field work. These data are mainly measured for structures such as faults, joints and flow banding by using Brunton compass and clinometer. The major structures like fault and liniments are visible and easily delineated from a satellite image.

Geological mapping of the study area is finalized by organizing and mosaicking on previously done geological maps by the use of Arc GIS 10.3 software. Compilation of the geological map also incorporated Satellite imagery interpretation and field observations to full fill the gaps of previous ones. The collected structures are represented on the geological map and those data are synthesized by an easy software package called Rose diagram.

1.5.3. Post-fieldwork

Post-fieldwork comprises analyze, synthesis, presentation, and interpretation of petrographic and geochemical data. During the different phases, a variety of tools are used, including topographic and geological maps at a scale of 1:250,000, standard field sampling and measuring tools, and ArcGIS 10.3, ENVI 4.5, Google earth pro, Global mapper 12, Petrograph beta 2, GCD tool kit 4.1,Strater, and Rose diagram software packages.

1.5.3.1. Petrographical Analysis

A total of eighty standard thin sections were prepared in the mineralogy and petrography laboratory of Geological Survey of Ethiopia. Thin sections preparation included removal of some weathered parts and cutting to a suitable size by splitting each specimen with various diamond blades. They are prepared by mounting a small cut and polished sample of rock, using a strong adhesive onto a plate of glass (usually 27x46 mm in size) and then the exposed surface of the rock is gradually ground or 'lapped' down to 0.03 mm thickness to be examined under a microscope using transmitted light microscope. Typically quartz is used as the gauge to determine thickness as it is one of the most abundant minerals.

The thin sections were described using a polarized petrographic microscope. A detailed petrographic study (thin section descriptions) including mineral identification, modal proportion, texture descriptions, and rock naming were performed. Representative mineral assemblage and peculiar textures were examined under the microscope. The main output of the thin section analysis is modal proportion of minerals, largest grain sized diameter along their longest dimension of each mineral, the average grain shape of those existed minerals and grain to grain relationship of the phenocrysts. This information will help lastly in the rock classification and understand the magmatic evolution; thereby allowing the different phases to be studied within their textural framework.

1.5.3.2. Geochemical Analysis

A total of twenty (basalt-eight samples: basanite-two samples: scoria-two samples: rhyolite-six samples: trachyte-two samples) were selected for whole-rock chemical analysis. These twenty rock samples are selected for geochemical analysis on the basis of lithological variations and spatial distributions. Then, the samples are crushed to 70% less than 6 mm, the pulverized entire sample to better than 85% passing 75 microns for geochemical analysis. The concentration of major and selected trace elements in volcanic rocks were determined by a combination of methods (code: ME-MS81d) Inductively Coupled Plasma-Mass Spectrometry (ICP-MS; code: ME-MS81) and Atomic Emission Spectrometry (ICP-AES; code: ME-ICP06) both by decomposing the sample by lithium metaborate fusion (code: FUSLIO1) at the laboratory of Australian Laboratory Services (ALS), Ireland.

In brief, a prepared sample (0.200 g) is added to lithium metaborate ($LiBO_2$) flux (0.90 g), mixed well and fused in a furnace at 1000°C. The resulting melt is then cooled and dissolved in 100 ml of 4% HNO_3, 2%HCl solution. Ions are extracted from the plasma through a pinhole-sized orifice into a pumped vacuum system and focused with ion lens into a mass spectrometer. This solution is then analyzed by Inductively Coupled Plasma-Mass Spectrometry for 31 trace elements including the rare earth elements (REE). Additionally, the same solution is then analyzed by ICP-AES and the results are corrected for spectral inter-element interferences. The concentration of thirteen oxides is calculated from the determined elemental concentration and the result is reported in that format (ALS, 2017). Calibration was done by an in-house CGM reference material and standard.

1.6. Review of Previous works

Lake Tana, the largest lake in the country, is circular basin 70 Km in diameter, is found in northwestern Ethiopian plateau. The nearby area and its vicinity are covered with Quaternary volcanic products. However, volcanic rocks around Lake Tana basin have not been studied to any detail prior to this work regarding its petrology and geochemistry. Earlier regional studies have included the Tana basin in the framework of Ethiopian flood basalt provinces. Recent works have provided some information on the age and overall petrological features of the northwestern Ethiopian plateau.

Primarily Mohr, (1962) classified the Cenozoic volcanic rocks of Ethiopia into Traps and Aden series. The geology of the Tana basin has been mapped by (Tefera et al., 1996) and BCEOM, (1998) which show that Pliocene-Miocene Tarmaber Basalt, Quaternary Basalt and Quaternary unconsolidated lacustrine and alluvial sediments cover the area. The geological and structural maps of the different parts of the Tana Basin have been prepared at a scale of 1:250,000 by the Geological Survey of Ethiopia (Haro et al., 2010; 2011; Hilemaryam et al., 2012 and Beshawered et al., 2010).

Pik et al., (1998) undertake detailed geochemical studies on the Oligocene flood basalt (Trap formation) of the North Western Ethiopian region, identified three distinct geochemical groups as the low Ti (LT), High Ti-1, (HT1) and high Ti -2 (HT2) corresponding to three magma types. Numerous dikes are discovered between Lake Tana and Mount Belaya, which are compositionally basaltic and silicic, with very few dikes of intermediate composition (Mège and Korme, 2004). The floor of the Tana Lake is covered by clay (Lamb et al., 2007). The first geophysical model of the deep structure beneath the Tana region reveals a 1.5-2 km thick sedimentary series beneath 0-250 m thick continental flood basalts (Hautot et al., 2006). The Tana basin, northwest Ethiopia is an uplifted dome possibly related to the Afar mantle plume and the Quaternary basalt cover in the area is assumed to 500-1500 meter in thickness (Pik et al., 2003).

The flood basalts mineralogical and chemical composition is relatively similar. The geology, geochemistry, and petrogenesis of felsic rocks from ELIP has been described (e.g. Ayalew et al., 2002; Peate et al., 2005; Ukstins et al., 2003). Volcano-,chemo-, and chronostratigraphic correlations between Yemen and Ethiopia indicate that the source of these felsic rocks may related to volcanic centers (e.g. calderas) now located in Yemen (Peate et al., 2005). Moreover, Abate et al., (1998) undertook the geochemical and petrographic studies on the area around Lake Tana including Gimjabet-Kosober and Dek Iceland. They mentioned that the rocks from the Eastern side of the Lake Tana are characterized as sub-alkaline rhyodacites displaying evidence of chemical differentiation and alkali basalts. The basaltic rocks have the typical characteristics of with-in plate basalts.

In terms of petrology Quaternary olivine basalt and subordinate alkaline lavas cover much of the southern Tana basin. Different ideasare exist respective to the occurrences of the Tana Lake. The

Lake Tana is formed during the later episodes of the renewed active faulting of Holocene basalts (Jepsen and Athearn, 1961). According to (Chorowicz et al., 1998) the Tana basin lies at the convergence of three grabens: the Debre Tabor graben from the east, the Gondar graben from the north-northwest, and the Dengel Ber graben from the south-southwest. Recently, Prave et al., (2016) suggest that the Tana basin is a caldera, that the ignimbrites and associated felsic rocks are thickest and coarsest adjacent to Lake Tana and thin and fine in all directions away from the lake.

Some works are also done regarding the age dating of plateau volcanism. Hofmann et al., (1997), Courtillot et al., (1999), Ukstins et al., (2002) and Kieffer et al., (2004) provide absolute $^{40}Ar/^{39}Ar$ age determination on Oligocene-Miocene flood volcanic and Miocene to Pliocene volcanoes from the western Ethiopian plateau. Geochronological $^{40}Ar/^{39}Ar$ (Riisager et al., 2005) and magnetostratigraphy data (Hofmann et al., 1997) of the eastern Tana basin indicate that the bulk of Ethiopian traps erupted at about 30 Ma, in two pulses, each possibly only a few hundred thousand years long. According to Kieffer et al., (2004) Mio-Pliocene volcanic rocks includes Choke (22.4 Ma) and Guna (10.7 Ma), and Quaternary volcanic rocks covers southern Tana basin.

Lake Tana area volcanic rocks are the part of Ethiopian large igneous provinces. These rocks surrounding the Lake are characterized by complex lithological and tectonic features. This complexity arises from the presence of variation in age, stratigraphy and volcanic products. The area is covered with Oligocene flood basalts and associate felsic rocks in some of western and north western sides. They have an age of 30 Ma with the short time eruption event. Considerably, Miocene to Pliocene volcanoes covers the most north, east and west directions of the area with 22 to present (Hofmann et al., 1997; Pik et al., 1998, 1999; Rochette et al., 1998; Ayalew et al., 2002), and the southern sector of the Lake Tana area is covered by recent Quaternary volcanic rocks (e.g. Hofmann, 1997; Peccerillo et al., 1997; Beccaluva et al., 2009), that are the barrier of the lake Tana not to drift out (Chorowicz et al., 1998; Hautot et al., 2006; Poppe et al., 2013; Prave et al., 2016). Volcanic plugs are conspicuous in the region surrounding Lake Tana compositionally basanite rocks (Abate et al.,1998) and trachytic plugs (Dercqet al., 2001) penetrate flows of the overlaid volcanic terrains.

The Oligocene basalt is situated at lower sequence of Ethiopian large igneous provinces (ELIP) which underneath Miocene-Pliocene volcanic rocks and overlaid on the Mesozoic sediments or Proterozoic basement rocks. According to (Mohr, 1963, Kazmin 1972, Merla et al., 1979 and Tefera et al., 1996) this unit is assumed correspondingly to the Aiba and Alaja basaltic units (Berehe et al., 1987; Pik et al., 1998; Kieffer et al., 2004; Piccirllo et al., 1997) which have a plateau age ranges from 29.6 and 31.1 Ma that obtained by 40 Ar/39 Ar dating (Hoffman et al., 1997) from numerous areas.

Recently, Prave et al., (2016) dated the oldest basaltic units within the present study area. The southern Lake Tana side near the Blue Nile fall 34.05 ± 0.54⁄0.56 Ma, north western Lake Tana 8 km west of Aykel and yielded a plateau age of 28.90 ± 0.12⁄0.14 Ma and south western lower part of the upper basalt unit ∼3 km south of Kunzla and yielded a plateau age of 23.75 ± 0.02⁄0.04 Ma. Ayalew et al., (2002) confirmed that most of the rhyolites were extruded shortly after the eruption of the Oligocene flood basalts, and nearly the whole Oligocene volcanic pile was emplaced in a time interval of 2 Ma. In the main, the basaltic rock which extends from Bahir Dar to Injibara is described as quaternary by Merla et al. (1979) and Tefera et al., (1996). Later, Piccirillo et al., (1997) characterize the Tana basalt as quaternary. The dating of Prave et al., (2016) from the Bahir Dar area determined its age about 0.033 ± 0.005⁄0.005 Ma.

In addition, the southern, northern and western peripheries of the Lake Tana are covered with recent lacustrine sediments. These sediments are situated where the lake is bordering flat to gently sloping land (Lamb et al., 2007; Poppe et al., 2013). These sediments may be deposited at the higher level of the lake with addition of eroded sediments and exposed after decline of water level. The Oligocene flood basalt and associated felsic rocks with Miocene-Pliocene volcanoes are mapped as Oligocene basalt, rhyolite, ignimbrite and pyroclastic deposits in the present study. The Quaternary basalt, basanite, scoria and lacustrine sediments are categorized under quaternary volcanic products. Oligocene basalts are characterized by their lower elevations, slightly weathered and intercalated with ignimbrites (Beshawered et al., 2010). Palaeosols, scoriaceous fall and flows are also visible in association with the lava flows (Asrat et al., 2012).

In most scenarios the Lake Tana area volcanic rocks are comparable with the northwestern Ethiopian large igneous province, such as: plateau basalt (Pik et al., 1998, 1999) and rhyolites (Ayalew et al., 2002; Ayalew and Yirgu, 2003). Recently, Prave et al., (2016) explained that

Oligocene rhyolites zirconium dating lapilli tuff near the base of the felsite unit ∼7 km southwest of Kunzla yield a mean age of 31.108 ± 0.020/0.041 Ma. A flow-banded stony rhyolite in the central part of the felsite unit exposed in an erosional window through Quaternary basalt around Zega which yield a mean age of 31.033 ± 0.018/0.041 Ma. Two Flow banded feldspar-phyric rhyolites from the upper part of the felsite around Yifag, yield mean ages of 30.858 ± 0.024/0.044 Ma and 30.844 ± 0.027/0.046 Ma, respectively.

Chapter Two

2. Regional Geologic Setting

2.1. Introduction

According to Gerra (2000) and Tadese (2009), the geology of Ethiopia is constructed by rock types range in age from Precambrian to Recent. These rocks are categorized into Precambrian metamorphic rocks, Paleozoic – Mesozoic sedimentary rocks and Cenozoic volcanic rocks and associated sediments which covers 25%, 25% and 50% of the country's landmass respectively.

2.1.1. Precambrian rocks

The Precambrian basement rocks are consisting of various high-grade gneisses and schists, Meta –volcano Sedimentary rocks, and associated syn to post tectonic plutonic rocks; these crystalline basement rocks are poly deformed and metamorphosed rocks of pan African age related to both the Mozambique belt (MB) and the Arabian Nubian Shield (ANS) (Gichile, 1991, Davidson, 1983, Asrat et al., 2001). These basement rocks had been categorized into lower, middle and upper Complex based on the variation in the grade of metamorphism, in linking the age Archean, Early Proterozoic, and Late Proterozoic respectively based on lithostratigraphic sequences (Kazmin, 1972; Kazmin et al., 1978). Although the ages of the basement rocks is conceded to Neoproterozoic ranging from 850 to 550 Ma as dated by Ayalew et al. (1990). These Precambrian rocks are not found as an outcrop in the present study area. Generally, metamorphic rocks are seen as an outcrop due to erosion (unloading) of overlaid material and uplifting processes.

2.1.2. Paleozoic – Mesozoic sedimentary rocks

Paleozoic-Mesozoic sediments with a thick succession of different types of sedimentary rocks covered several distinct sedimentary basins unconformably deposited on the Precambrian basement. The Abay (Blue Nile) Basin is the one which encompasses the Lake Tana locality (study area) inside. According to Gani et al. (2007), it exceeds 1400 meters horizontal to sub-horizontal successions of both continental siliciclastic and marine carbonate rocks. In age, it ranges from Triassic to Cretaceous where this succession contains evidence for different phases of marine transgression and regression. The Blue Nile is incised into a Northwestern Ethiopian

Plateau which high 2500meters. Hautot et al. (2006) presented that the presence of NW trending sub-basins underneath around Lake Tana area as evidence.

2.1.3. Cenozoic volcanic rocks and associated sediments

According to Berhe et al. (1987) volcanism of Ethiopia taking place in two different phases within separate places; NW and Central Ethiopia as early Eocene (<40 Ma) and SW Ethiopia as Oligocene to Miocene (~49 Ma). However, there is evidence for older around 45 ma, which is less extended flood magmatism further south in Ethiopia (Ebinger et al., 1993). Most of the flood basalts in the northern sector of the study area were extruded over a short time period around 30 Ma (Hofmann, 1997; Hofmann et al, 1997) significantly predates the main extensional phases (Menzies et al., 1992). This extensive basaltic flow ranges 500–2000 meters thick and (Rochette et al., 1998).

The volcanism of Ethiopian large igneous province is a bimodal type (basaltic - rhyolitic in composition), with a lack of intermediate products (Ayalew et al., 2002; Ayalew and Ishiwatari, 2011) erupted mainly around 30 Ma for short period of time (Berhe et al., 1987; Hofmann et al 1997; Rochette et al., 1998; Ukstins et al., 2002; Kieffer et al., 2004). It is located near the triple junction of the Red sea, the Gulf of Aden and East African Rifts is considered as a young example of continental flood basalt volcanism associated with the continental break up. The CFB province was formed because of the impingement of the Afar mantle plume beneath the Ethiopian lithosphere (Mohr, 1983; Mohr and Zanettin, 1988; Marty et al., 1996; Hofmann et al., 1997; Kieffer et al., 2004).

2.2. North Western Ethiopian Plateau Volcanism

In a country there are two major plateaus are present which are separated by SW and NE trending Ethiopian rift valley. The northwestern covers the Tigray and Amhara Regions, including the Semien Mountains Ras Dashan (4620 m), are the highest peak in Ethiopia. The elevation is generally highest just before the point of origin to the Great Rift Valley, which splits the plateau diagonally (Asrat et al., 2012). Several rivers are crossing the plateau; notably the Blue Nile rising from Lake Tana. The plateau gradually slopes to the lowlands of the Sudan on the west and the Somali-inhabited plains to the east.

The North-western Ethiopian Plateau, with a mean elevation of ~2.5 km, it reaches 4.5 km at some places. It is located on the western flank of the tectonically active Main Ethiopian Rift and the Afar Depression. It records magmatic events from initiation through high flux and shut down to the onset as well as initiation of sea floor spreading (Kieffer et al., 2004) and 30-10 Ma ago (Pik et al., 2003) the part of Oligocene volcanism. Ethiopian volcanic plateau is covered by fissure fed basaltic lavas with subordinate rhyolite bounding the current Afar and MER (Kieffer et al., 2004). Now a days, the volcanic activities are continuingin Afar rifts.

The plateau was uplifted due to the combined effects of the rising Afar mantle plume and flank uplift of the Main Ethiopian Rift and the Afar Depression. Plume related uplift caused deep-seated faults within the Ethiopian lithosphere, leading to the collapse that formed the Afar Depression at~24 Ma (Beyene and Abdelsalam, 2005). This event was followed by shield volcano constructing episodes, which gave rise to the development of the Choke and Guguftu volcanoes around 22 Ma (Kieffer et al., 2004) which are situated southern and eastern side of the Lake Tana area respectively. According to Wolfenden et al., (2004), the Ethiopian Plateau is separated by the Northern Main Ethiopian Rift into northwest and southeast sectors nearby 11 Ma. In the meantime, the Guna shield volcano shaped at 10.7 Ma (Kieffer et al., 2004). Based on stratigraphic relationships and geochronological studies (Woldegabriel et al., 1990) suggested that the western boundary fault of the Main Ethiopian Rift initiated at least by 8.3 Ma.

However, as the structural, petrological and geochronological study of Bonini et al., (2005) concluded that extension forming the Main Ethiopian Rift started near 5-6 Ma Based on $^{40}Ar/^{39}Ar$ age dating and magnetostratigraphy data. Hofmann et al., (1997) suggested that extensive basaltic flows (500 –2000 m thick) erupted on 30 Ma over a short period of interval. This eruption, covering an area of >500,000 km^2, is inferred to mark the appearance of the Afar mantle plume (Mohr and Zanettin, 1988; Hofmann et al., 1997; Kieffer et al., 2004). Felsic rocks and pyroclastic deposits are inter-bedded with the flood basalts, particularly at superior stratigraphic units (Ayalew et al., 2002, Kieffer et al., 2004).

The mineralogical and chemical composition of the flood basalts is relatively uniform. Mostly aphyric to sparsely phyric, and contain phenocrysts of plagioclase and clinopyroxene with or without olivine. Most have tholeiitic to transitional compositions (Mohr, 1983; Mohr and Zanettin, 1988; Pik et al., 1998). Inter-layered rocks within the flood basalts are felsic lavas and pyroclastic rocks of rhyolitic compositions which is very similar with the field probe and petrographic investigations through this study.

2.3. Geology and Stratigraphyof Lake Tana Region

Generally, the Ethiopian Cenozoic volcanisms are volumetrically predominated by basalts. Alkaline and tholeiitic basalts are equally abundant. The ELIP has been host to tholeiitic and alkaline basalts. The detailed study of local stratigraphy and radiometric age determination (Mohr, 1962; Zanettin, et al., 1974) has shown that the volcanic rocks have been emplaced during two phases of volcanic activity. The first phase is known by extensive fissural basaltic eruptions built up thick piles of plateau lavas around 30-20Ma with the maximum frequency being 30Ma (Hofmann et al., 1997).These are overlain by locally inter-fingered with rhyolitic and trachytic ignimbrites (Ayalew et al., 2002; Ayalew and Yirgu, 2003) and by shield like volcanoes (Kieffer et al., 2004). The second phase (15 Ma to recent) is related to the Main Ethiopian Rift (MER) opening and extrusion of silicic volcanic and subordinate basalt flows (Kazmin et al., 1980).

Lake Tana is situated which is a faulted depression between erosional escarpment to the west overseeing the Sudan plains and tectonic escarpment of plate margin overseeing the Afar depression to the east (Chorowicz et al., 1998).The main geologic features of the basin are subsidence, block fault formation and accumulation of Miocene organic rich sedimentary rocks (Yemane et al., 1985). All through Plio-Pleistocene basin volcanism, late quaternary volcanic activity and recent lacustrine and alluvial deposition were successively happened along the margin of the lake (Chorowicz et al., 1998).

The stratigraphic evolution of the Lake Tana Basin is not fully understood since much of the basin's geological record (Mesozoic and Precambrian rocks) is buried beneath the extensive 500–2000 meters thick Cenozoic volcanic rocks (Hofmann et al., 1997; Coulie et al., 2003; Kieffer et al. 2004) and no subsurface data is available. Therefore, much more information is deciphered from the ~1.6 Km deep Gorge of the Nile (Gani and Abdelsalam, 2006; Gani et al., 2007) formed by the Blue Nile River on the Northwestern Ethiopian Plateau. Generally, it is covered with Quaternary volcanics (Merla et al., 1973; Gani et al., 2008) alluvial deposits around the lake margin (SMEC, 2007)which may have a thickness of up to 130m (Mohr, 1971) and Oligocene-Miocene CFB (Hofmann et al., 1997; Kieffer et al., 2004).

Some authors like Mohr, (1971); Kazmin, (1972) and Merla et al., (1979) mentioned that Lake Tana basin is formed by recent volcanic activity related to a set of north-south faults, known as the Lake Tana Rift. According to Merla et al., (1979) minor basaltic eruptions have occurred on the Ethiopian plateau during the Quaternary time in the Tana area. The Quaternary basalts from this area show a similar alkalinity spectrum to the Danakil block and Ethiopian Rift (Mohr, 1983). Although, this Quaternary volcanism from south of Lake Tana is related to local rifts and fractures zones (Hofmann et al., 1997).

Merla et al. (1979) suggested that the Tana Lake was formed due to Quaternary lava damming the river of Abay. Therefore, as a confirmation Blue Nile river falls down over basaltic fence like lava pile (Poppe et al., 2003). Lake Tana also resulted from the convergence of three grabens together and quaternary lava damming (Chorowicz et al., 1998; Hautot et al., 2006). According to Chorowicz et al., (1998) Lake Tana appeared at 8 Ma, marked by the deposition of lignitiferous sediments. It is also characterized by complex lithological and tectonic features with erosional escarpment on western side of Lake Tana (Sembroni et al., 2016 and reference therein).

In addition, Tana area is characterized by a widespread dike and pipe feeders which contributed to the mid-Tertiary flood basalt flow of this sector of the Ethiopian plateau (Mohr and Zanettin, 1988; Mege and Korme, 2003).Therefore, these volcanic rocks are associated with the Afar Mantle Plume are the outcome of subsequent opening of the Afar Depression and the Main Ethiopian Rift (Hofmann et al., 1997). After this plateau basalt the area was affected by uplift. The uplift brought intrusions of trachytic plugs. This event was followed by Tana rift. This rift formation favored lake accumulation in to which the Pliocene Chilga sediments deposited. Later Quaternary trachyte lava flow is followed by Quaternary basalts. Later with increase of the sea level Quaternary lacustrine sediments were formed (Haro et al., 2010).

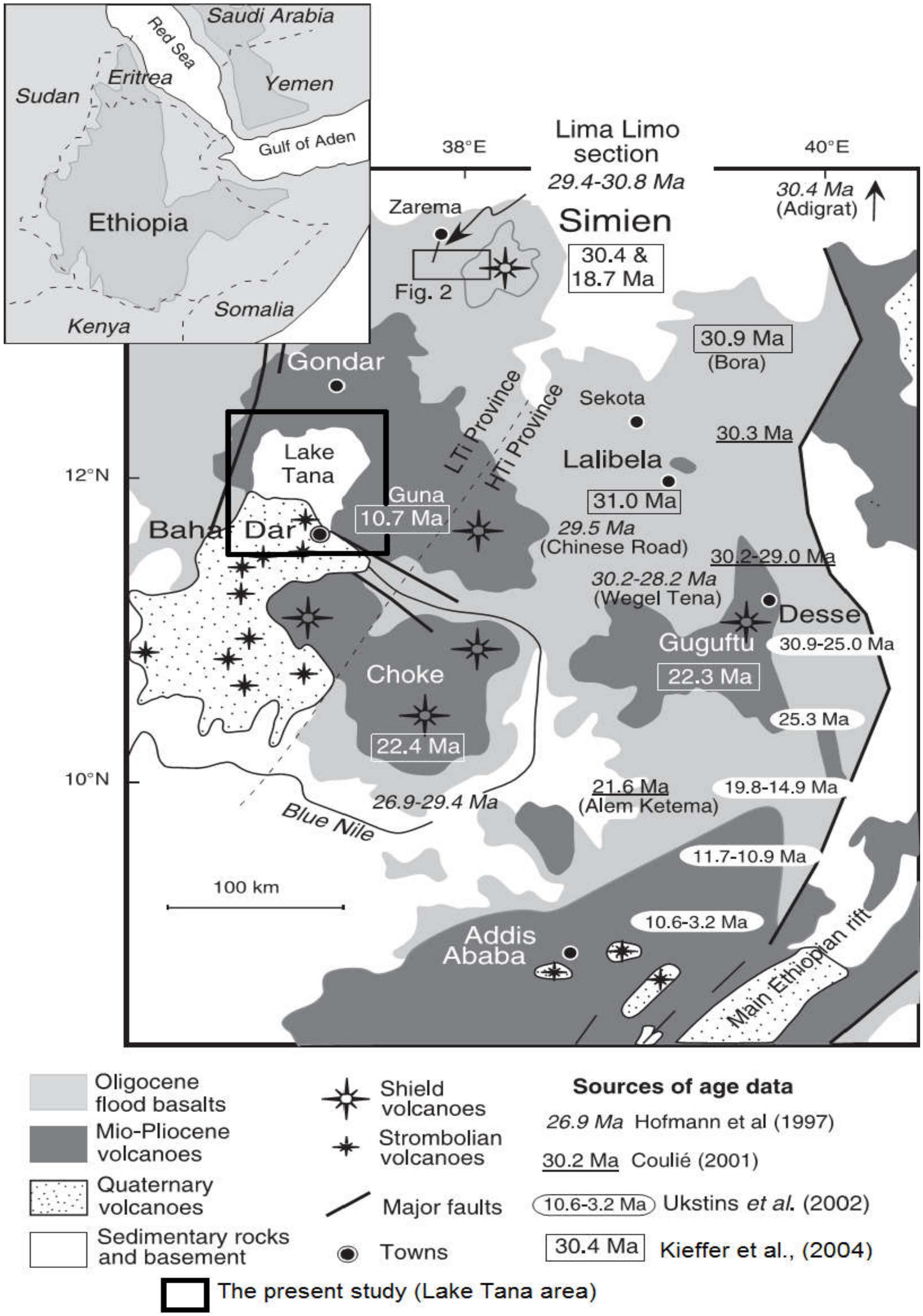

Figure 2.1: Geological map of the central and Northwestern Ethiopian plateau showing the extent of the flood volcanism, modified after (Kieffer et al., 2004).

Chapter Three

3. Geology of the Study area

3.1. Introduction

The major part of the studied area is covered with water (Lake Tana). Due to this, the geology beneath the lake has not been given much emphasis during the study. Rather, the study focused on the land masses surroundings the lake and some islands inside the lake. The geology of Tana area comprises different lithologies and geological structures. It is geologically complex with rough geomorphology and heterogeneous lithologies. Traverse lines were devised to encounter the accessible types of exposures in the area. Among those hillsides, river cuts, road cuts, and quarry sites exposures were common during the field study. From those exposures, the field rock identification and collection of representative samples were done.

The study area shows the lager coverage of volcanic rocks with different varieties and characteristics with the later formed weathered materials (sediments). It is believed that these sediments are formed from the nearby volcanic rocks. During the study, both felsic and mafic rocks are encountered with columnar jointing. Mostly, the basaltic rocks are found as lava flow, dome (ridge) and sometimes intercalated with Pyroclastic ejecta in the area; the felsic units are also exposed as rhyolitic lava flow and dome with extensive Pyroclastic flow deposits.

The basalts are generally stratified and cover extensive areas with flat and undulating geomorphology. The basalts are generally variable in composition, color and texture. They are often aphanitic, slightly phyric, porphyritic, vesicular and scoriaceous basalts. Those vesicular basalts are filled with secondary material most commonly zeolite and calcite. As a result some basalt has amygdaloidal textures. Then, basalts in the studied area are categorized in to two groups based on their field relations and age on the basis of literatures as Quaternary basalt and Oligocene basalt. Straightly aligned and spattered scoria cones are also the distinctive features within the area. In addition, a huge volcanic dome has been observed. In some places, those basaltic units area weathered and eroded, as a result, the beneath felsic units area exposed. From the overall field observation of the Lake Tana area, the basaltic units have greater areal coverage with respect to the felsic ones.

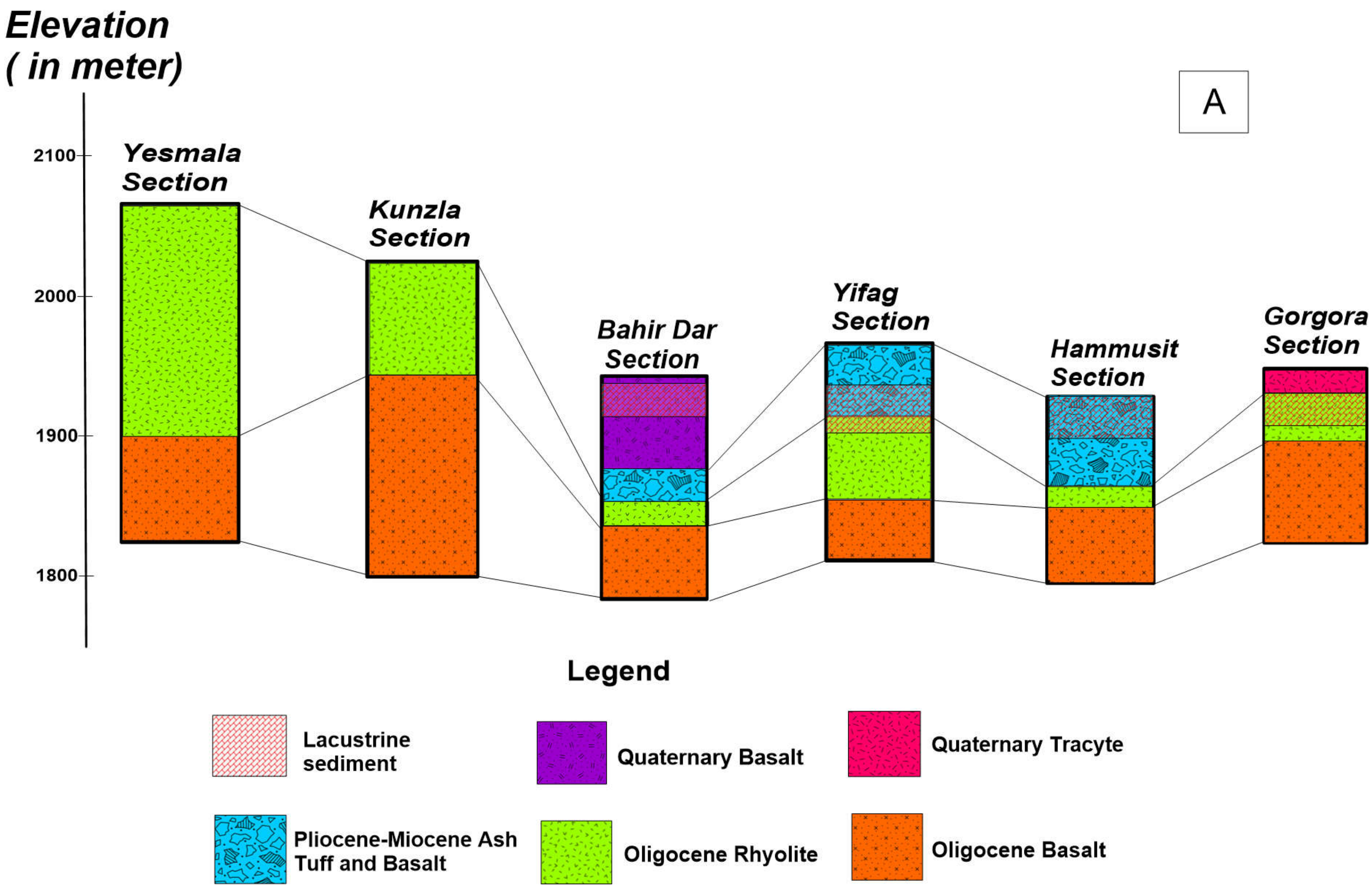

Elevation
(in meter)
A
2100
2000
1900
1800
Yesmala Section
Kunzla Section
Bahir Dar Section
Yifag Section
Hammusit Section
Gorgora Section
Legend
Lacustrine sediment
Quaternary Basalt
Quaternary Tracyte
Pliocene-Miocene Ash Tuff and Basalt
Oligocene Rhyolite
Oligocene Basalt

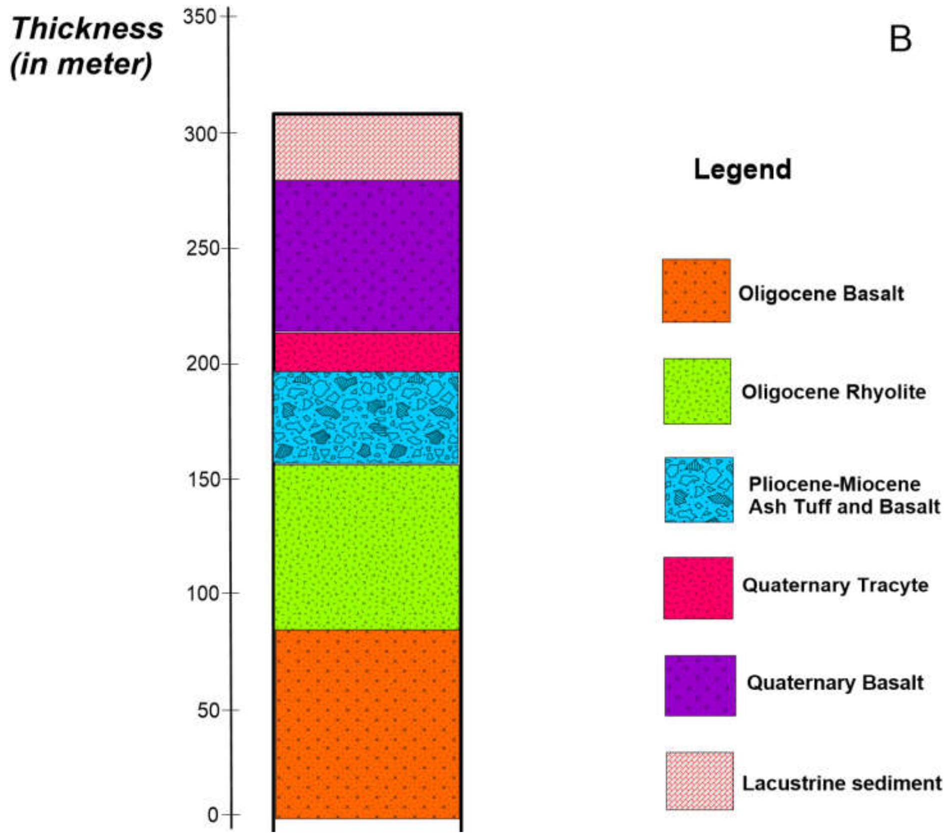

Figure 3.1 (A) Intra-basin correlation between different sections of Lake Tana surroundings (B) Composite stratigraphic of Lake Tana area based on field observation

The overall stratigraphy of the studied area is characterized based on the field observation and positions of the lithologies (altitude). Due to the complexity of the lithological units, it was difficult to represent single stratigraphic log initially. However, it is quite relevant to construct the stratigraphic log by selecting an ample section with varied lithologies. Additionally, it was very helpful to produce the composite volcano-stratigraphy by making correlation among the individual sections. Throughout the circumstance of the Lake Tana the volcano-stratigraphic sections are almost similar.

The major lithological units identified in the studied area includes: recent lacustrine sediments, Quaternary basalt, Pliocene to Miocene ash tuff and associated basalt, Oligocene rhyolite and basalt. Basanite intrusions and scoria cones are also discussed under the Quaternary volcanics. Those smaller outcrops like basanite are not included in the map and stratigraphic column but, they are discussed in the descriptions separately. The geological structures that are identified in the area include joints, fractures, faults and dikes.

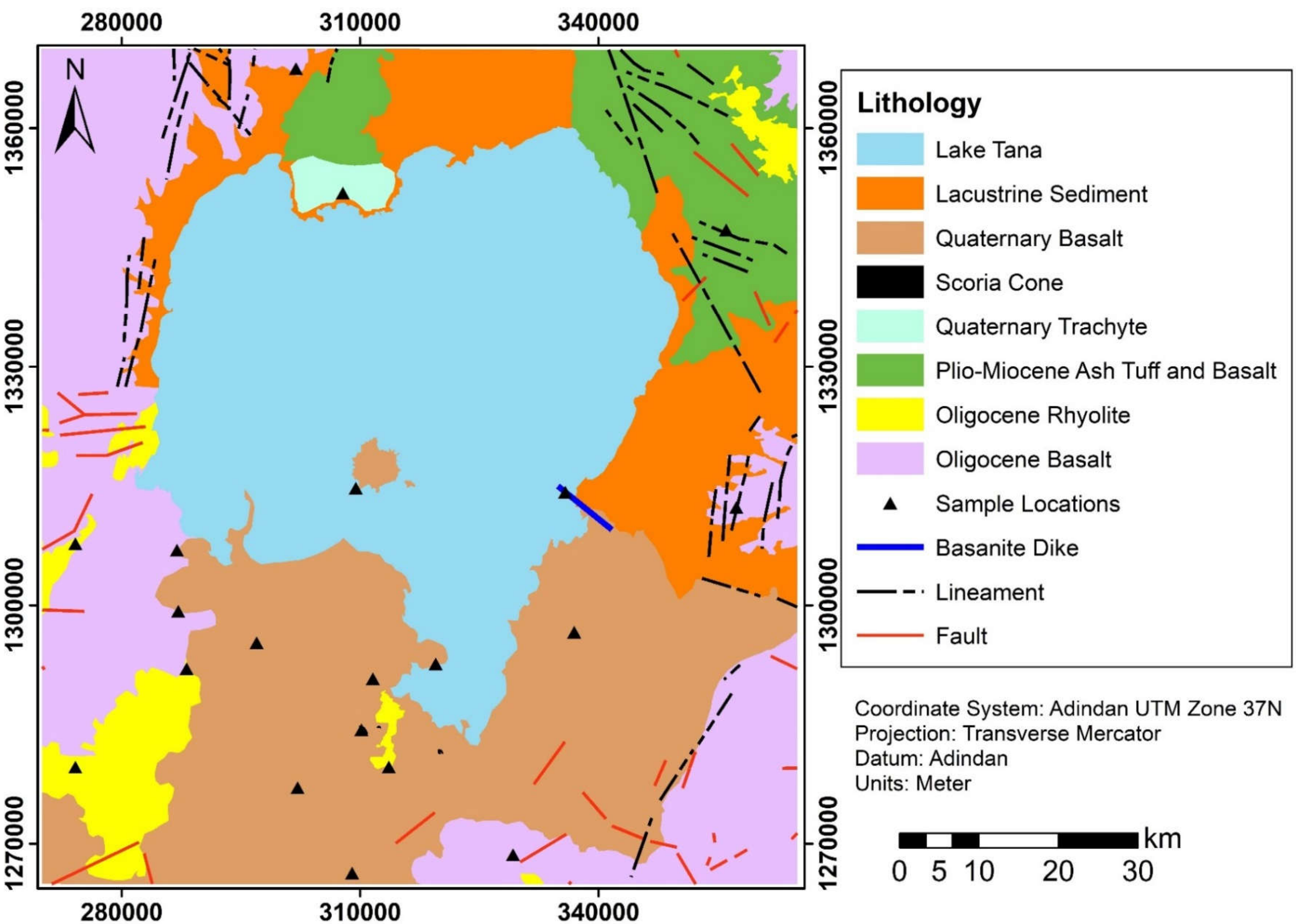

Figure 3.2: Geological Map of the Study Area

3.2. Lithological Description

3.2.1. Quaternary Lacustrine Sediments

These lacustrine sediments are occurring to the north of Lake Tana area continuation of the Fogora and Dembia floodplain sediments. They also occur to the west of Lake Tana around Delgi town and north western side around Yifag villages. It forms flat-lying topography and marshy areas. It consists of loose, brown to grey colors and, silt, and clay bearing clasts. This clast includes boulders of basalt, rhyolite, and scoria.

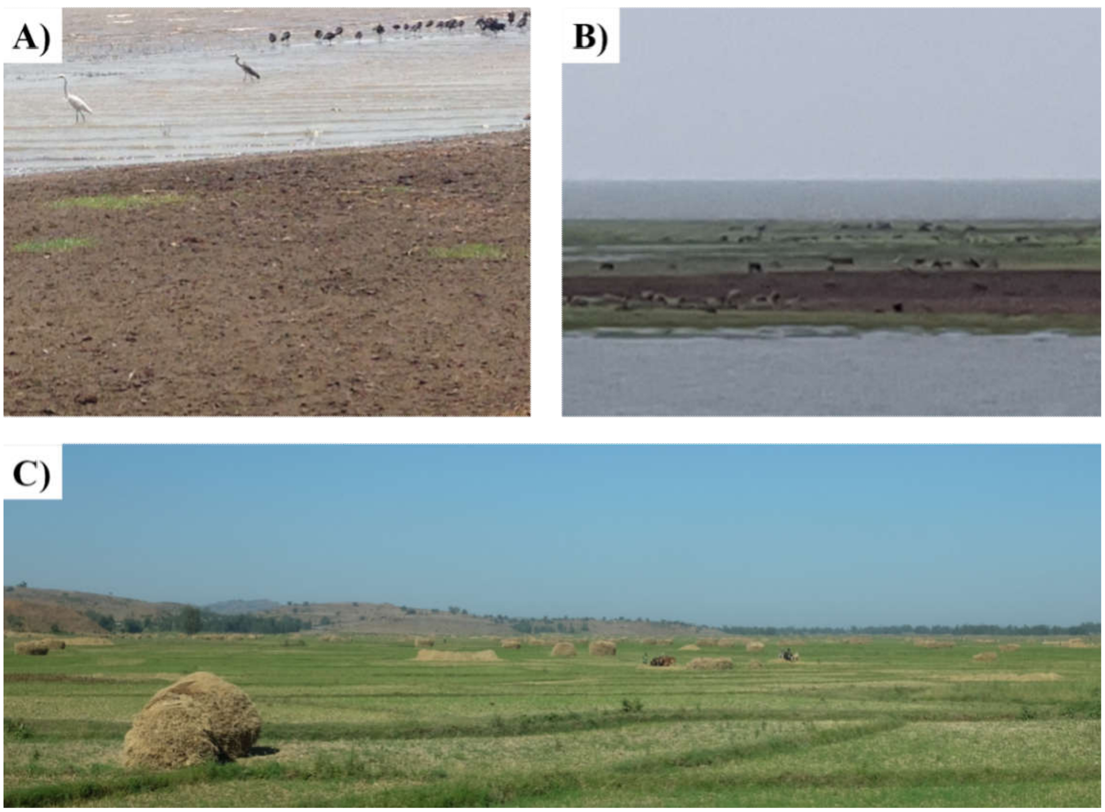

Figure 3.3: (A) Quaternary lacustrine sediments northern side of Lake Tana (B) Lacustrine sediments southern side of Lake Tana (C) Fogera floodplain

3.2.2. Quaternary Basalt

The Quaternary basalt is found relatively at higher stratigraphic positions. They form lava plain and randomly distributed variable exposures with some cliffs. They show porphyritic and vesicular textures with black to dark grey color. These basalts are underlain by Miocene ash tuff and partly cover by Quaternary Lacustrine sediments in and around the vicinity of the Lake Tana area. Mineralogicaly, they constitute olivine, plagioclase and some pyroxene. The olivine and plagioclase phyric basalts are black and compact. Around Zega, Merawi and Gordema area the vesicles on this basalt are very less based on hand specimen and at the outcrops.

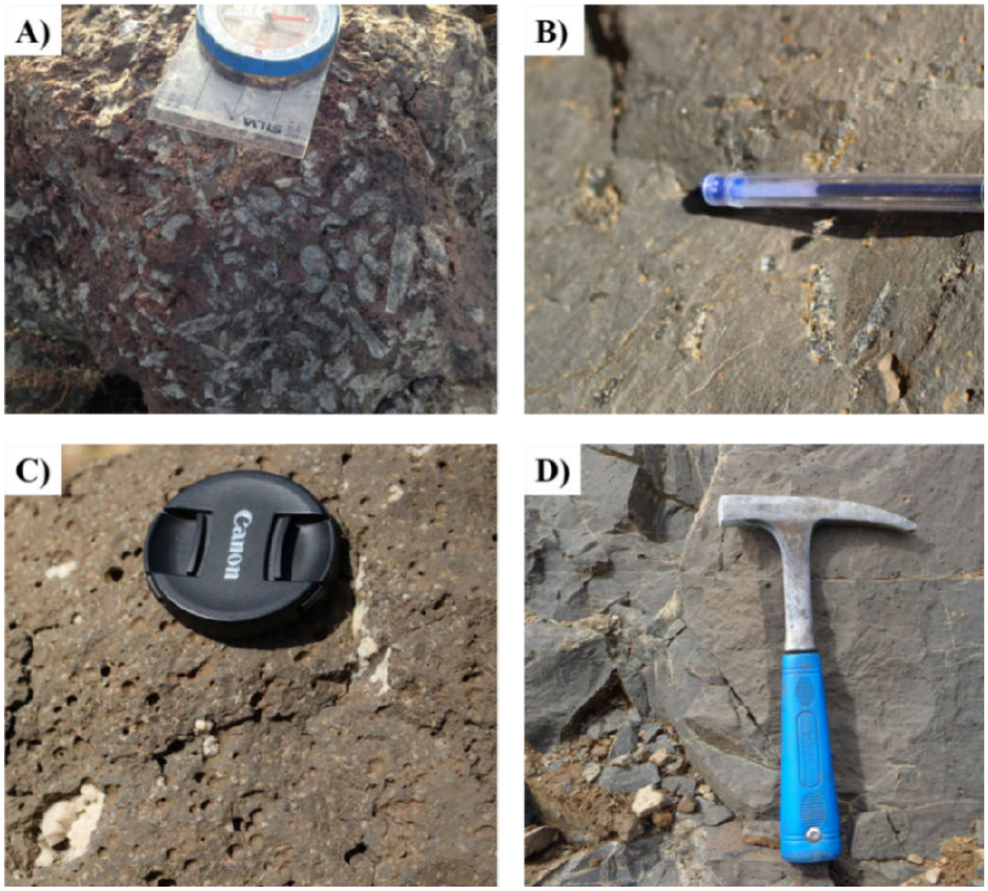

Figure 3.4: Quaternary Basalt A) & B) Extremely porphyritic plagioclase pyric C) Olivine phyric vesicular Basalt with secondary infilling materials D) Pyroxene pyric basalt

Sample # Tan 10, Tan 19 and Tan 20 are collected from those areas. Near Bahir Dar, Weramit and Hamusit area the basaltic lava flows has the porphyritic and vesicular textures. Sometimes the vesicles are filled by secondary infilling materials (precipitates). Those filled vesicles with zeolite, calcite and green color secondary minerals has amygdaloidal texture. The olivine and plagioclase phyric basalts are coarse grained, black and compact. On the way to Delgi it is characterized by a coarse grained mineral ~3-5 cm of plagioclase (Fig 3.4.A) and around Shobele village coarse crystal ~3-5 cm of pyroxene mineral is set in medium to fine grained groundmass of plagioclase and some pyroxenes dark rock with porphyritic texture. Basaltic domes are found around Delgi and Asinora villages. They have smaller elevation as compared to felsic ones having columnar joints. They are characterized as flat top ridges and wide area coverage.

Scoria cones are generally small volcanoes produced by quick eruptions with a total vertical relief of 90-150 meters in study area. Around Bahir Dar area the scoria cones are highly excavated as a row material for construction (Fig 3.5.A). From the sections of each quarry it is visible to observe the bedding pattern which infers the flow direction and venting sequence of the magmas. Parasitic sill (Fig 3.5.D) which is measured 2.5m is also observed with in scoria cones. Its color looks dark grey with aphanitic texture. It shows hardened and compacted nature which is different from the host scoria cone. This parasitic cone may be formed due to post magmatic tectonics processes when the basaltic magma flows in to fractures.

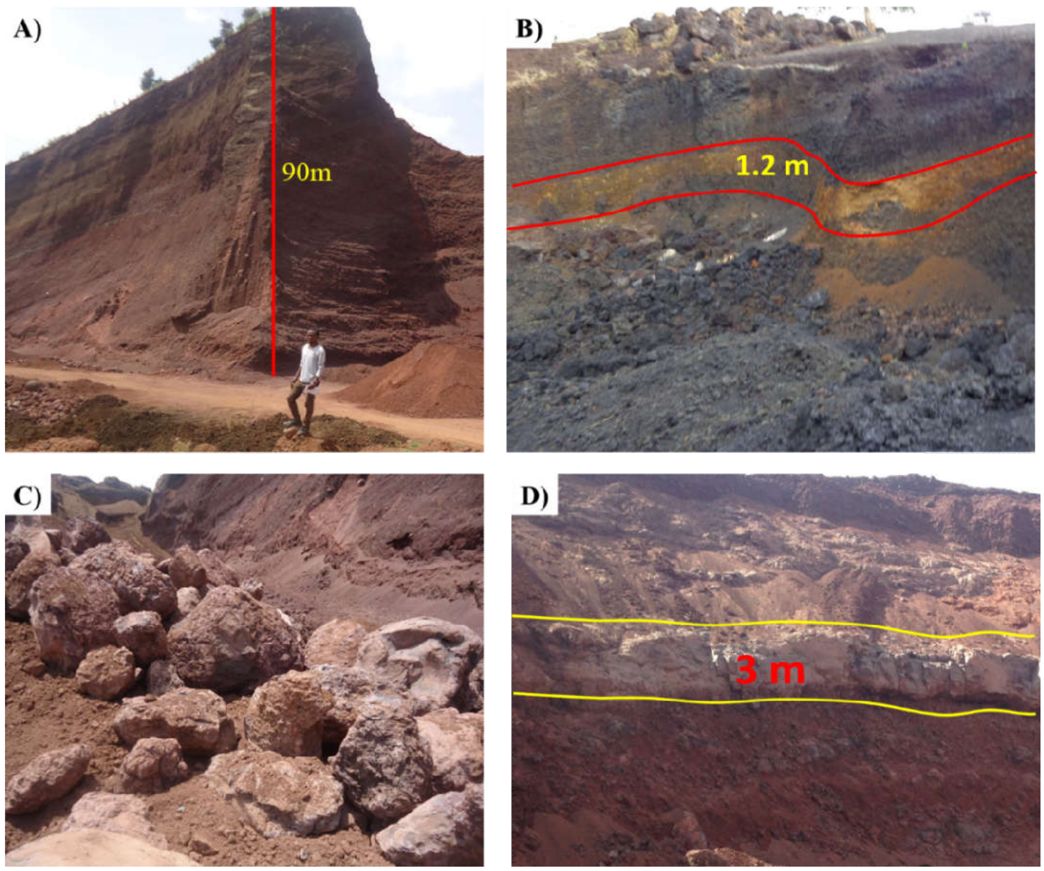

Figure 3.5: Scoriaceous basalt A) Scoria cone under quarrying around Bahir Dar city B) Fresh black scoriaceous basalt with 2.5 m thick paleosol C) Volcanic Blocks and Bombs near scoria cones D) parasitic sill within the scoria cone showing horizontal layering.

Volcanic blocks and bombs (Fig 3.5.c) are dominantly seen in and around scoria cones. These unmodified scoria fragments have equant, elongate and irregular shapes bounded by rough and ragged surface. These juvenile basaltic pyroclasts are deposited near scoria by basaltic fallout.

The spindle bombs looks spherical to elliptical shapes (rugby ball) with relatively smooth surface. These blocks and bombes are modified by surface tension (aerodynamic effects) in the atmosphere during flight.

3.2.3. Quaternary Trachyte

Quaternary trachyte lava dome is observed around Gorgora, north of Lake Tana (Fig.3.6.A). It forms smaller area and lava flow laterally overlain by lacustrine sediment. These trachytes are greenish grey, fine to medium grained and locally contain phenocrysts of quartz, plagioclase and alkali feldspars. The Quaternary trachyte often displays porphyritic texture, where acicular to tabular sanidine feldspar phenocrysts align in one direction. This trachytic texture is suggestive of flow prior to cooling. This unit is also exposed in North West side of Lake Tana around Yifag in association with the other rhyolitic and basaltic rocks with unknown age.

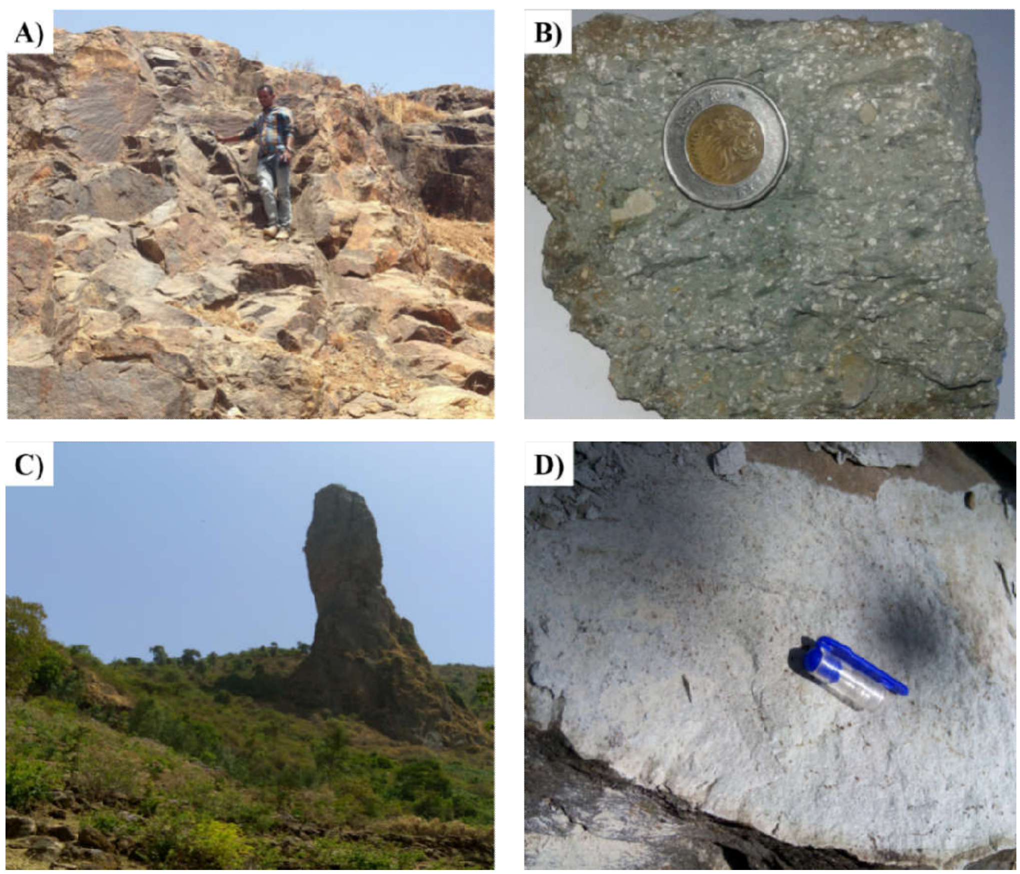

Figure 3.6: (A) and (B) Trachytic lava dome showing porphyritic texture (C) and D) Trachytic volcanic neck near Addis Zemen town and hand specimen of the Trachyte sample respectively.

Additionally, along asphalt road takes to Gonder town near Addis Zemen the trachyte plugs which have continuation to Guna shield are seen. The plug is rocky and resistant to erosion and formshigh rising hill. It is composed of sanidine and quartz crystals. But, it is slightly aphanitic to porphyritic texture and pink to light grey color. The trachytic plug around Addis Zemen area (Fig.3.6.C) is a typical example of a volcanic neck. It is silica rich rock due to this it is highly resistant to weathering. Most of the trachytic plugs are existed by penetrating the surroundings pyroclastic and basaltic rocks. These trachytic plugs have columnar jointing with 10-40 cm polygonal colonnades.

3.2.4. Pliocene-Miocene Ash Tuff and Basalt

Miocene ash tuff deposits are found in the study area at different localities. These formations are found as intercalated units with basaltic rocks, unwelded tuff, and slightly welded rhyolitic ignimbrites. This unit contains compositionally different rock type fragments with variable size. The size of the lithic fragments ranges from ash to block sizes. It is coarse to very coarse grained containing rock fragments of basalt and rhyolites (such as pumice) are cemented by volcanic ashes. The constituent phases include biotite, quartz and feldspar minerals. The color of lithic fragments varies from light blue to grayish, commonly characterized by fine to medium grained textures. This unit weathered color is dull to bluish gray. Along the fractures of these units, Fe-oxide minerals such as, hematite is precipitated.

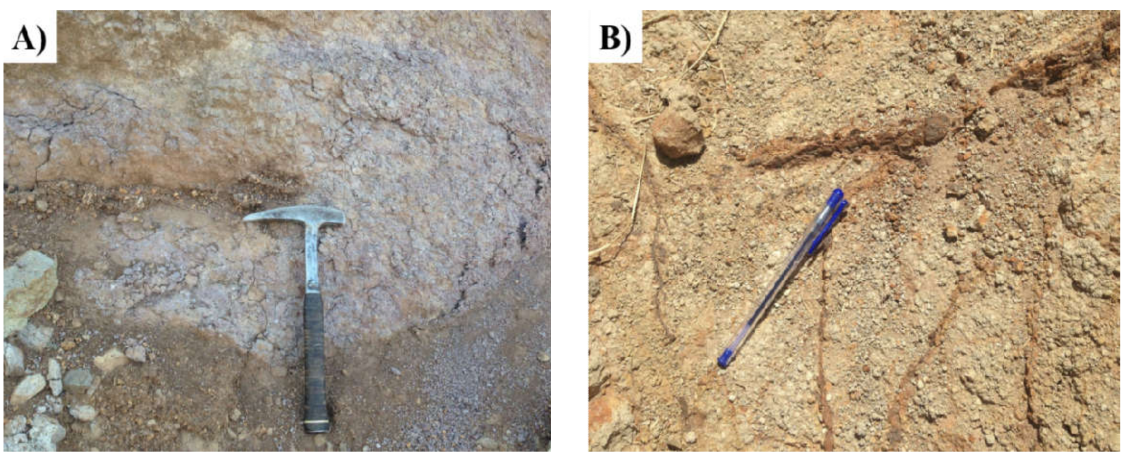

Figure 3.7: A) Grayish color pyroclastic flow deposit B) Weathering and hematization alteration on the Miocene ash tuff

Whereas, the Miocene basalts are situated at the middle of upper Quaternary and lower Oligocene formations by stratigraphic positions and exposed in eastern side of the study area and far south eastern side of Lake Tana. Texturally, it ranges from slightly aphyric to porphyritic and often shows moderately weathered appearance. It is dark to grey in fresh samples and reddish to yellowish brown in weathered ones. Plagioclase and clinopyroxene are present as phenocrysts.

3.2.5. Oligocene Rhyolite

In the study area, rhyolitic lava is found in to two different types of volcanic landforms. The first one is rhyolitic lava flow which dominantly shows flow banding. The other is Rhyolitic dome with columnar joints. It is light grey to pink in color composed of alkali feldspar, quartz, and biotite micas. Several smaller rhyolitic domes are encountered around Zege, Kunzla, Yesmala Giyorgis and Yifag. The outcrops of extensive rhyolitic lava are also found around Kunzla, Dengel Ber, Yifag, Gurashka and Yesmala area. The rhyolitic domes around Chuahy Dingiya SW of Lake Tana and Yifag area west of Lake Tana are indicated that they are resulted from rhyolitic lava flows.

On many outcrops of Oligocene rhyolites the hematite veins are observed with cross cutting relationship to the outcrops and vertically in association to the columnar jointing (Fig 3.8. A). In addition these rhyolitic rocks are identified as a dyke. In some places, they show intercalation of fine ash and un-welded tuffs. It forms horizontal flow banding with ~5-20 cm beds thickness. Locally, these rocks are affected by joints weakly to strongly with vertical as well as horizontal attitude.

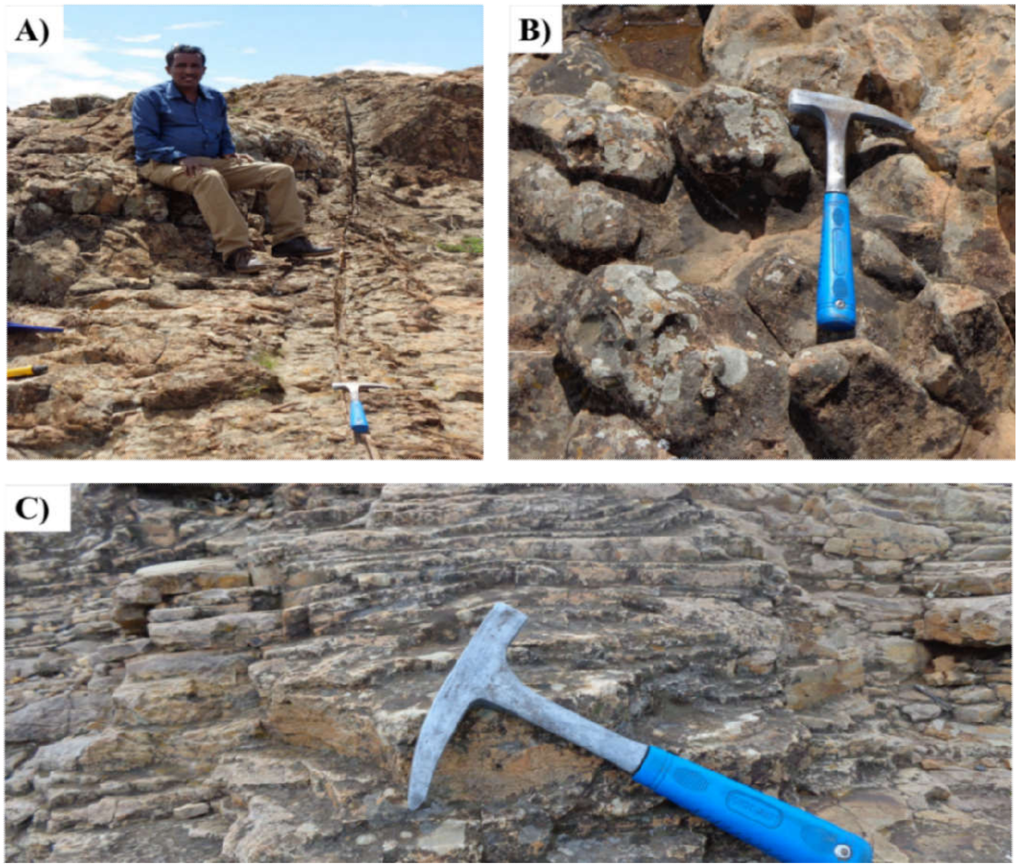

Figure 3.8: Rhyolite lava A) Rhyolitic lava dome with the extensive hematite vein B) Columnar jointing on rhyolitic lava dome C) Layering and flow banding of rhyolitic lava

Other varieties of Oligocene rhyolitic ignimbrite composed of pumice, volcanic glasses, and basaltic rock fragments. And also quartz and biotite minerals are present as an accessory. It is coarse-grained, densely welded rock containing vitrophyric fiamme (Fig 3.9.C) and lithic fragments with associated rhyolitic lava flows interleaved with ash and un-welded tuffs (Fig. 3.9.A and B). The size of the lithic fragments ranges from ash to block sizes. These rock units are exposed to Wanzaye hot spring and Dengele Ber areas. Locally Teda area near Gondar city,these ignimbrites have a reddish color. Also, some locale people called this reddish ignimbrite ‘Fasil Dengaye’ as the result, this rock has been used as construction material for the Palace of “emperor Fasil” in Gondar city at the past period.

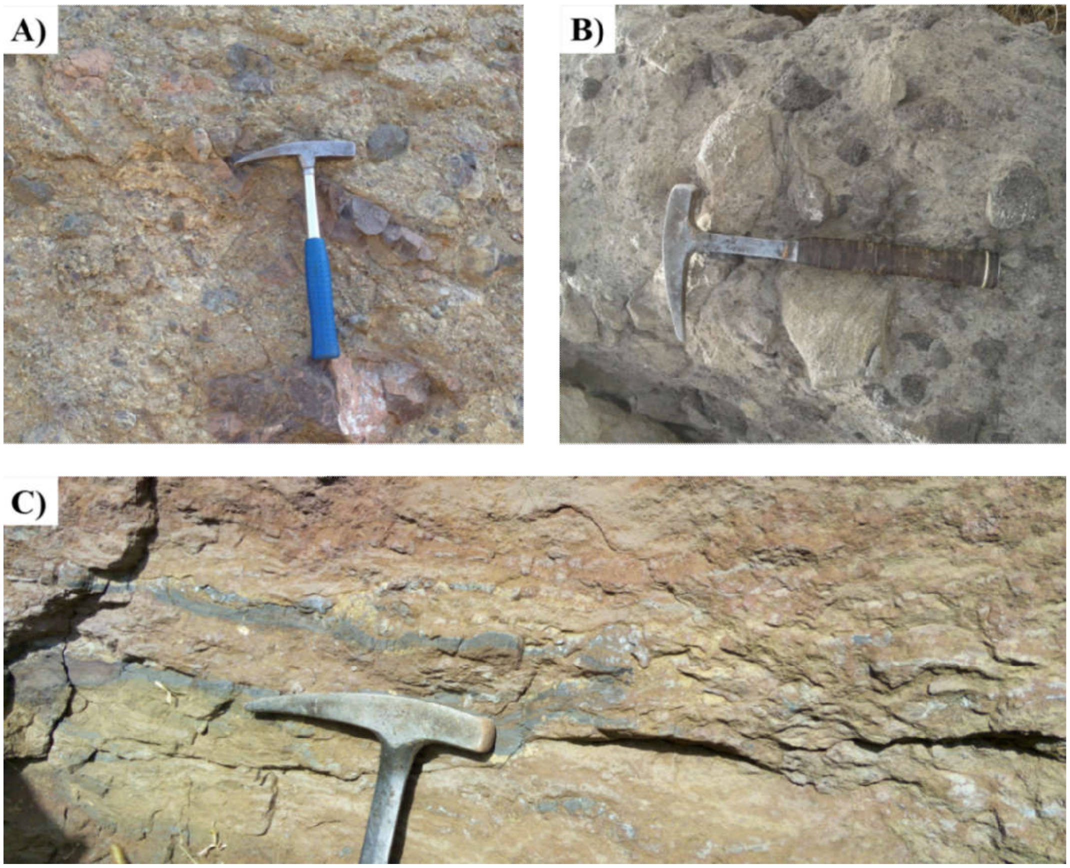

Figure 3.9: (A) and (B) un-welded Ignimbrite with volcanic rock fragments and volcanic glasses C) Reddish color layered and compacted ignimbrite

3.2.6. Oligocene Basalt

Oligocene basalt is situated at the lowest stratigraphic position exposed western and south western and northern side of Lake Tana which has higher altitudes for example; they are exposed at Azezo, Makesegnite and Addis Zemen areas. This unit has an exposure horizontally stratified manner and deeply weathered at places. It has dark grey color, very fine grained texture and often slightly weathered. Those slightly weathered basalts are intercalated with pyroclastic deposits in many places of these areas.

These aphanitic Oligocene basalts are commonly characterized by columnar jointing (Fig.3.10). The columns typically have six sides mostly straight and parallel sided. In some places, iron oxide (hematite) is precipitated within the joints and chlorite on the outer surface. The jointing pattern in these outcrops defines two distinct zones. The thin lower colonnades comprise well developed wide columns oriented at right angle to the flow base and the overlaying entablature, less regular, narrow and fanning columns. The Basaltic units shows that coarse grained texture occurs in the central part of the lava flow and fine grained textures occurs in the bottom and in the top of the same flow.

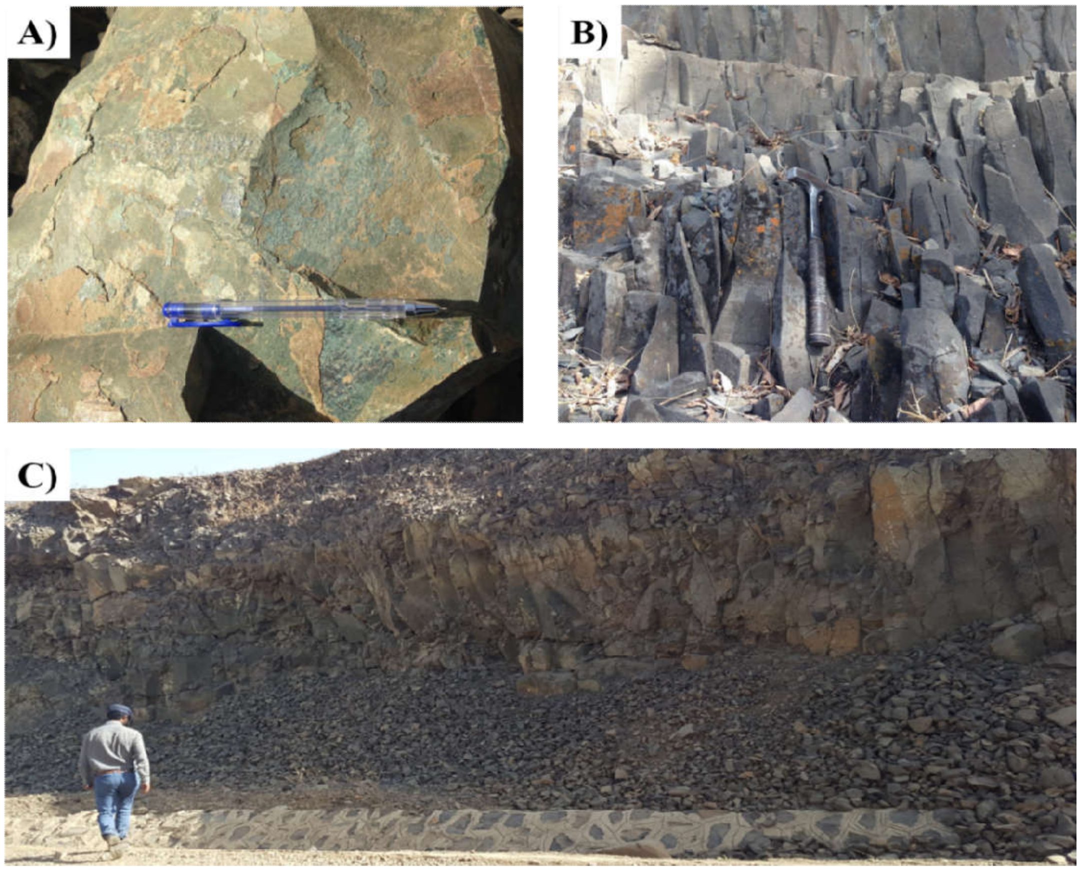

Figure 3.10: (A) Oligocene basalt showing chloritization alteration (B) Columnar joints on Oligocene basalt (C) Road cut exposure showing weathered Oligocene basalt on the way Kunzla to Delgi

3.2.7. Basanite Intrusion

These rock types are found as mafic lava dome around Asinora Village south eastern Lake Tana (Fig.3.11.A) and monastery of Tana Kirkos (Fig.3.11.B) is also found on mafic intrusion. Tana Kirkos is one of the islands on Lake Tana which is ~2 km longer and 10 m wider dike like structure having basanite composition. This basanite rocks in the area have a well-developed columnar jointing structure. In hand specimen, their color ranges from greenish grey- to-grey and greasy luster or appearance. It has very compact dense texture, poorly to highly porphyritic with phenocrysts of alkali feldspar and olivine minerals. They have flow features and give a sonorous ring when struck by a hammer. A well-developed thin slate like sheets characterizes them, and that the rocks break in to platy parting.

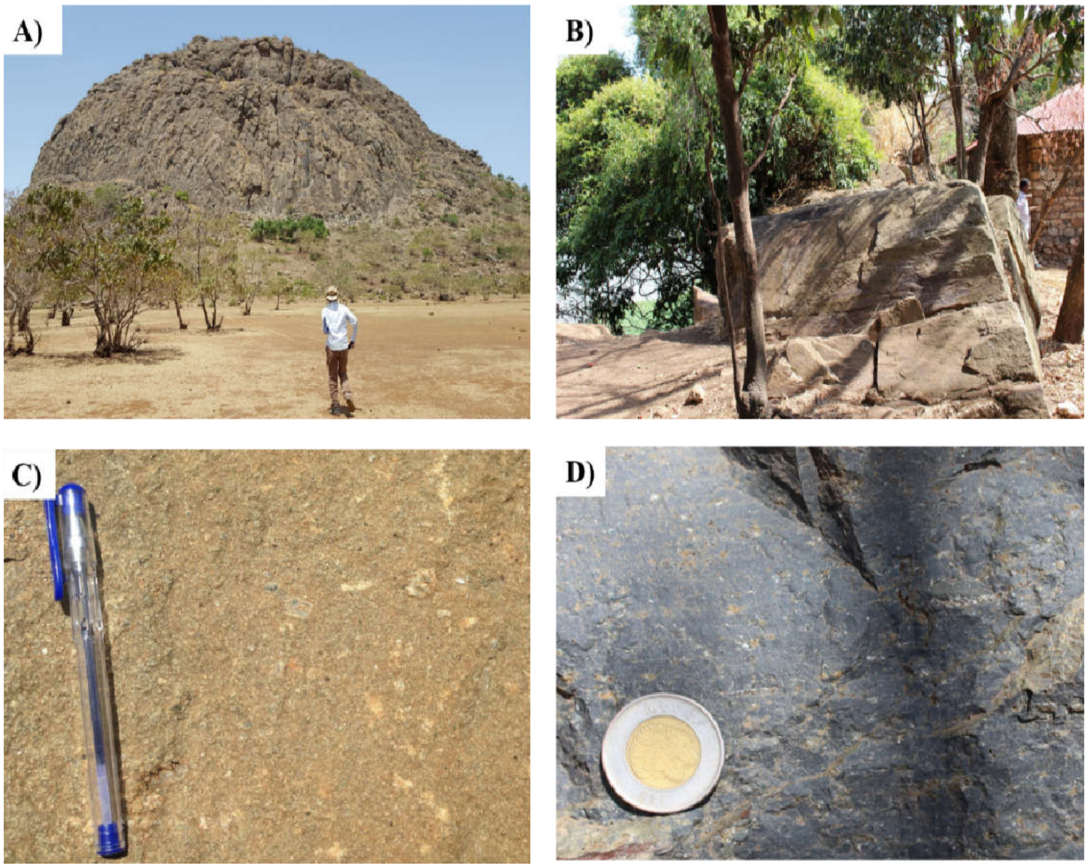

Figure 3.11: (A) and(C) Basanite dome near Asinora village (B) and (D) Basanite dike at Tana Kirkos Island with their hand specimen samples respectively.

3.3. Geological Structures

According to Chorowicz et al., (1998) Lake Tana basin was formed by the processes of collapsing occurred at the focus the three half grabens, called the Gonder, Debretabore and Dengle Ber grabens. The first subsidence was in Mid-Tertiary while the subsequent subsidences were due to revival of graben faults in Late Miocene and Quaternary. Subsidence was due to purely tensional forces.

These structural elements within the study area are identified by the combination of results from Landsat imagery and DEM analysis, and field observations. Most of the structures are associated with the extensional tectonics. They include faults, lineaments, fractures, and joints, having variable magnitude and orientations. The major geologic structures in the studied area are mostly localized in the western and northeastern side of Lake Tana having a series of NW-SE normal faults and other linear features or lineaments have also been interpreted from satellite imageries of the study area. All these faults have their fault planes with very steep dips. May be those lineaments are product of tectonic derivation. These lineaments have the following trends: NNE-SSW and NE-SW with variable strike length (few meters up to kilometers).

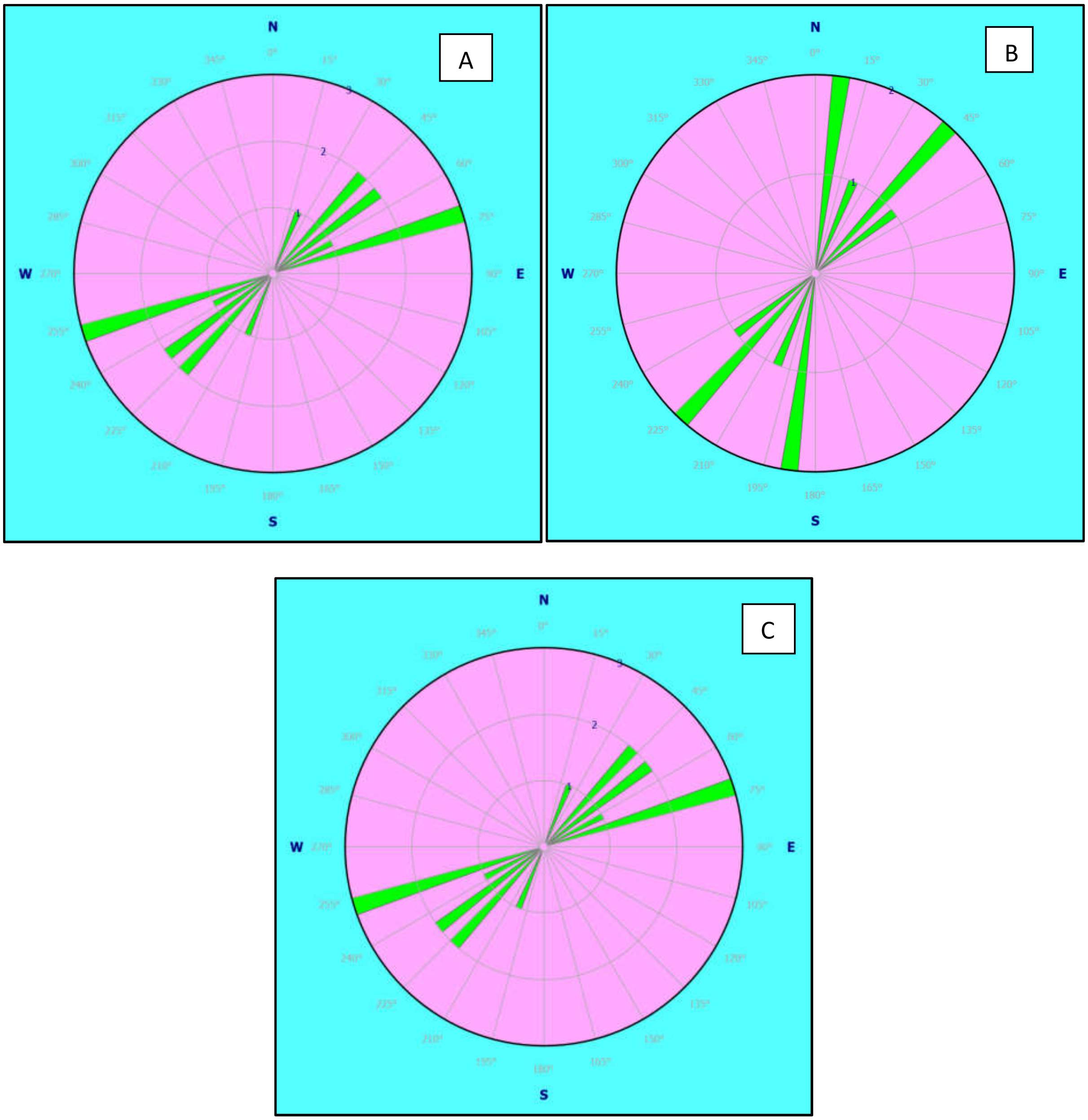

Figure 3.12: Rose diagram (A) Strike of the faults (B) strike for the joints and (C) Strike for dikes

Chapter Four

4. Petrographic Descriptions

4.1. Introduction

Modal analysis is one of the most common microscopic methods in the igneous petrographic practice. Based on the mineralogical composition of the igneous rock, and the percentage by volume of essential minerals (minerals influencing its classification and constituting more than 5% of the rock). By the aid of this method, it is possible to determine the relative abundance of the rock-forming minerals and microscopic texture of a given rock. These data commonly used to give petrological conclusions about the type of textures and mineral assemblages; moreover, it's cooling history. Eighty thin sections were investigated under the plane and crossed polarized view by using Leica microscope.

The representative pictures from the microscopes are captured automatically by using LAS EZ version 3.0 inbuilt-camera. The rocks are classified accordingly as olivine, plagioclase and sometimes pyroxene phyric with porphyritic and vesicular textures Quaternary basalt, aphanitic Oligocene basalt, and porphyritic and glassy Oligocene rhyolite. In addition, porphyritic Eocene trachyte and poikilitic and glomeroporphyritic basanites are among the samples investigated under petrographic microscope.

4.1.1. Quaternary Basalt

From the upper stratigraphic section of the basaltic rocks four samples Tan 10, Tan 11, Tan 19, and Tan 20 are examined microscopically (Fig. 4.1). Sample Tan 10 (Fig. 4.1.A) is composed of 50% phenocrysts 50% groundmass. The phenocrysts assemblage consists of 30% lath euhedral plagioclase, 11% clinopyroxene, 9% olivine. The groundmass is also composed of lath-shaped Plagioclase, pyroxene (augite), opaque and volcanic glass. Sample Tan 19 (Fig. 4.1.D) shows 5% olivine, 18% augite, 70% plagioclase and 7% opaque mineral (magnetite).

Also, sample Tan 20 shows 50% phenocrysts and 50% groundmass. Phenocrysts are olivine 3%, 7% pyroxene, 40% plagioclase and 3% opaque minerals (Fig. 4.1.B). In all samples, phenocrysts of olivine display 0.3-1mm maximum size and euhedral to anhedral shape. They show glomeroporphyritic and porphyritic textures. Additionally, sample # Tan 11 shows (Fig. 4.1.C) vesicular and dissolution textures. Clinopyroxene and plagioclase phenocrysts are set with in a fine grained groundmass of strongly flow aligned plagioclase lath displays trachytic texture.

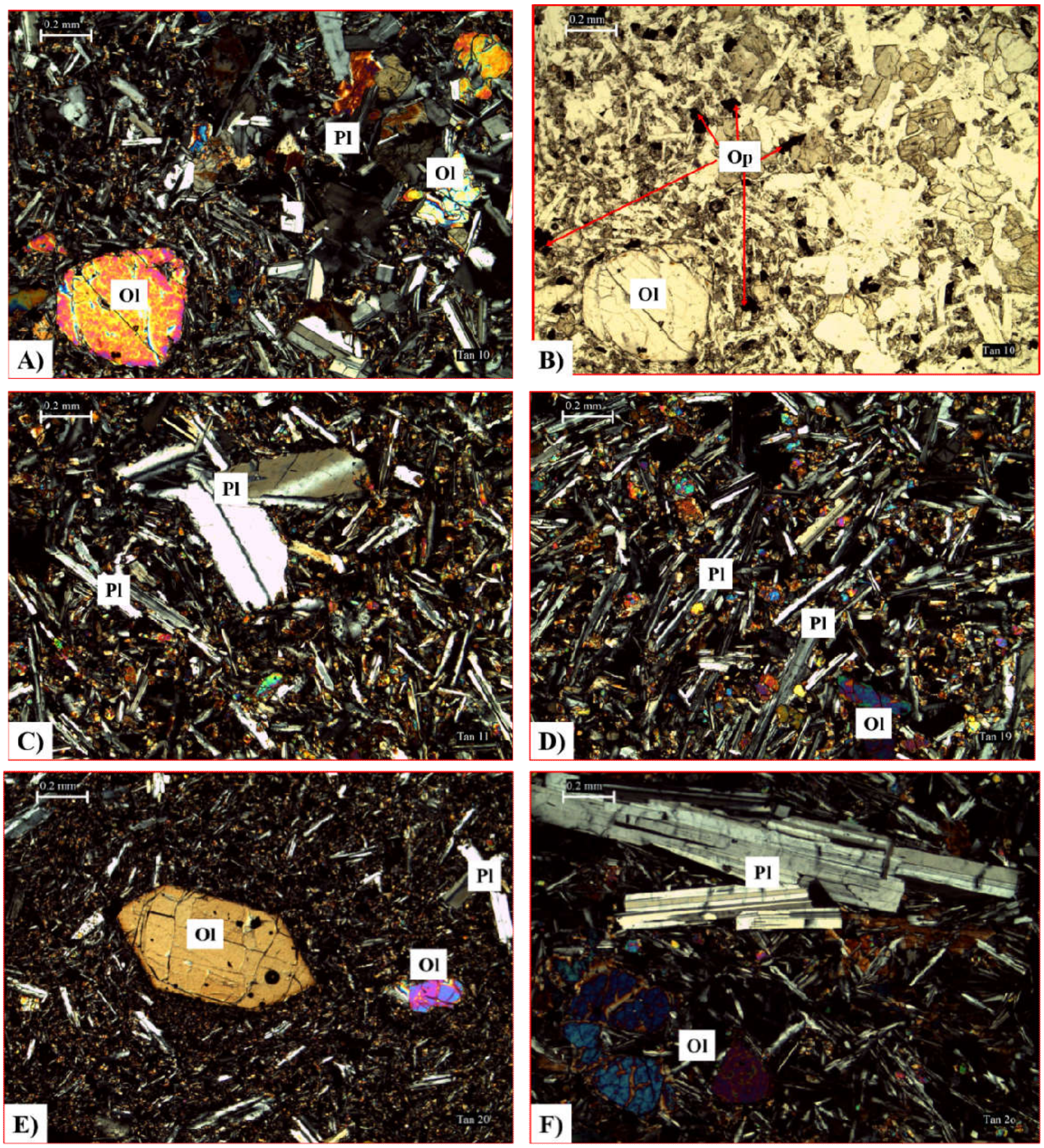

Figure 4.1: Microphotographs of Quaternary basalt; sample Tan 10, 11, 19 and 20 (A, C, D, E and F) under XPL and (B) under PPL view. The labels stand for; Pl-for plagioclase feldspar, Ol-for olivine, Op-for opaque (Fe, Ti oxides) and Cpx-for clinopyroxene.

4.1.2. Scoriaceous Basalt

The scoria cones throughout the study area have similar petrographic characteristics. Sample code Tan 15 is fresh black scoria and Tan 21 oxidized reddish scoria showed the vesicular texture. The vesicles are circular to elliptical shape with 0.4 mm maximum diameter (Fig. 4.2). The olivine and clinopyroxene minerals are identified as phenocrysts having 0.3 mm of maximum sizes. Both have euhedral to subdural crystal habit. It composed of 54% vesicles, 36% plagioclase as microphynocryst and ground mass, 5% olivine, and clinopyroxene 3%. Opaque minerals Fe, Ti oxides as inclusion in olivine minerals and as ground mass is about 2%. Both samples of scoria from the study area show that vesicular or scoriaceous texture (Fig. 4.2).

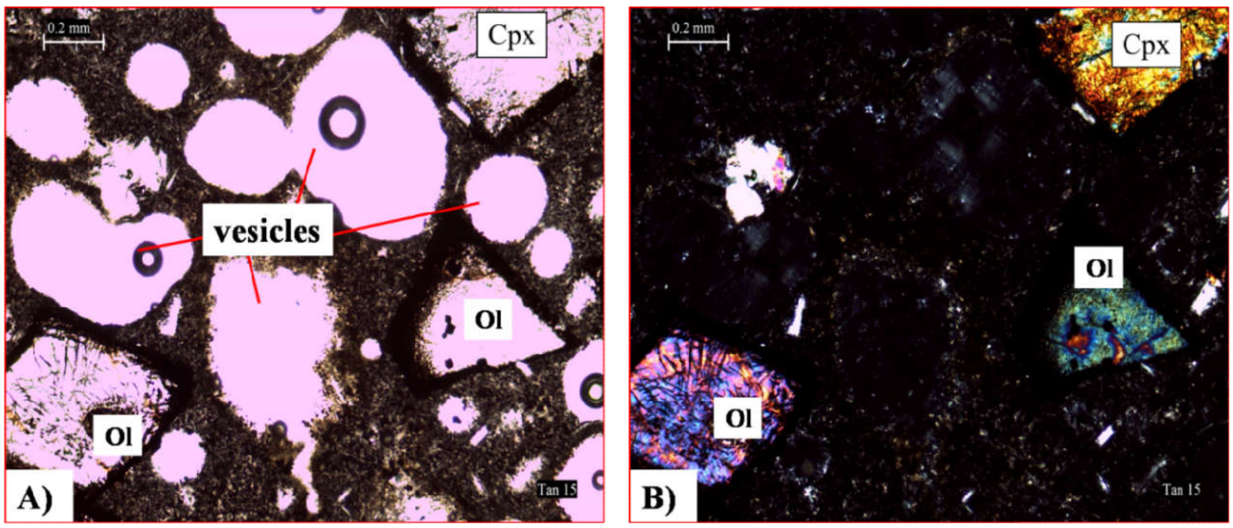

Figure 4.2: Microphotographs of scoria; sample Tan 15 and Tan 21 (A) under plane- polarized microscope in PPL and (B) in XPL view. The labels stand for; Ol-for olivine and Cpx-for clinopyroxene

4.1.3. Oligocene Rhyolite

Five rhyolitic samples have been analyzed petrographically such as samples are Tan 6, Tan 13, Tan 14, Tan 16, and Tan 17. These rhyolitic lavas show hypocrystaline with vitrophyric, porphyritic, perlitic (glassy), and flow banding texture. Phenocrysts are alkali feldspar (sanidine), plagioclase and quartz. The groundmass is mainly volcanic glass. Larger phenocrysts of quartz and sanidine are embedded in a glassy groundmass. Sample Tan 6 shows that flow banding (Fig. 4.3.A) microstructure and felsic texture (Fig. 4.3.B) with phenocrysts of quartz (10%) within the devitrified groundmass (90%). Quartz phenocrysts have 0.34mm maximum size and subhedral partially resorbed shape.

Sample # Tan 13 and Tan 16 have similar petrographic nature. They show porphyritic texture with 20% phenocrysts and 80% groundmass (Fig. 4.3.C&D). Compositionally, 12% sanidine, 3% quartz, 1% plagioclase, 2% opaque and apatite set in a groundmass of microlithic lath sanidine, volcanic glass, quartz and opaque. Once more, sample # Tan 14 and Tan 17 shows similar petrographic characteristics. Fibrous Alkali feldspar and quartz microphenocrysts are radiating within the glassy groundmass. This generally indicates the spherulitic texture (Fig. 4.3.E&F).

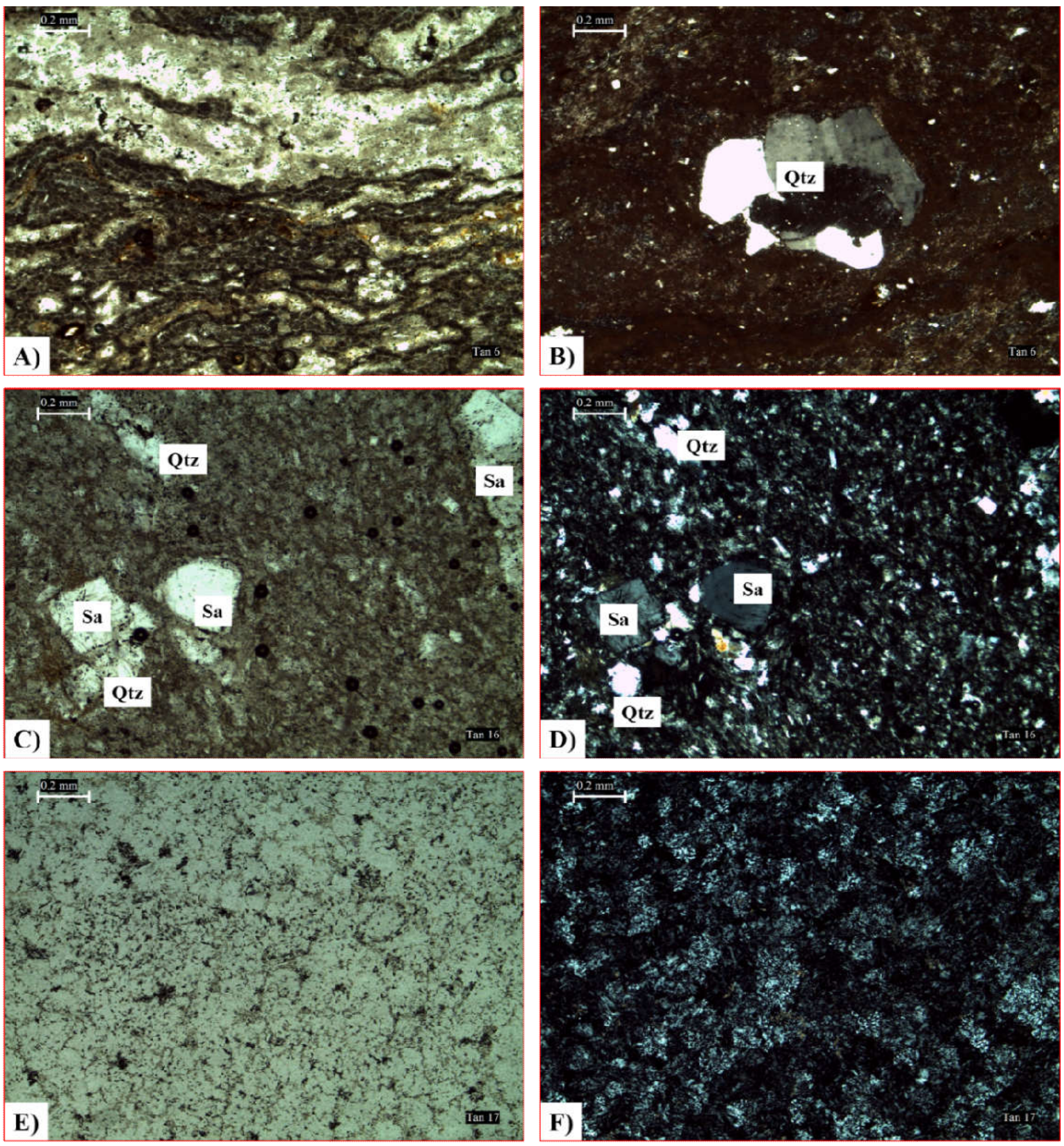

Figure 4.3: Microphotographs of Rhyolite; samples # Tan 6, 13, 14, 16, and 17 (A, C&E) under PPL (B, D&F) under XPL view. The labels stand for; Qtz-for quartz and Sa-for sanidine

4.1.4. Quaternary Trachyte

From trachytic unit, two samples are selected for petrographic analysis. These are Tan 7 from trachytic lava dome and Tan 8 from the trachytic plug. Sample # Tan 7 shows that porphyritic textured with 32% phenocrysts and 61% groundmass. The phenocrysts phase is made of 26% large euhedral and tabular crystals of alkali feldspar (sanidine), 4% plagioclase, 1% opaque minerals and 1% pyroxene. They are set in a finely crystalline groundmass composed of alkali feldspar (sanidine), clinopyroxene, and biotite. The plagioclase in sample # Tan 7 typically shows oscillatory zoning (Fig. 4.4.A). Unlikely, sample # Tan 8 (Fig. 4.4.D) shows that the groundmass without phenocrysts. The groundmass contains volcanic glasses and consists of minute tabular crystals of sanidine microlites. The groundmass of both samples shows that sub-parallel orientation of microlithic sanidine which is typical characteristics of trachytic texture (Fig. 4.4.C&D).

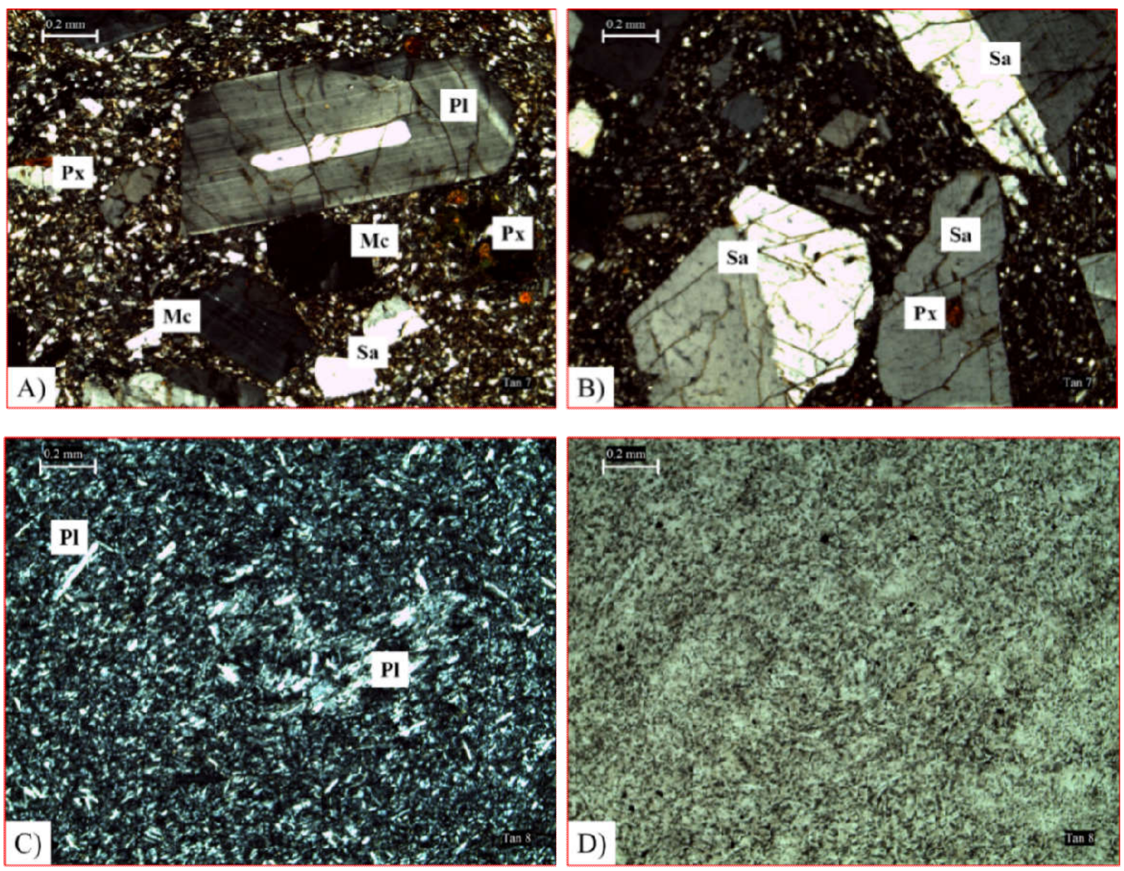

Figure 4.4: Microphotographs of Trachyte; samples # Tan 7 and Tan 8 (A, B & C) under XPL and (D) under PPL view. The labels stand for; Pl-for plagioclase feldspar, Mc-for microcline, Px-for pyroxene and Sa-for sanidine

4.1.5. Oligocene Basalt

From the lower successions of Oligocene basaltic units, four samples are analyzed petrographically. Samples are Tan 4, Tan 9, Tan 18, and Tan 22. From those samples, Tan 18 (Fig. 4.5.D) shows that 85% groundmass of plagioclase, olivine, and opaque minerals with 10% clinopyroxene and 5% plagioclase phenocrysts.

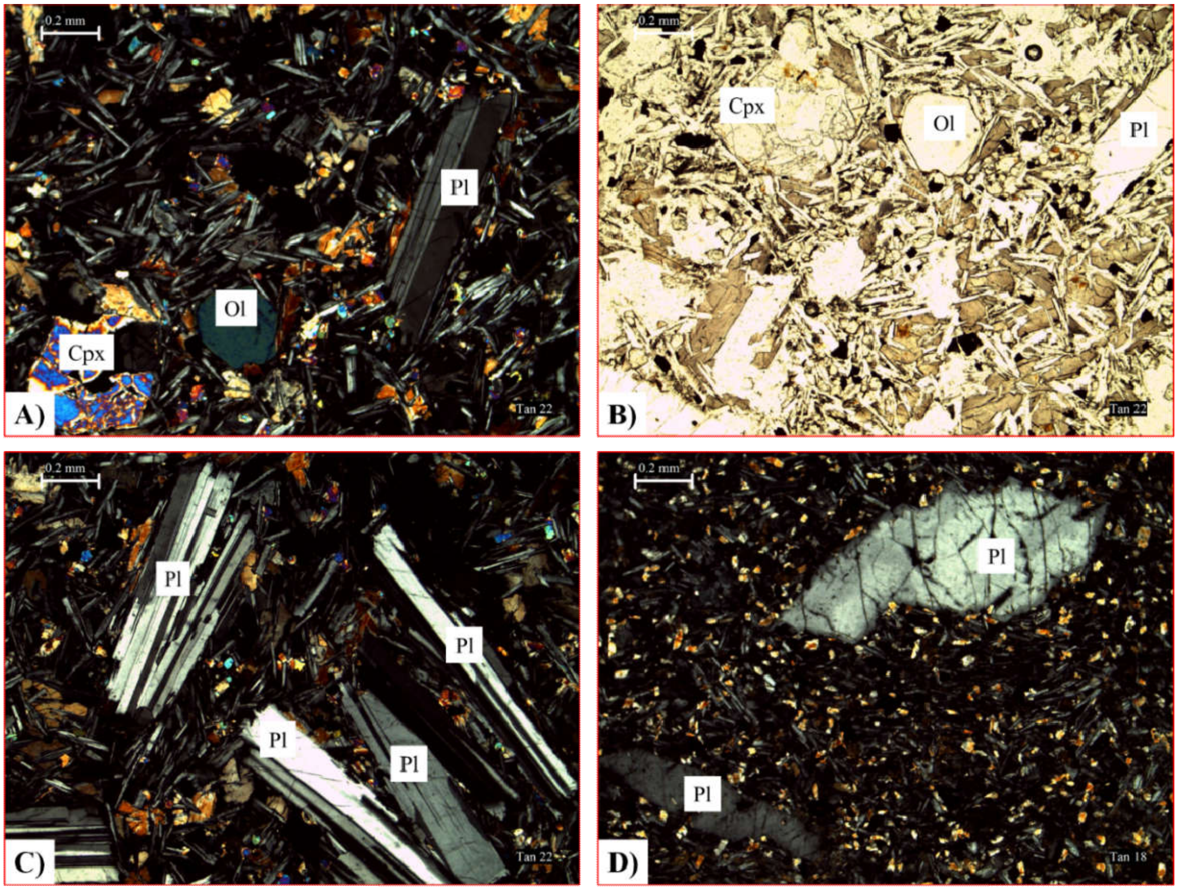

Figure 4.5: Microphotographs of Oligocene basalt; sample Tan 18 and Tan 22 (A, C and D) under XPL and (B) under PPL view. The labels stand for; Pl-for plagioclase feldspar, Ol-for olivine, and Cpx-for clinopyroxene.

Sample # Tan 22 (Fig. 4.5.A-C), shows that porphyritic texture with 70% phenocrysts and 30% groundmass. Phenocrysts are 52% plagioclase, 8% olivine, and 10% clinopyroxene. The groundmass of this sample is an aggregate of microphenocrysts of plagioclase, olivine, and clinopyroxene with some opaque minerals. The trachytic texture is typical of basaltic rocks in the study area, in which plagioclase minerals in the groundmass are arranged in sub-parallel mode.

Dispute other samples # Tan 4 and Tan 9 (Fig. 4.6.A and B) shows that an aphanitic and trachytic texture with and without phenocrysts respectively. Their groundmass is composed of microphenocrysts of plagioclase, pyroxene, olivine and opaque minerals. Sample # Tan 9 shows a single sanidine lath ~1% with 2mm size. Whereas, the sample # Tan 4 shows hematization alterations.

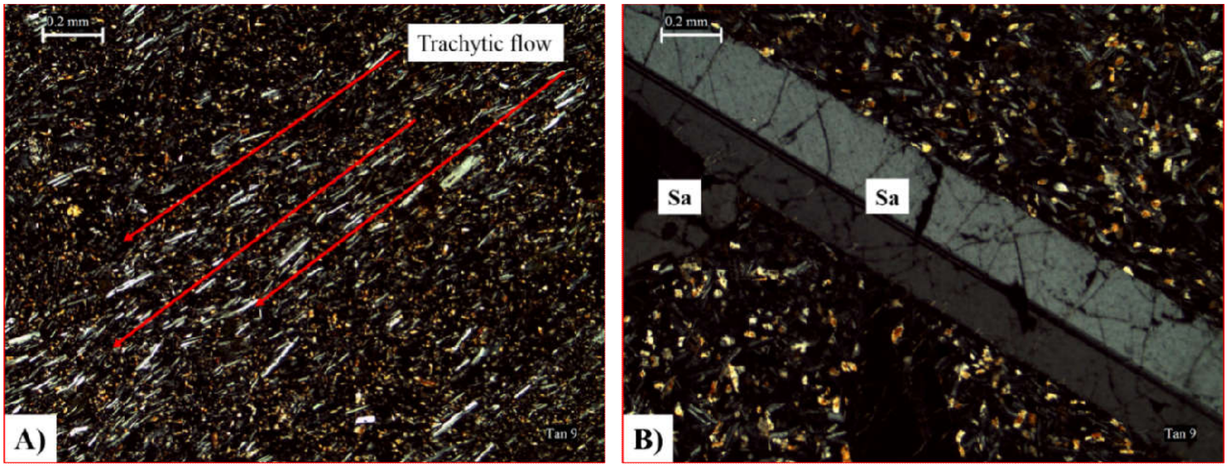

Figure 4.6: Microphotographs of Oligocene basalt; sample Tan 4 and Tan 9 (A&B) under XPL view, Sa-sanidine.

4.1.6. Basanite Intrusion

Basanite intrusion has phenocrysts of olivine, plagioclase, nepheline and clinopyroxene minerals. In addition, the groundmass is identified as microphenocrysts of these minerals. Based on petrographic analysis Tan 2 shows 55% of groundmass and 45% phenocrysts. Mineralogically it is composed of 5% olivine, 11% clinopyroxene, plagioclase 23%, and 7% of nepheline phenocrysts. The sample Tan 2 which shows that highly porphyritic texture with the plagioclases phenocrysts having the maximum size >3mm. Olivine phenocrysts has subhedral to euhedral shape with 0.3-0.5 maximum size and they are highly altered and changed to iddingsites (Fig. 4.7.A). Plagioclase minerals show normal zoning (Fig.4.7.C) that Ca-rich plagioclase as a core and Na rich plagioclase as a rim. Iddingsites and pigeonites minerals are incorporated within plagioclase phenocrysts as inclusion. This shows that the poikilitic texture (Fig. 4.5.A).

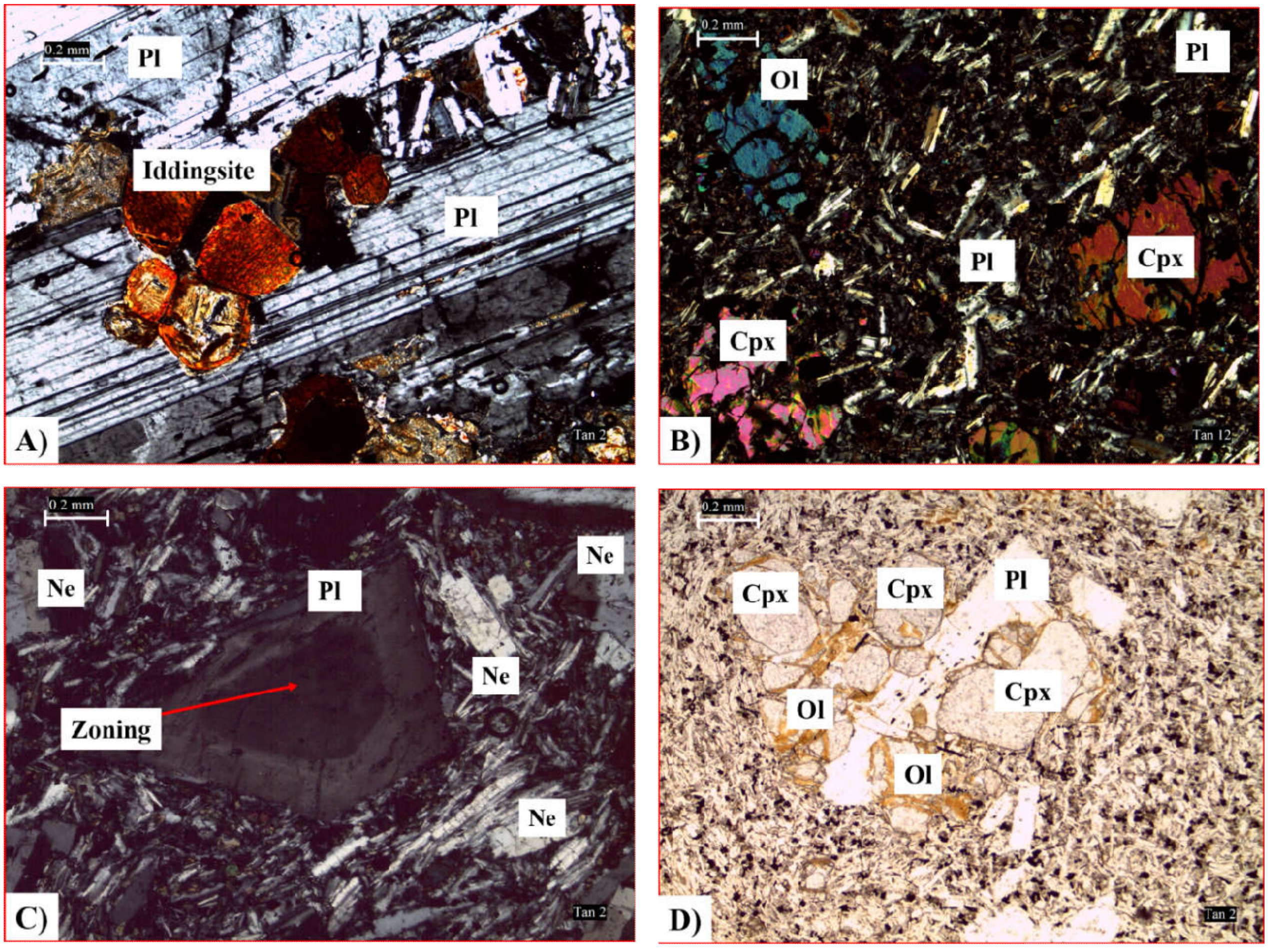

Figure 4.7: Microphotographs of Basanite intrusion; samples # Tan 2 and Tan 12 (A, B&C) under XPL and (D) under PPL view. The labels stand for; Pl-for plagioclase feldspar, Ol-for olivine, Ne-for nepheline and Cpx-for clinopyroxene

Whereas the sample# Tan 12 shows that 75% phenocrysts and 25% groundmass. Olivine 6% and clinopyroxene 14% phenocrysts are highly fractured. Their maximum size ranges 1-1.2mm with anhedral to subhedral shape. Almost 20% plagioclase and 50% opaque minerals (Fe, Ti oxides) phenocrysts have been identified. These phenocrysts are surrounded by microphenocrysts of plagioclases by having trachytic (flow) texture (Fig. 4.7.B). The opaque minerals in sample Tan 12, which are integrated within the olivine minerals, are chromite. Although in the sample # Tan 2 ilmenite has found as an opaque. In general, these, samples of basanites are shown glomeroporphyritic textures.

Chapter Five

5. Whole Rock Geochemistry

5.1. Introduction

Geochemistry is one of the best tools to understand chemical changes on the Earth in terms of analyzing absolute and relative abundances of chemical elements. Basically, chemical elements are found in rocks, minerals, soils, water, and atmosphere of the earth. The abundance of these elements is determined on the basis of their distribution along with the movement of these elements in various environments of the earth. Geochemical studies of ancient rocks, fluids and gases provide insights into the evolution of Earth's crust, oceans, primordial atmosphere, etc. (e.g. Cox, 1979; Rolinson, 1993; White, 2013).

The major elements include SiO_2, Al_2O_3, Fe_2O_3, CaO, MgO, Na_2O, K_2O, TiO_2, and P_2O_5 whose oxides constitute more than 1% by weight. Becausetheir concentration is expressed in wt. % in oxide form and the total should sum to100% ideally. However, acceptable totals lie in the range 98.5 to 101wt. %. Those major elements are used in this study basically to understand magmatic process under which the given rock is formed and to which magma source it belongs. Most of the information's are gained from the chemical (mineralogical) composition of the source rocks. Therefore, the source and process of magma evolution have been analyzed by examining the concentration of major elements initially. The analysis and interpretation will be further implemented by trace element data for confirmation. Moreover the petrographic analysis of the samples, CIPW normative mineral calculation gives information about the type of the rock.

It is well known that the concentration of trace elements will vary with the rock type. Variations of trace elements provide additional information about the sources and major processes that controlled the formation of the volcanic products. The relative abundances of trace elements are used to identify the minerals that were present during melting or fractional crystallization. Trace elements most commonly used for the interpretation of the petrogenesis of igneous rocks include: Ni, Cr, Sc, V, Rb, Ba, Sr, Zr, Y, Nb and the rare earth elements (La to Lu).Rare earth elements (REEs) are very useful to deal about igneous petrogenesis in detail because they have similarity in their geochemistry as a group.

Table 5.1: Whole-rock geochemical data for volcanic rocks around Lake Tana

Sample Code	**Tan-2**	**Tan-5**	**Tan-6**	**Tan-7**	**Tan-8**	**Tan-9**	**Tan-10**	**Tan-11**	**Tan-12**	**Tan-13**
Rock Type	**Basanite**	**Basalt**	**Rhyolite**	**Trachyte**	**Trachyte**	**Basalt**	**Basalt**	**Basalt**	**Basanite**	**Rhyolite**
Easting(m)	**287132**	**301944**	**286969**	**280421**	**365347**	**336934**	**319507**	**309468**	**336043**	**313621**
Northing(m)	**1299261**	**1367487**	**1306938**	**1317281**	**1342992**	**1296589**	**1292595**	**1314738**	**1315261**	**1279656**
Wt%										
SiO_2	48.3	45.1	76.7	69.3	65.5	45.5	48.6	47.5	43	74.5
TiO_2	1.85	2.78	0.05	0.36	0.37	3.74	1.76	1.61	3.42	0.19
Al_2O_3	17.15	15	12.45	13.9	17	14.65	16.85	16.4	15	13.2
Fe_2O_3	11.45	10.75	1.23	5.43	3.39	15.95	11.15	12.05	15.05	2.04
FeOt	10.31	9.68	1.11	4.89	3.05	14.36	10.04	10.85	13.55	1.84
MnO	0.17	0.17	0.03	0.12	0.36	0.2	0.17	0.18	0.19	0.01
MgO	6.93	10.1	0.05	0.02	0.27	5.23	6.04	7.23	8.45	0.05
CaO	9.89	10.05	0.25	0.29	0.52	8.8	10.25	9.72	9.31	0.4
Na_2O	3.7	2.54	3.68	6.34	6.86	2.94	3.52	2.79	3.12	4.15
K_2O	1.13	1.73	3.98	4.17	5.63	0.8	1.14	0.9	1.19	3.82
P_2O_5	0.45	0.77	0.05	0.04	0.09	0.36	0.3	0.3	0.54	0.03
LOI	-0.25	2.23	2.28	0.97	0.97	2.11	-0.4	1.17	2.17	1.66
Total	**100.77**	**101.22**	**100.75**	**100.94**	**100.96**	**100.28**	**99.38**	**99.85**	**101.44**	**100.05**
#Mg	40.21	51.07	4.32	0.41	8.13	26.70	37.57	40.00	38.42	2.65
ppm										
V	187	194	<5	<5	<5	329	212	202	267	8
Cr	140	400	10	<10	10	60	150	230	50	10
Ni	107	175	5	6	19	73	48	93	129	6
Cs	0.12	0.31	2.2	0.08	0.73	0.05	0.1	0.04	0.11	0.44
Rb	19.9	34.6	205	74.6	154.5	11.9	19.8	12.9	21.8	75.6
Ba	324	499	23.1	420	58.4	185	328	331	244	794
Sr	528	823	11.2	15.3	8.7	406	474	350	560	40.9
Th	2.55	4.28	40	6.39	28.9	1.98	1.94	1.84	1.83	9.16

U	0.49	1.11	10.05	1.58	5.54	0.59	0.61	0.42	0.6	2.87
Nb	39.2	63.3	153	81.6	292	19.7	24.9	22.7	25	28.7
Ta	2.3	3.5	14.7	5	18	1.2	1.6	1.2	1.5	2.1
Zr	129	188	157	802	1250	225	110	99	207	458
Hf	3.2	4.4	7.2	20.2	26.4	5.7	3.1	2.8	5.5	14
Y	21.8	22.2	39.1	41.5	39	35.9	21.3	21.8	26.5	67
La	23.6	39.6	18.9	53.5	141	20.8	17	17.5	21	44.8
Ce	45.6	76.3	39.8	116	243	49.6	34.2	32.7	46	115
Pr	5.43	8.69	4.65	14.05	26.5	6.88	4.17	4.25	6.36	13.15
Nd	21.3	33.8	14.6	55.3	79.4	29.9	16.9	16	28	51.1
Sm	4.64	6.72	4.12	12.4	12.2	7.26	3.81	3.89	6.69	11.9
Eu	1.61	2.2	0.06	2.25	2.44	2.57	1.35	1.33	2.61	2.55
Gd	4.73	6.19	4.22	11.7	8.39	8.62	4.38	4.16	7.14	12.25
Tb	0.7	0.79	0.75	1.87	1.24	1.23	0.63	0.69	1.08	1.99
Dy	4.2	4.58	5.58	11.05	7.33	6.95	3.74	4.18	5.95	11.75
Ho	0.87	0.92	1.31	1.98	1.63	1.39	0.87	0.86	1.12	2.59
Er	2.49	2.27	4.44	5.74	4.23	3.75	2.35	2.43	2.24	7.78
Yb	1.83	1.89	5.32	5.62	5.15	3.17	2.17	2.04	2.07	7.57
Lu	0.26	0.27	0.82	0.82	0.79	0.43	0.29	0.31	0.29	1.15
Eu/Eu*	1.05	1.04	0.04	0.57	0.74	0.99	1.01	1.01	1.15	0.65

Sample Code	Tan-14	Tan-15	Tan-16	Tan-17	Tan-18	Tan-19	Tan-20	Tan-21	Tan-22	Tan-24
Rock Type	**Rhyolite**	**Scoria**	**Rhyolite**	**Rhyolite**	**Basalt**	**Basalt**	**Basalt**	**Scoria**	**Basalt**	**Rhyolite**
Easting(m)	**308661**	**296991**	**274177**	**280453**	**276616**	**309004**	**311612**	**312272**	**346669**	**287161**
Northing(m)	**1283968**	**1295260**	**1279625**	**1301037**	**1269119**	**1266304**	**1290728**	**1284778**	**1306568**	**1299261**
Wt%										
SiO_2	74.2	47.1	73.6	73.3	51.5	48.2	47.6	42.7	45.2	56
TiO_2	0.25	1.82	0.07	0.25	1.84	1.44	1.81	2.03	2.8	1.18
Al_2O_3	12.85	16.05	13.85	11.7	15.65	16.55	17	14.9	14.85	13.35
Fe_2O_3	2.32	11.75	1.55	3.2	10.9	11.55	11.25	14.55	14.4	7.1
FeOt	2.09	10.58	1.40	2.88	9.81	10.40	10.13	13.10	12.96	6.39
MnO	0.01	0.18	0.02	0.03	0.16	0.18	0.17	0.2	0.18	0.13
MgO	0.02	7.37	0.07	0.06	5.09	7.13	6.61	8.51	6.32	1.33
CaO	0.36	10.7	0.23	0.17	7.76	10.85	9.85	11.35	8.67	3.51
Na_2O	4.61	3.38	4.28	4.08	3.07	3.22	3.62	2.72	2.66	1.76
K_2O	3.31	1.12	4.53	4.13	1.44	0.75	1.11	0.98	0.79	1.29
P_2O_5	0.05	0.4	0.02	0.02	0.43	0.29	0.44	0.35	0.34	0.22
LOI	1.49	0.34	1.7	1.99	1.66	-0.2	0.05	0.15	1.72	12.35
Total	**99.47**	**100.21**	**99.92**	**98.93**	**99.5**	**99.96**	**99.51**	**98.44**	**97.93**	**98.22**
#Mg	0.95	41.07	4.78	2.04	34.16	40.68	39.50	39.39	32.78	17.23
ppm										
V	<5	195	<5	<5	221	205	187	435	301	24
Cr	<10	220	10	10	30	220	130	190	70	<10
Ni	<5	91	5	8	44	71	98	114	122	<5
Cs	0.72	0.2	1.65	0.05	0.23	0.1	0.2	0.19	0.03	0.67
Rb	63.2	21.4	288	73.8	25.9	13.6	19.1	26.6	12.7	35.7
Ba	689	318	18.4	457	392	252	306	375	250	505
Sr	41.6	477	7.8	11.4	444	432	527	594	454	524
Th	7.66	2.85	43	7.87	2.86	1.5	2.5	3.69	1.95	5.1

U	2.48	0.68	9.21	2.13	1.11	0.32	0.65	0.86	0.61	1.79
Nb	27.2	37.8	144.5	53.4	13.2	22.6	39	42.7	19	28.6
Ta	1.7	1.9	17.5	3.2	0.8	2	2	2.3	1.1	1.8
Zr	627	107	228	791	197	84	127	97	201	394
Hf	16.8	2.9	8.8	19.1	4.8	2.2	3.2	2.7	5.3	10.8
Y	82.7	22.6	22.1	95	31.3	20.7	21.8	20.9	31	56.9
La	48.6	23.6	26.3	28.1	22.2	15.8	23.2	27.4	21.4	38.4
Ce	95.7	43.6	45.2	30.4	48.1	31.1	44.2	50.1	48.7	79
Pr	13.75	5.27	5.47	8.62	6.34	3.77	5.29	5.64	6.61	11.6
Nd	56.6	20	16.5	32.5	27	16	21.1	21.4	28	47.2
Sm	13.5	4.41	3.21	9.38	6.18	3.81	4.53	4.39	6.61	11.95
Eu	2.42	1.46	0.11	1.77	2.03	1.37	1.53	1.52	2.32	3.37
Gd	14.25	4.79	2.89	12.45	6.35	4.07	4.48	4.57	6.87	12.3
Tb	2.46	0.71	0.51	2.4	0.97	0.56	0.71	0.71	1.04	1.83
Dy	14.4	4.22	3.37	15.8	5.67	3.85	4.11	3.77	6.22	10.75
Ho	3.18	0.86	0.79	3.49	1.25	0.85	0.87	0.83	1.22	2.19
Er	9.05	2.38	2.65	10.45	3.39	2.4	2.05	2.39	3.29	5.89
Yb	8.56	2.02	3.21	9.88	3.01	1.93	2.07	1.84	2.53	5.09
Lu	1.24	0.3	0.47	1.53	0.42	0.26	0.29	0.3	0.35	0.69
Eu/Eu*	0.53	0.97	0.11	0.50	0.99	1.06	1.04	1.04	1.05	0.85

#Mg=MgO/ (MgO+FeOt) x100% (Cox, 1979)

FeOt=Fe_2O_3** 0.9 +* Fe_2O_3 *(Rollinson, 1993)*

Eu/Eu=Eu/EuN/√SmN*xGdN (Rollinson, 1993)*

5.2. Major Element Geochemistry

In general, the Tana Volcanic rocks shows SiO_2 contents that range from 42.7%-74.6%. Loss on ignition varies between 0-2.3 wt. % which is low; implies that most of the samples are not altered. From the total of twenty samples, only one sample has a larger LOI value of 12.35 wt. %. This sample is obtained from moderately welded ignimbrite outcrop. As a result, the larger LOI could be from the conditions of alteration and weathering (Peccerillo, 2003). The normative mineral olivine value for basaltic rocks ranges from 6.05-15.13 wt. %. Also, for felsic normative mineral quartz reaches up to 39.33wt. %.

In addition, normative minerals olivine >10wt. % (11.5 and 15.13wt. %) and nepheline has a maximum value of 6.93 wt. % for the basanite. Alkaline rocks are essentially ultrabasic to intermediate in terms of SiO_2 content, and range from transitional (olivine and hypersthene-normative) to mildly alkaline (relatively low normative nepheline contents). As showed below TAS diagram which is useful for the classification of volcanic rocks and also useful for distinguishing between two types of parental magmas (or of magmatic rock series or trends): alkalic and tholeiitic.

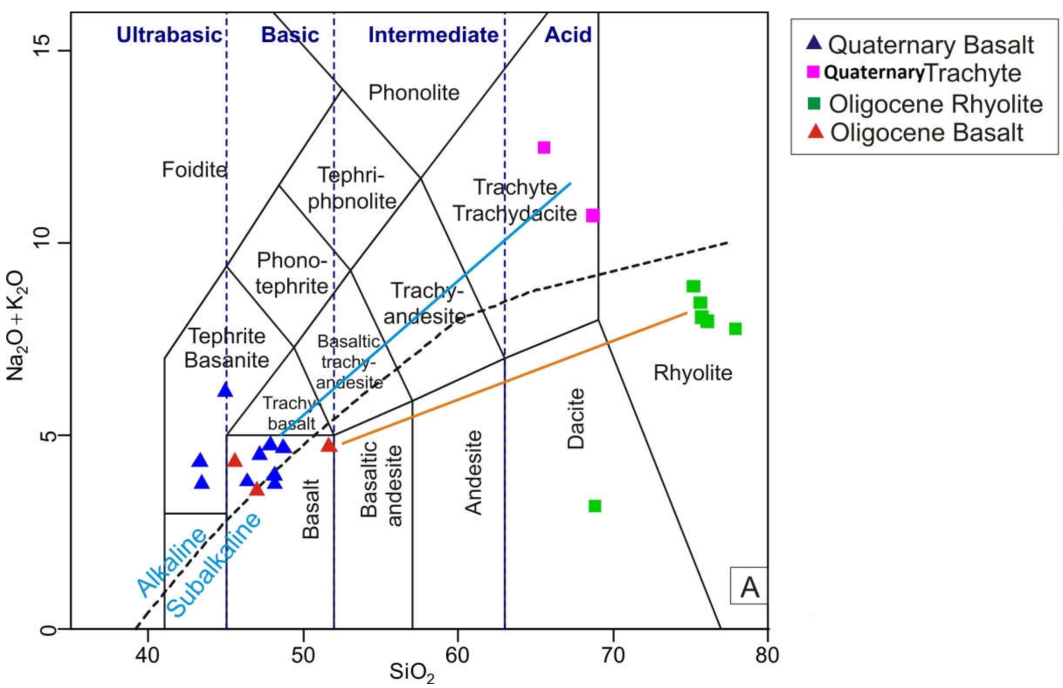

Figure 5.1: Classification of rocks from Tana volcanic rocks based on the total alkalis versus silica (TAS) diagram after Le Bas et al., 1986. The orange and light blue line implies the magma series in the Lake Tana area.

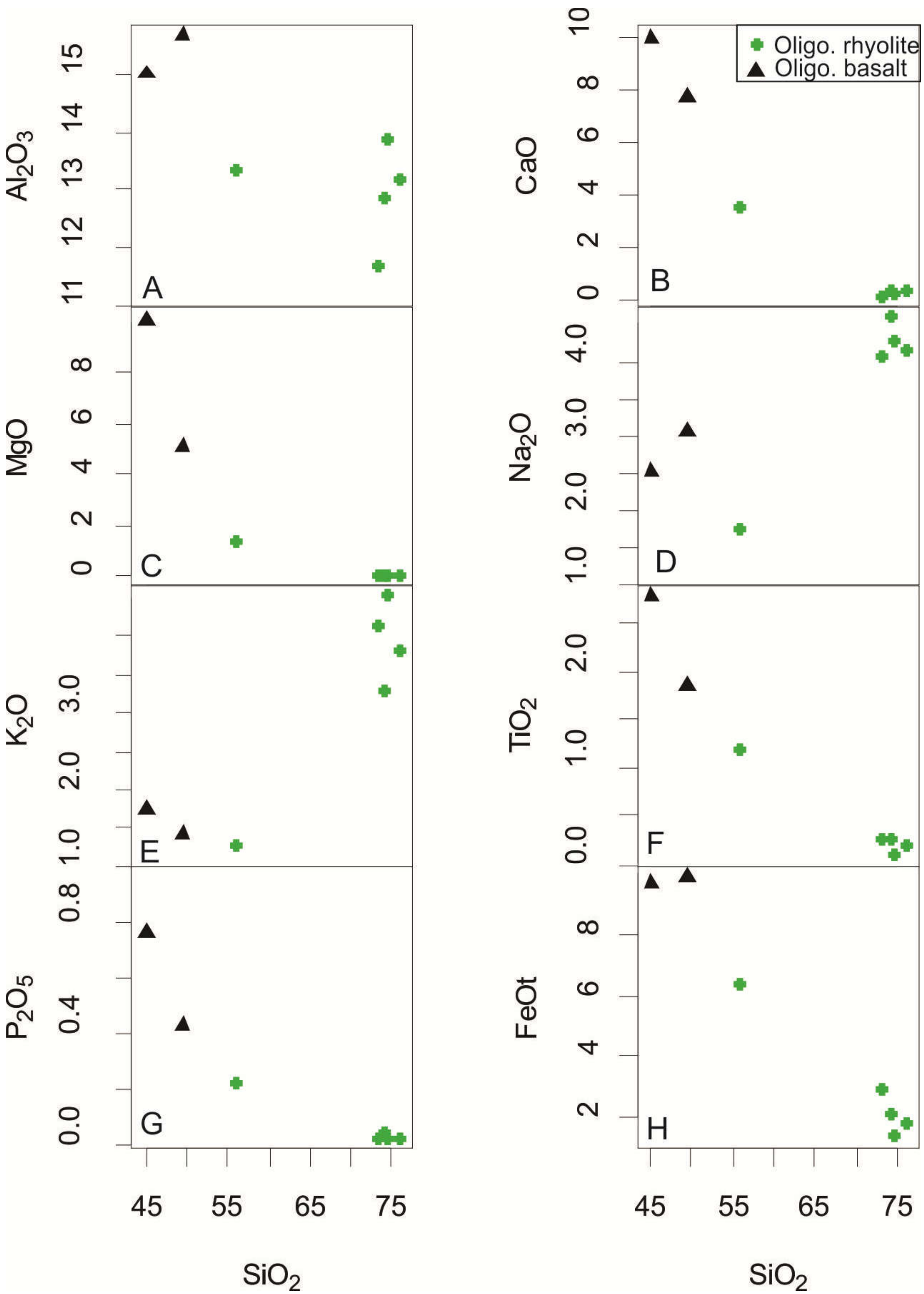

Figure 5.2: Harker variation diagram for major oxides against silica for Oligocene rocks

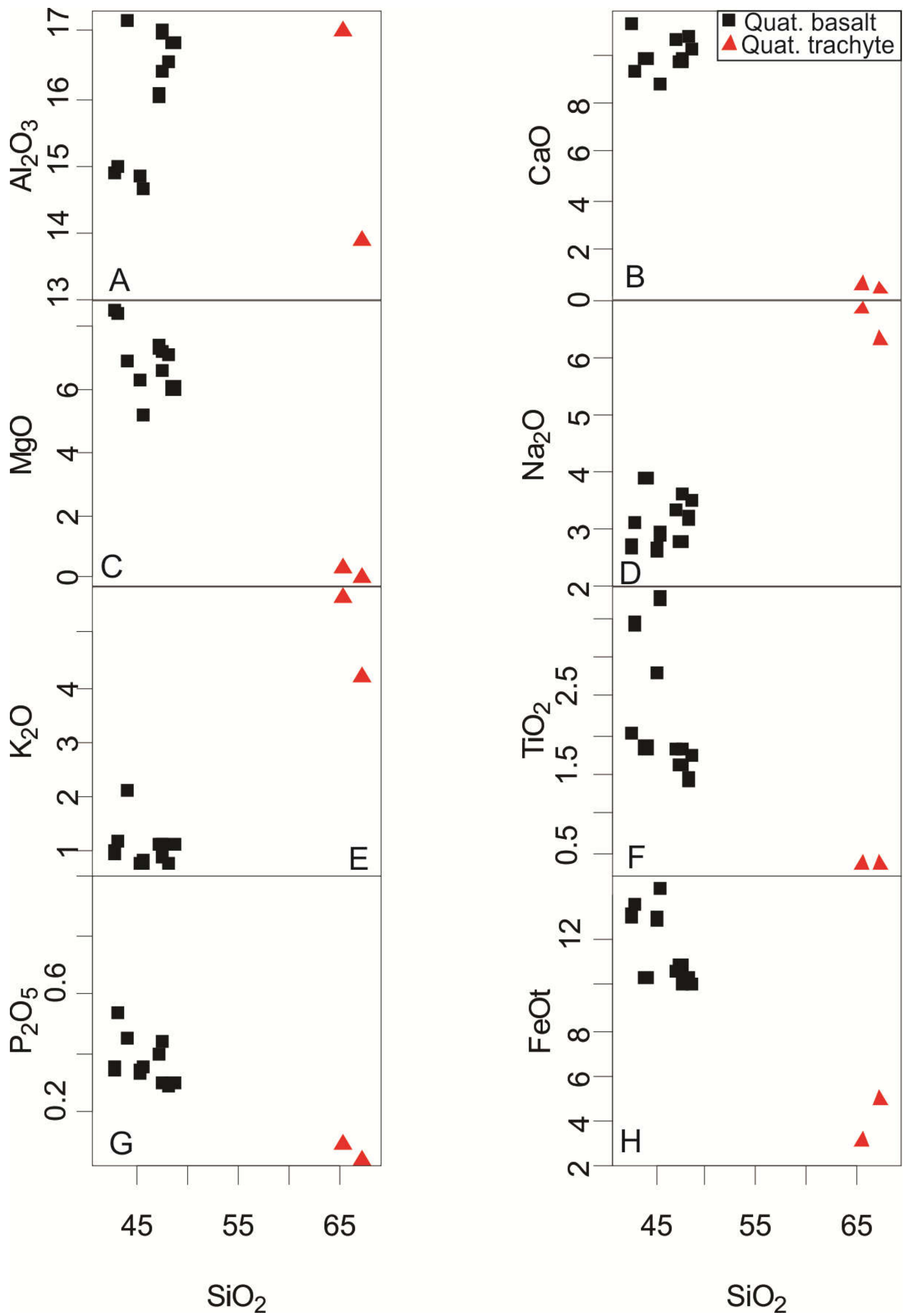

Figure 5.3: Harker variation diagram for major oxides against silica for Quaternary rocks

Based on the total silica-alkali (TAS) classification (Fig. 4.1) the twenty samples of Tana area volcanic rocks classified in to trachyte, rhyolite, dacite, basalt, and basanite groups (Le Bas et al., 1986). From the twelve mafic samples, only three of them fall on the basanite group. The rest samples are fall on the basaltic group. Whereas, from the eight felsic samples only one sample fall on the dacite group and two of them fall on the trachyte-trachydacite range but the rest of the samples are rhyolitic in composition.

From TAS diagram mainly mafic rocks fall on transitional to alkaline basalt and felsic samples fall beneath the sub-alkaline boundary with higher silica values. The slightly curved broken line on TAS diagram separates alkaline and tholeiitic basalts (Irvine and Baragar, 1971).Their distribution from the TAS classification diagram shows that the widespread occurrence of basalt and rhyolite without significant intermediate rocks. The TAS diagram shows the absence of rocks with silica range between 49.5-65.5 wt. %. Two magmatic rock series or trends are visible from the TAS diagram. Due to huge age gap between Oligocene and Quaternary the alkaline Tana basalts are not genetically related to Oligocene rhyolites.

The mafic samples are characterized by low SiO_2 (42.7-49.5 wt. %), high Al_2O_3 (14.65-17.15 wt. %), and high FeO (9.7-14.4 wt. %) with MgO (5.09-10.1 wt. %). They have variable amount of alkaline contents Na_2O and K_2O total (3.34-6.03 wt. %). The felsic samples have high silica (56-76.7 wt. %), and Na_2O and K_2O (3.05-12.49 wt. %) and lower MgO (0.02-1.33 wt. %) and Al_2O_3 (11.7-17 wt. %) which is common. The Harker variation diagram of the major oxides against silica plot (Fig. 5.2 and 5.3) for the Tana area volcanic rocks shows a negative correlation on Al_2O_3, FeOt, CaO, MgO, $TiO_{2,}$ and $P_2O_{5.}$ But Na_2O and K2O shows positive correlations indicating fractionation as probably the major process in the formation of these volcanic rocks.

5.3. Trace Element Geochemistry

Trace elements are those which occur in very low concentrations in common rocks (usually < 0.1 % by weight). Their concentrations are therefore commonly expressed in parts per million (ppm; 1 ppm = 10^{-4} wt. %) (Rollinson1993). Unlike major elements, trace elements tend to concentrate in fewer minerals, and are therefore more useful in formulating models for magmatic differentiation, and in some cases, in predicting the source of a particular magma (Winter, 2001).Compatible elements, such as Ni and Cr, have low concentrations (Ni <129 ppm, Cr <400 ppm).The variation plots for trace element against silica is presented in Fig 5.4. The compatible trace elements mainly Ni and Cr show a negative correlation against silica. These elements show a general negative trending with a concentration below the detection limit for some silicic rock samples (Table 5.1). Although, high field strength (HFSE) incompatible elements (Nb, Hf, Th, Y, and Zr) and LILE mobile element (Rb) against SiO_2 shows positive correlations. Also, the rhyolitic samples have a higher concentration of these elements. The trend of Ba and Sr shows a difference relative to the above incompatible trace elements. Ba against SiO_2 variation plot shows more a gentler slope but Sr show negative correlation that reaches very low values only on the rhyolitic rock. The Ba versus SiO_2 plot shows a steep variation trend within the mafic and silicic rocks.

On account of the ionic size of Zr, it does not enter into the major crystalline phase. Because of this, Zr prefers the liquid phase so it‘s very important to study behavior of elements in magmatic evolution by taking Zr as an index. The incompatible trace element (Ta, Y, Nb and Rb) against Zr show a positive correlation (see Fig. 5.5). This trend shows the genetic relationship or co-magmatic nature of the same age Oligocene mafic and silicic rocks.

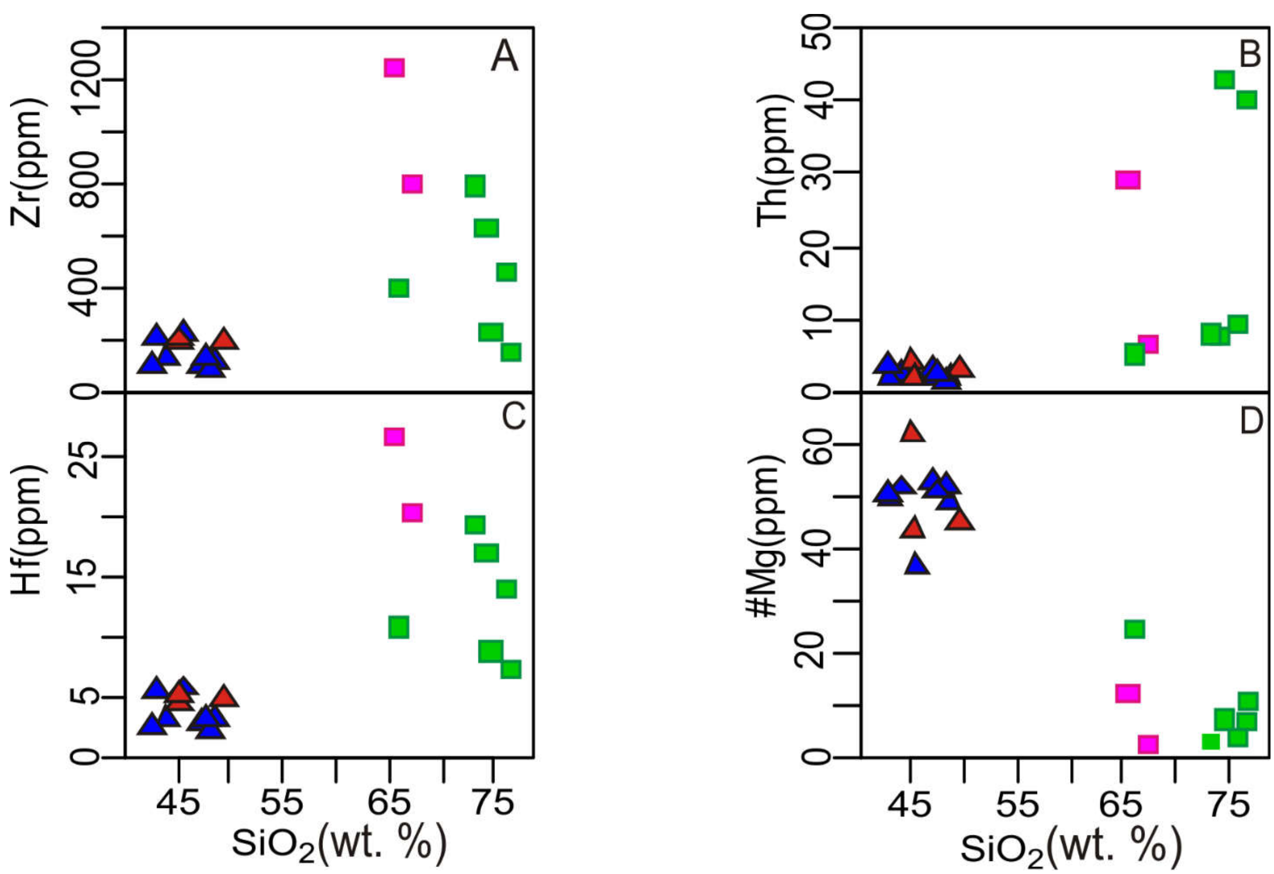

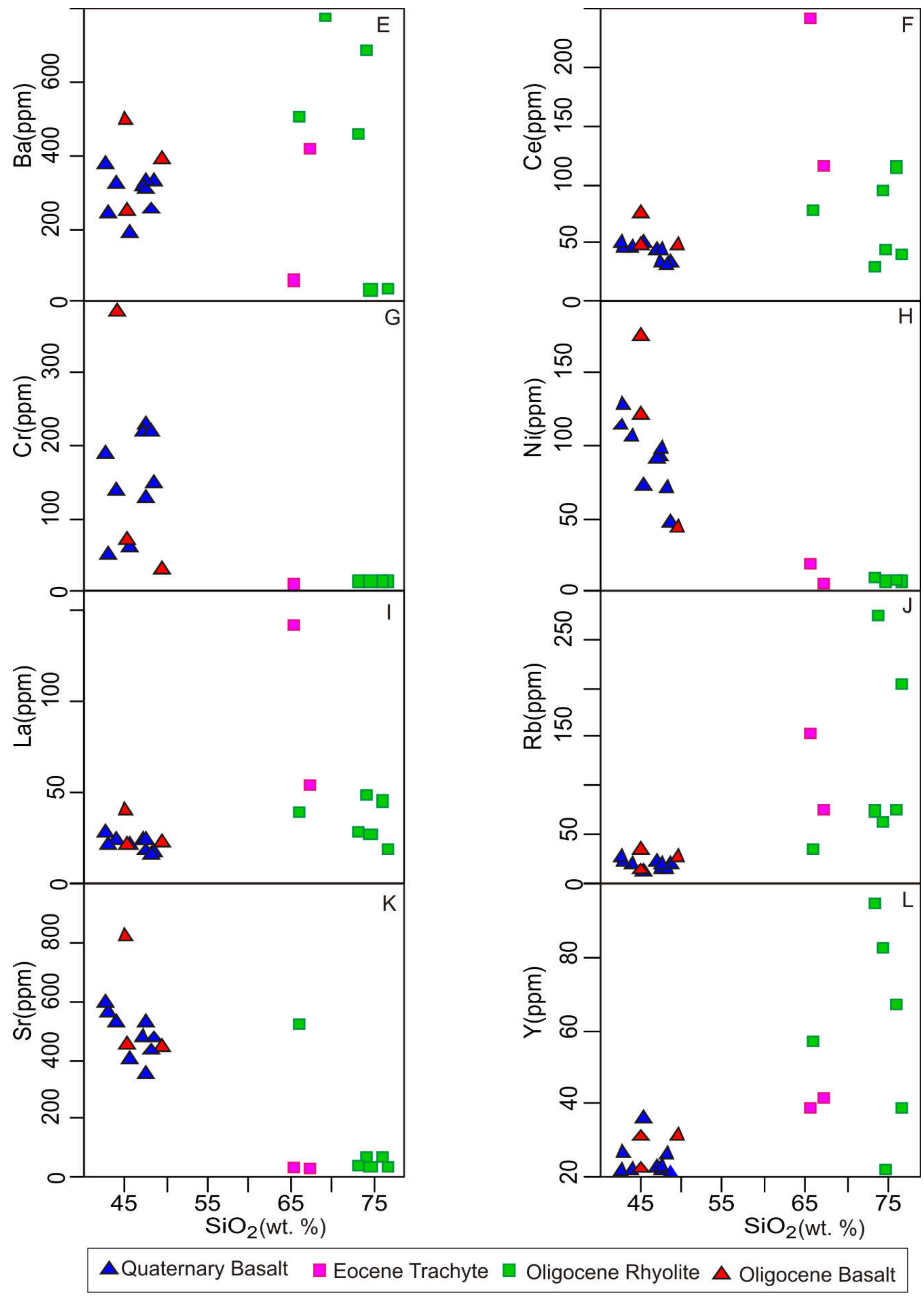

Figure 5.4: Harker variation diagram for trace elements against silica

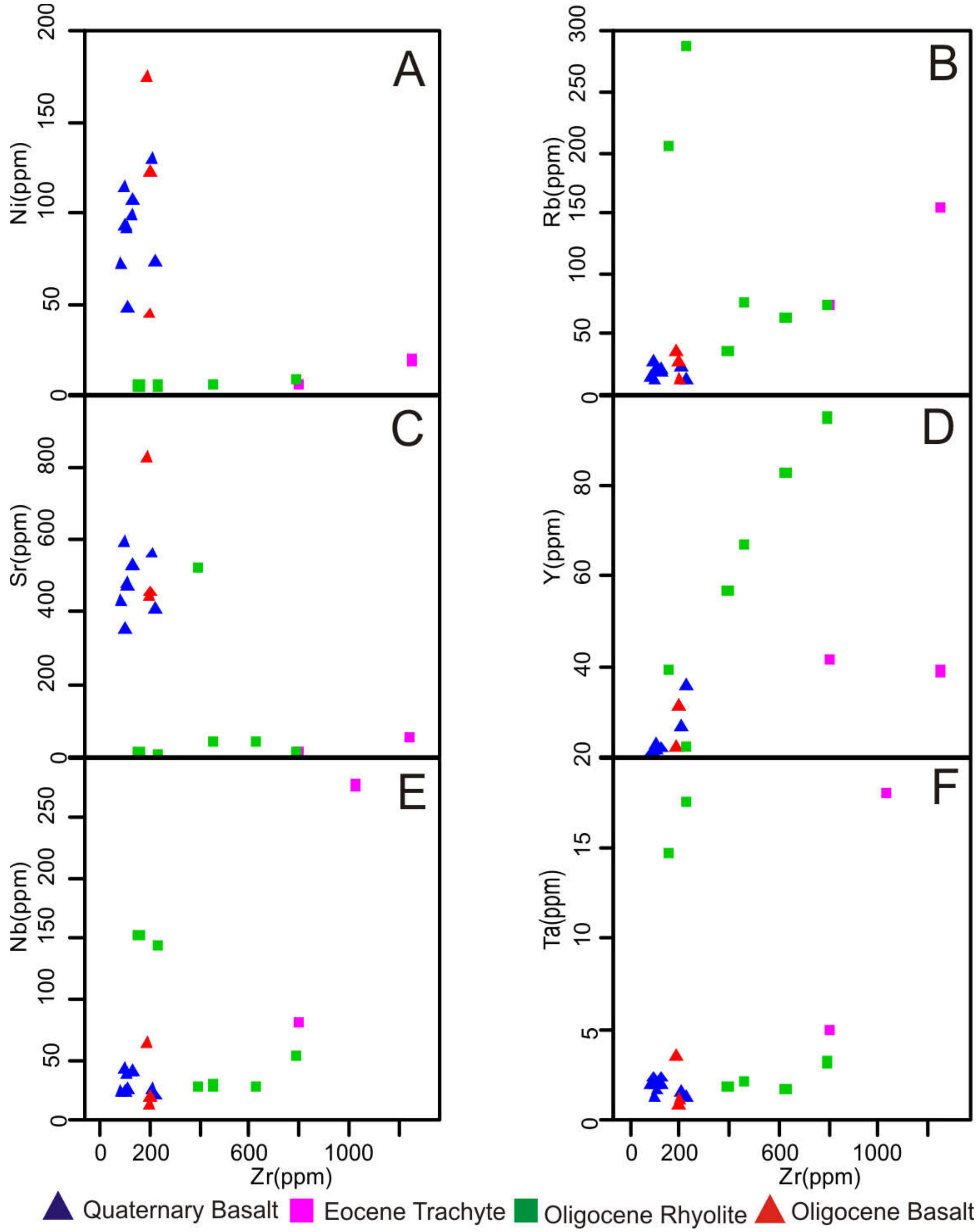

Figure 5.5: Some of selected trace element variation against Zr diagram

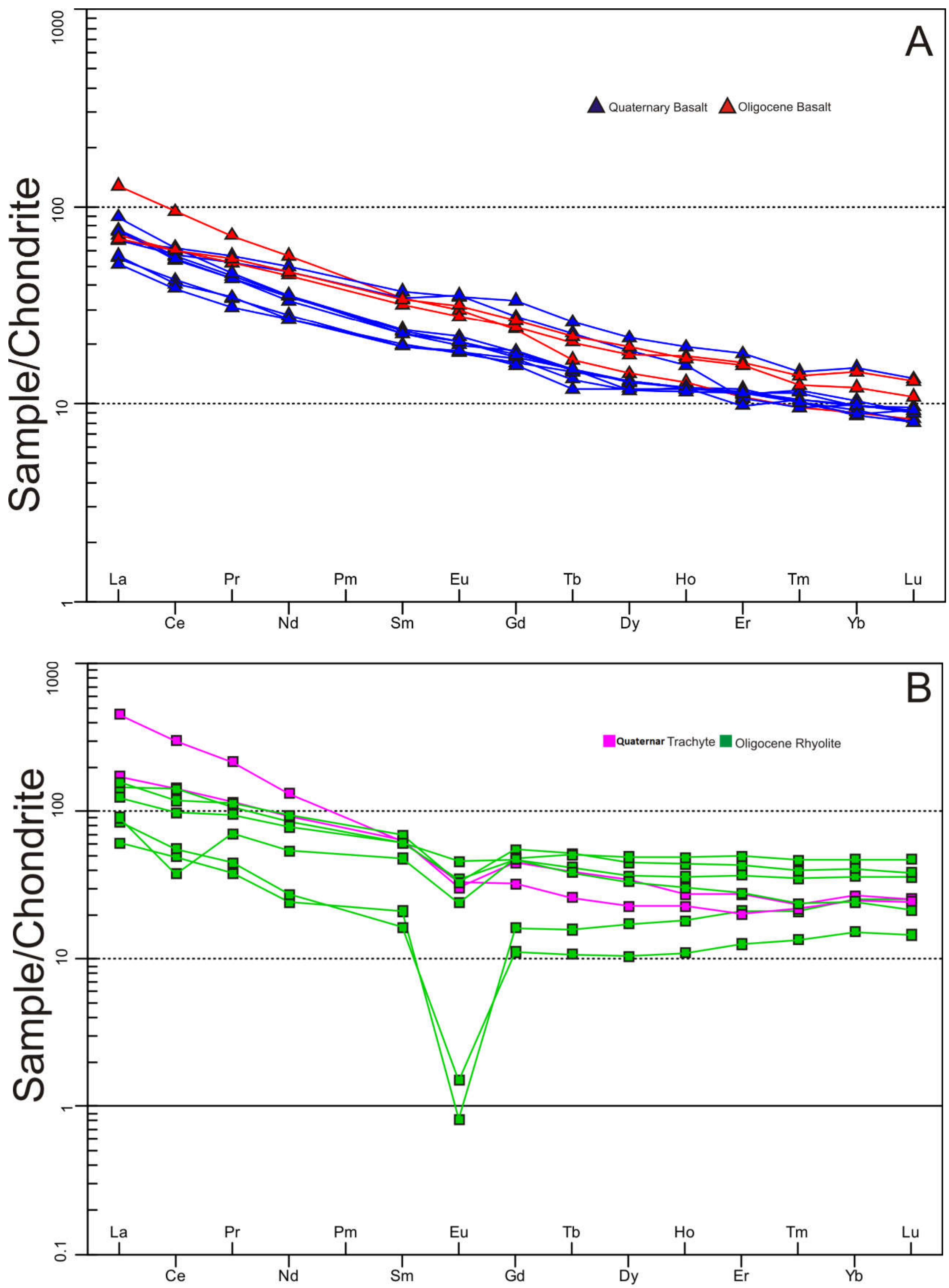

Figure 5.6: REE spider diagram of mafic (A) and felsic (B) rocks from the Tana area. The concentration value of the rock sample is normalized to chondrite value determined by Boynton (1984).

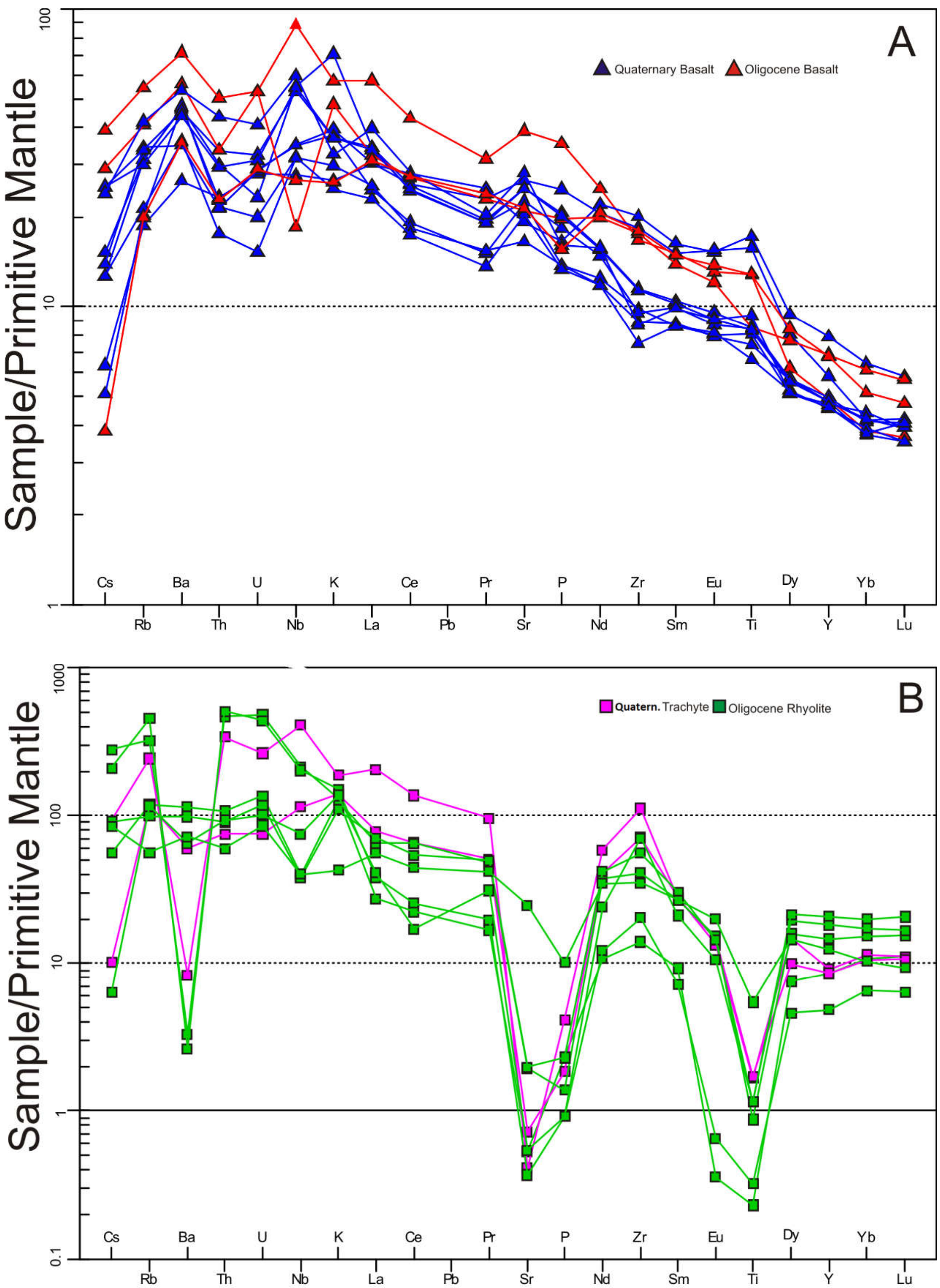

Figure 5.7: Multi-element variation diagram of mafic (A) and felsic (B) rocks from Lake Tana area. The samples are normalized to primitive mantle value determined by Sun and McDonough (1995)

Both Spider diagram and multi-element variation diagram of mafic and silicic rocks are plotted (Fig.5.6 and 5.7 respectively). All the samples show a parallel to sub parallel patterns. The chondrite normalized REEs diagram (Fig.5.6.A and B) for the mafic rocks are enriched in LREEs elements with $(La/Yb)_N$ (the subscript N indicate the normalized value hearafter) in the range of (4.7-15) andnearly flat HREEswith a positive Eu*anomaly ranges in (1.0-1.2). The consequent enrichment in LREEs with respect to MREEs and HREEs of the Lake Tana area volcanic rocks results in slightly upward concave patterns in the REE diagrams. The gentle slope in HREE show the source for mafic rock is garnet free. The chondrite normalized diagram for the mafic samples shows nearly alike pattern with OIB basalt. Felsic samples from Tana area shows that LREEs enrichment is relatively higher than the HREEs with $(La/Yb)_N$ in the range of (2.0-19.6) and significant negative Eu* anomaly (0.1-0.8). While the overall pattern of the chondrite normalized REEs diagram show parallel for almost all samples. REE scattering have smoother slope pattern which tend to flatten toward HREEs. But, two felsic (rhyolitic) samples show slight pulling out from the general pattern of the sample by showing strong negative Eu anomaly spikes.

To further understand and clarify the magmatic evolution of Lake Tana area volcanic rocks the multi-element variation diagram is plotted (Fig 5.7.A and B). Because, estimated primitive mantle concentration values are all about three times the chondritic concentrations. Thus, the samples are normalized to primitive mantle concentration values determined by Sun and Mcdonugh (1995). Commonly, in the dataset for almost all analyzed rocks show a positive Ba anomaly. The multi elements variation diagram for the mafic rocks show parallel patterns with enriched LRREs with strong enrichment in Ba and Nb. Some mafic rocks show Th–U troughs and positive spikes at Ba, Nb, and Ta with respect to neighboring trace elements. The Tana area rhyolites as compared to the primitive mantle (Fig.5.7) they are variably enriched in the incompatible trace elements (LREE) such as Rb, Th and Zr. Also, they present marked troughs at Ba, Sr, P, and Ti; little troughs in HFSEs, especially in Nb and Ta.

Chapter Six

6. Petrogenesis of Tana Volcanic Rocks

6.1. Lithology and Petrography

Petrographically, most basaltic rocks show different textures from the upper and lower sections within the same lava flow. Basalts from the upper part exhibit fine grained groundmass and the phenocrysts either consist of plagioclase or assemblages of plagioclase, clinopyroxene and olivine. They are often glomeroporphyritic, porphyritic and rarely aphyric. The basalts from the lower part have intergranular to intersertal textures contains groundmass of plagioclase, clinopyroxene, olivine and Fe–Ti oxides. Olivine phenocrysts are also present in these basalts exhibiting a subophitic textures and rarely iddingsitised. Clinopyroxene and plagioclase phenocrysts are also set with in a fine grained groundmass of strongly aligned plagioclase lath displays trachytic (flow) texture.

Phenocrysts of olivine result from a slower cooling beneath the surface in the magma chamber prior to eruption. Therefore, they indicate the presence of enough time to equilibrate with the melt at mantle depth. Upon eruption, the remaining liquid crystallizes to form fine laths and tabular or equant crystals comprising the groundmass and resulting in a dense network of plagioclase microlites and pyroxene granules, with opaque oxides of a small size. In the ophitic texture, laths of plagioclase enveloped by larger pyroxene (augite) are commonly interpreted as indicating that the clinopyroxene (augite) formed later Winter, (2007). Also, these basalts with sub-ophitic texture having interstitial clinopyroxene and plagioclase lath groundmass. Phenocrysts of olivine and some pyroxenes has euhedral and subhedral shape with complete and unbroken crystals evenly distributed and ranging up to 3 cm in size due to relatively slow cooled and suspended in the melt (McPhie et al., 1993).

The porphyritic nature of the magmas in the study area may result from the two stages of magmatic processes. Initially, some crystals grow early, slow and subsurface cooling of magma. Then after, following eruption relatively rapid solidification of the melt by consisting of the already crystallized phenocrysts results the formation of groundmass. In addition, subophitic to ophitic textures with variable grain sizes that correspond to different cooling rate of a crystal. A Glomeroporphyritic texture consists of a small number of phenocrysts clustered together and also typical of coherent lava flows. Vesicles on the some of the basaltic rocks are recorded due to steam bubbles enclosed in magma (McPhie et al., 1993; Winter, 2007).

6.2. Chemical classification of Tana volcanic rocks

Based on the total silica-alkali (TAS) diagram (Fig. 4.1) Tana area volcanic rocks are classified in to trachyte, rhyolite, dacite, basalt, and basanite groups. Mainly, mafic rocks fall on transitional to alkaline basalt and felsic samples fall below the sub-alkaline boundary with higher silica values (Le Bas et al., 1986); agrees with transitional to alkaline fields of Ethiopian basaltic lava (Piccirillo et al., 1979). This shows that the widespread occurrence of basalt and rhyolite, with the absence of intermediate rocks. This indicates the bimodal volcanism nature of the Tana area. Several studies on both plateau and rift volcanism documents the lack of intermediate rocks (Ayalew et al., 2002; Keiffer et al., 2004; Pecccerillo et al., 2003; Pik et al., 1998; Ayalew et al., 2006). Bimodal magmas are universally found at continental rifts and hotspots. Initially, partial melting of the mantle originates basaltic magma. Then after, the rising of this magma partly melts continental crust, resulting dual occurrence of mafic and felsic rocks (Peccerillo, 2005) with a characteristics of extensional tectonic settings volcanic suites (e.g., Wilson, 1989).

However, the present study argues with the transitional to alkaline nature of the Lake Tana area Quaternary basaltic rocks. The alkalinity index of felsic rocks was determined by the ratio of total alkalis with respect to Al_2O_3 (Le Bas et al., 1986). Based on this calculation, these felsic samples collected from the Tana area posses sub-alkaline nature with the value less than one (<1). Probably, it may resulted due to alkali loss during deuteric mobilization (Ayalew and Yirgu, 2003 and reference therein). The A.I. value ranges from 0.4-0.9 except Tan 24 (A.I. 5.88) which is highly altered ignimbrite sample due to low temperature or hydrous alteration subsequently loss of Na (Ayalew et al., 2002; Giordano et al., 2014 and reference therein).

6.3. Fractional crystallization

The role of fractional crystallization in the formation of basaltic rocks can be accessed from a plot of SiO_2 versus the other major oxides (Cox, 1979; Winter, 2001).The observed correlations in the Harker diagrams (Fig. 5.2 & 5.3) for Lake Tana area volcanic rocks probably reflect the significant role of fractional crystallization processes during their evolution. The decrease in MgO, FeOt, Co and Ni with increasing SiO_2 is probably related to ferromagnesian mineral (olivine) fractionation. The CaO and MgO decrease with increasing SiO_2 reflects clinopyroxene fractionation. The negative trends in FeOt, TiO_2 and MgO may be related to fractionation of Fe-Ti oxides.

Whereas, negative CaO correlation parallel to Sr and negative K_2O and Na_2O trends with increasing SiO_2 are probably linked to plagioclase and K-feldspar joined fractionations. K_2O and Na_2O are sequentially enriched in the lavas during the course of differentiation. Because, sanidine is a common phenocrysts phase in high K_2O felsic samples (trachyte and rhyolite). Also, negative P_2O_5 correlations with increasing SiO_2 probably result from apatite fractionations. Al_2O_3 remains constant in basaltic and slightly increases in rhyolitic rocks. But, it shows some increment in trachytic rocks due to the presence of Lucite and nepheline minerals (Wilson, 2007). The positive trend for Sr and the negative trend for Ba with fractionation index SiO2 (Fig 5.4 J and E respectively) indicates the differentiation process and removal of feldspar.

A decrease in Rb with increasing SiO_2 indicates the removal of Rb from the liquid where Rb is accommodated therefore feldspar fractionation will happen. Sr favorably enters the plagioclase structure or other Ca bearing phases and shows a negative correlation. Therefore, the decrement of Sr is attributable to removal of feldspar and apatite. The presence of Eu anomaly, whether positive or negative, is related to plagioclase feldspar fractionation or accumulation. Slight Eu anomalies may be obtained by fractionating equal proportions of plagioclase and clinopyroxene (Hanson, 1980) and the low oxygen fugacity for the rhyolites (e.g. Ayalew et al., 1999). The Tana area rhyolites as compared to the primitive mantle (Fig.5.7) they are variably enriched in the incompatible trace elements, such as Rb, Th, K, LREE, Nb, Ta, Zr, and Hf. Also, they present marked troughs at Ba, Sr, P, and Ti indicative of feldspar, apatite, and Fe-Ti oxide fractionation. They are moderately fractionated La_N/Yb_N (2-19.6) with negative Eu anomalies.

Models of incompatible against compatible trace elements are potentially powerful tools to further discriminate between fractional crystallization and melting processes. Sr against Rb is plotted for this purpose (Fig. 6.1). The plots show a clear process of fractional crystallization with high concentration variation of compatible element (Sr) and low concentration variation of incompatible element (Rb). This is the result of compatible element responds in opposite manner for fractionation/partial melting process relative to incompatible element. From this the evolution of Tana silicic magma is modeled. For the modeling the parent magma is selected from the Tana samples, sample Tan 5, which show least differentiation relative to the other samples. The sample has MgO (10.1 wt. %) and Ni (107 ppm). The partition coefficient taken for the model is 5-Sr and 0.05-Rb (after Ewart and Griffin, 1994) that best fit the trending line on the plot. For the genesis of Tana felsic rocks the mafic magma need at least a degree of fractional crystallization 70- 80%. Since the fractionation of ferromagnesian minerals would decrease the concentrations of the compatible elements and increase the concentrations of the incompatible elements. Partial melting might have also contributed to the composition of these volcanic rocks. During partial melting incompatible elements are concentrated in the melts thereby becoming depleted in the source rocks (Rollinson, 1993).

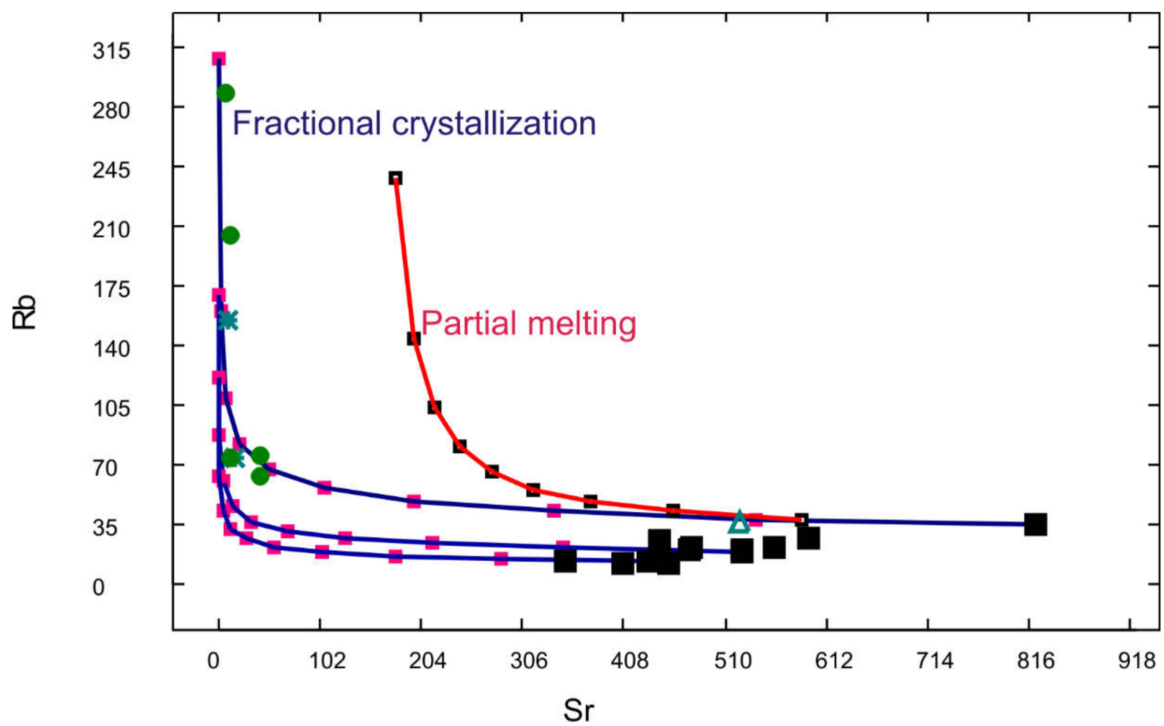

Figure 6.1: Fractional crystallization model that explain the evolution of silicic volcanic products of Lake Tana area basaltic lava.

6.4. Petrogenesis of felsic rocks

Temporal, spatial and geochemically associated basaltic and rhyolitic volcanic rocks nearby the Lake Tana are belonging to a bimodal suite. In general, the origin of the felsic rocks in a bimodal suite has remained a classic petrogenetic problem. Silica gap can be produced in a co-genetic suite of rocks by fractionation of basaltic parent magma (Xu et al., 2010). Perhaps, this Daly gap might simply reflect the onset of significant amounts of Fe-Ti oxide fractionation, which accelerate accumulation of SiO_2 contents (Garland et al., 1995). Another argument used besides fractional crystallization of basaltic magmas is voluminous of felsic rocks. However, studies on felsic magma generation (e.g., Bachmann and Bergantz, 2008) suggest that immense volumes of magma can be rapidly removed from crystal mush zones (e.g., Wilson et al., 2007). Comparably, 20% of felsic lava is estimated for the Ethiopian plateau bimodal suite (Ayalew et al., 2002) considering Lake Tana surroundings.

Two hypotheses have been proposed to account for the generation of silicic end-members. One hypothesis suggests that felsic rocks and associated basalts represent two genetically independent melts, with the basalts coming from the mantle and the silicic liquids being generated in the crust, by melting of either old crust or young under plated basalts. The other hypothesis proposes continuous fractional crystallization, starting from the basaltic parents, possibly with a role for crustal contamination (Ayalew et al., 2002; Ayalew and Ishiwatari, 2011; Trua et al., 1999; Peccerillo et al., 2007). Fractionation of clinopyroxene and/or olivine could account for the positive correlations in the Cr and Ni vs. SiO_2 diagrams (Fig.4.3 G and H respectively). However, the fractional crystallization of mafic magmas alone may not be able to explain the centralized geochemical features of the high-silica Tana area rhyolites. Furthermore, it is hard to explain the fractionation of basaltic melts that generated these rhyolites without producing intermediate compositions (Wang et al., 2017).

According to Pik et al., (1998, 1999) and Ayalew et al., (2002) plateau rhyolites are genetically related with subordinate and superimposed Oligocene low Ti-basaltic sequences. The plot of TiO_2 vs. SiO_2 (Fig 5.2.F) shows negative correlations and diagrams of Zr vs. Nb, Zr vs. Ta, Zr vs. Y and Zr vs. Rb (Fig. 5.5) form a positive correlation by forming a single trend that show the genetic relationship or co-magmatic nature of the Oligocene LT basaltic and rhyolitic rocks around Lake Tana area either by Fractional crystallization or Partial melting (Ayalew et al., 2002). The similarity in pattern of REE and multi-element variation diagram implies the magmas are derived from similar source or melting conditions (Ayalew et al., 2016).

Eventually, Tana area basalts and rhyolites are interlayered in the same volcanic bodies, it is quite possible that they could have a common origin, i.e., it is probable that they originated within the same magma chamber and that the felsic volcanic rocks were derived from crystal fractionation of the primary basalt melt. The felsic rocks show trace element spider-diagrams and chondrite-normalized REE patterns (Fig.6.2) similar to those of the mafic rocks, except for the negative Eu and Sr anomalies. The large negative Eu and Sr anomalies require major plagioclase fractionation (Rollinson, 1993). These intermingling of rhyolites and basalts imply that there may have been several episodes of magmatic recharge in the underlying chamber (Ayalew and Gibson, 2009).

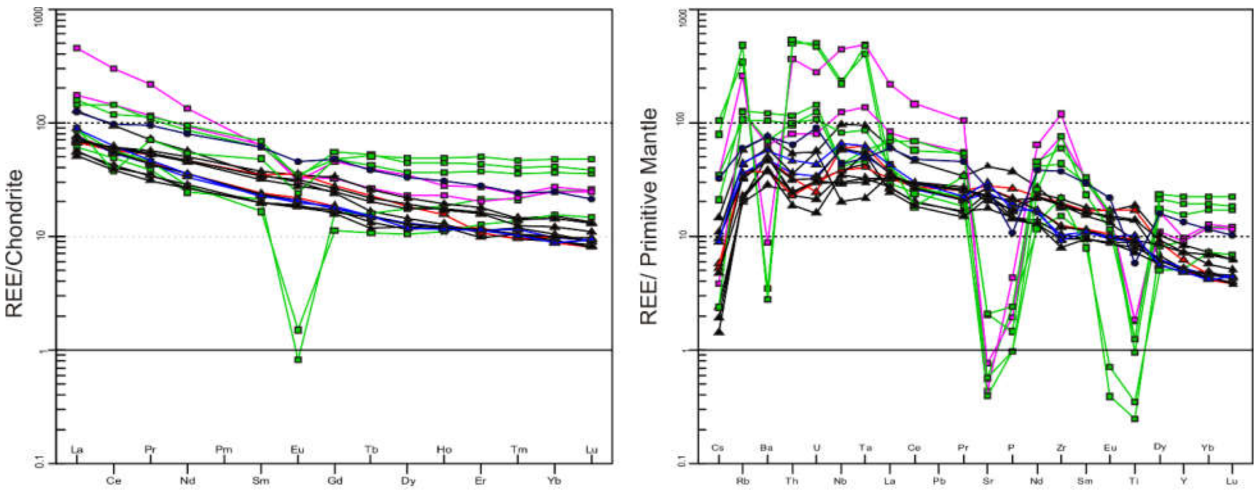

Figure 6.2: Spider diagram and multi-element variation diagram for the whole samples to show similarity of the REE and multi-elements

6.5. Crustal contamination

Primarily, the origination of basaltic magma and their transportation through crust with staying in magma chambers located at different crustal level processes, favors the possibility of crustal assimilation that has an impact upon incompatible trace element compositions (e.g. Gill, 2010; Wilson, 2007, 2007; Winter, 2001; Rollinson, 1993). Thompson et al., 1984 suggested that crustal contamination in basaltic magmas from La/Nb values. That OIB, MORB and continental alkali basalts all have La/Nb value < 1, whereas La/Nb values for continental flood basalts range from 0.5 to 7 suggesting variable degrees of contamination. The negative Nb anomaly in some samples from multi-element plot (Fig.5.7) ratifies the crustal nature or crustal contamination (Rollinson, 1993). Accordingly, Tana area volcanic rocks have La/Nb value ranges <1. Thus implies that these volcanic rocks are not affected by crustal contamination.

According to Sun and McDonough, 1989 mantle-derived magmas are considered to be categorized by Nb/Ta and Zr/Hf average values of 17.6 and 36.3 respectively. The mafic volcanic rocks from the Lake Tana area are characterized by Nb/Ta and Zr/Hf values of 16.46 and 37.13 respectively. Although, the felsic rocks from the Lake Tana area are characterized by the Nb/Ta and Zr/Hf values of 15.21 and 37.23 respectively. Hence, the volcanic rocks are not distinctly affected by crustal contamination. However, little troughs in HFSEs, especially in Nb and Ta, suggest that the felsic rocks are present with little evidence for crustal contamination (Rolinson, 1993).

6.6. Tectonic significance and magma source

Tectonic discrimination diagrams reveal that the Tana Basaltic samples consistently plot in the within-plate basalt fields. Likewise, the Zr/Y versus Ti/Y, Zr versus Zr/Y, Zr versus Ti and Th-Hf-Nb diagrams show the same relationships. As shown in the plot Zr vs. Zr/Y (Fig 6.3) the within plate tendency for the Tana area basaltic rocks are pronounced in the Zr/Y-Zr diagram (Pearce and Norry, 1979). On the other hand, incompatible trace element ratio diagram of Nb/Yb vs. Th/Yb most of this intra plate magmas are plotted in the field of OIB groups (Pearce, 2008).The geochemical characteristics of the LT and HT1 lavas are consistent with shallow level fractionation, dominated by plagioclase plus various amounts of olivine and clinopyroxene. These fractionating mineral assemblages are compatible with the sequence of fractionation and phase proportions observed experimentally at low pressure for similar basalt compositions (Cox and Bell, 1972).

As stated by Smith et al., (1999), it is accepted that HFSE's such as Nb and Ta are depleted in the lithospheric mantle sources compared to LEE's and therefore Nb/La ratio is lower in the lithospheric mantle (<0.5) and the ratio is higher (>1) in the astenospheric mantle originated OIB's. Similarly, De Paolo and Daley, (2000) suggest that the ratio of La/Nb is ~0.7 for an astenospheric source and if the ratio is > 1, it indicates a lithospheric source. Consequently, the Tana area mafic volcanics are derived from asthenosphere and the other felsic groups are from the lithosphere. From the geochemical point of view the mafic rocks have a sub-alkaline character, with an affinity to a continental within-plate tectonic setting.

The trace element distribution patterns of the studied rocks is similar to OIB, which probably represents basaltic melts from the enriched asthenosphere mantle source, often associated with an uprising mantle plume (Wilson, 1989). The basaltic lava sequences around the NW Ethiopian plateau area have been affected by plume impact to generated greatest volume of melt (Ayalew and Gibson, 2009). The basalts of the area representing all rocks were formed in an intra-continental (within plate) tectonic setting and they represent alkali to transitional basalt, most of them having undergone slight to moderate fractionation. Probably the volcanic activity responsible for these basalts occurred in a zone of initial continental rifting. The geochemical data based on trace element variation of mafic and felsic volcanic rocks, which are alternating in the lithological sequence, suggest two different sources, an upper lithospheric mantle and crust.

6.7. Comparisons of Quaternary Tana volcanic rocks with the Ethiopian Oligocene CFBs

Most of the southern Lake Tana area is covered with the recent volcanic products. However, the rests are occupied by relatively older Pliocene to Oligocene lavas. It is usually known that there is a huge gap between the Oligocene and Quaternary volcanic episodes. Numerous samples are collected from these varied geological formations in terms of areal distribution and their age. Among the basaltic samples collected for the present study, from the twelve of them three samples have similar characteristics with transitional to tholeiitic Low Ti (LT) Oligocene plateau basalts. The rest nine basaltic samples overlay with alkaline to transitional character of Tana Quaternary basalt. TAS and AFM diagrams (Fig. 6.3) reveal that two different magma series of the Tana area in relation to the other plateau volcanic rocks.

The petrographic description of LT Oligocene basalts from the Lake Tana surroundings confirmed the Pik et al., (1998) petrographically characterization of plateau basalts as intergranular to glomeroporphyric with rarely aphyric textures consisting of plagioclase, clinopyroxene and olivine phenocrysts. Basically, sub ophitic nature with glomerophyric aggregates of clinopyroxene led them to have tholeiitic affinity (Fig. 6.3). In the meantime these LT basalts show the olivine and hypersthene normative. The less explored Quaternary volcanics presented near Lake Tana area and extend towards the south. According to Abate et al., (1998)all these units in hand specimen expressed as dark, vesicular and fine grained to aphanitic with the absence of separate crystal phases which is a wholesale overview.

Particularly, some discussions of this study on the samples which are collected from the very near Tana area (Dek Island, eastern and southern localities) showed similarities to the earlier works. Essentially, the basalts from Dek, Zega, Merawi and Bahir Dar area are porphyritic olivine rich basalt. Also, the basanitic intrusions of Tana Kirkos dike and Asinora hill are characterized with nepheline normative. Subhedral to euhedral olivine, randomly aligned tabular plagioclase, splintered clinopyroxene and sometimes nepheline crystals are hosted in a fine-grained groundmass. The matrix has similar mineral assemblages with the phenocrysts. In reason to this, Quaternary basalts are described as alkaline to transitional magma series (Fig. 6.3).

The bimodality nature of Ethiopian large igneous provinces have been disscused over various times (Gasparonetal., 1993; Trua et al., 1999; Ayalew et al., 2002; Peccerillo et al., 2003, 2007; Rooney et al., 2007; Kabeto et al., 2010; Ayalew and Ishiwatari, 2011). Likewise to other Afro-Arabian volcanisms the Lake Tana area exhibited as bimodal Oligocene volcanism. Ayalew and Yirgu, (2003) commenced the strongly bimodal compositions of North western Ethiopian plateaus in relation to alternation of felsic and mafic lava on the uppermost successions after discerning Lima Limo and WgeleTena sections. However, the Quaternary basaltic lavas are not genetically linked to the Oligocene products due to the differences in geochemistry and age. The Felsic lavas from the Tana area are dominantly rhyolites which verified as porphyritic to glassy textures. Sanidine, quartz, biotite and ilmenite set in fine grained (glassy) groundmass. Petrographically, Lima Limo rhyolite which has glassy and perlitic characteristics is comparable to Tana rhyolites.

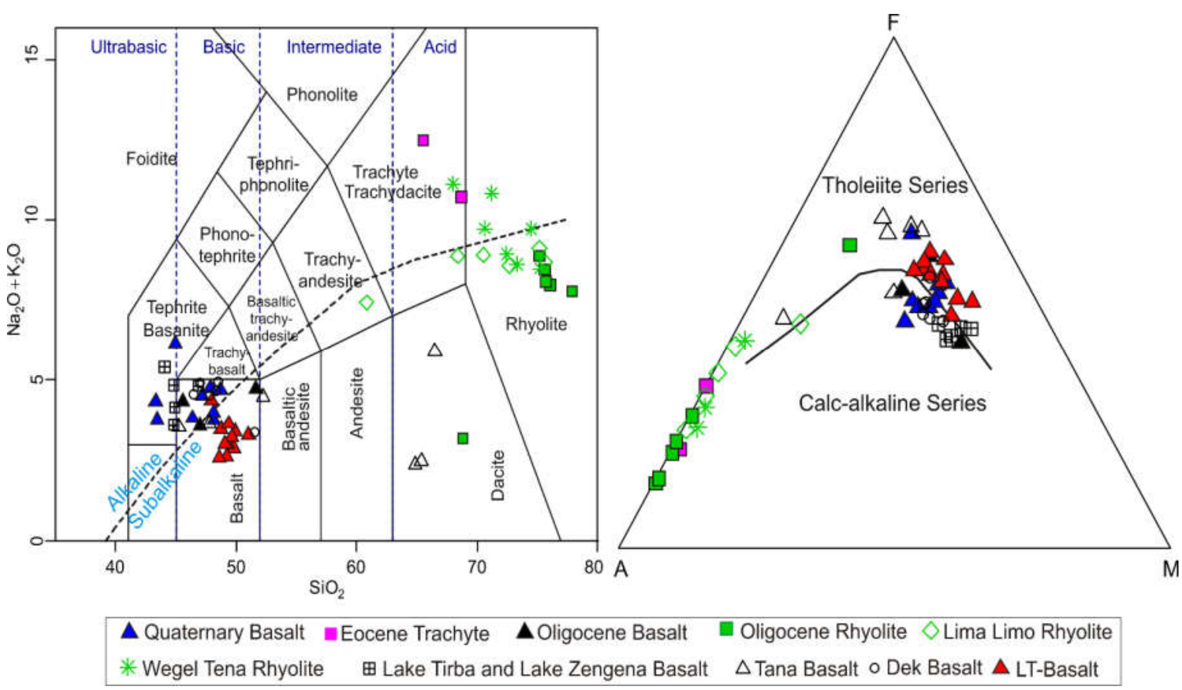

Figure 6.3: TAS diagram after Le Bas et al., (1986) for the plateau volcanic rocks (B) AFM diagram after Irvine and Baragar, (1971): LT basalt samples from Pik et al., (1998), Lake Tana, Tirba, Zengena and Dek basalt from Abate et al., (1998) and Lima Limo and Wegel Tena from (Ayalew and Yirgu, 2003).

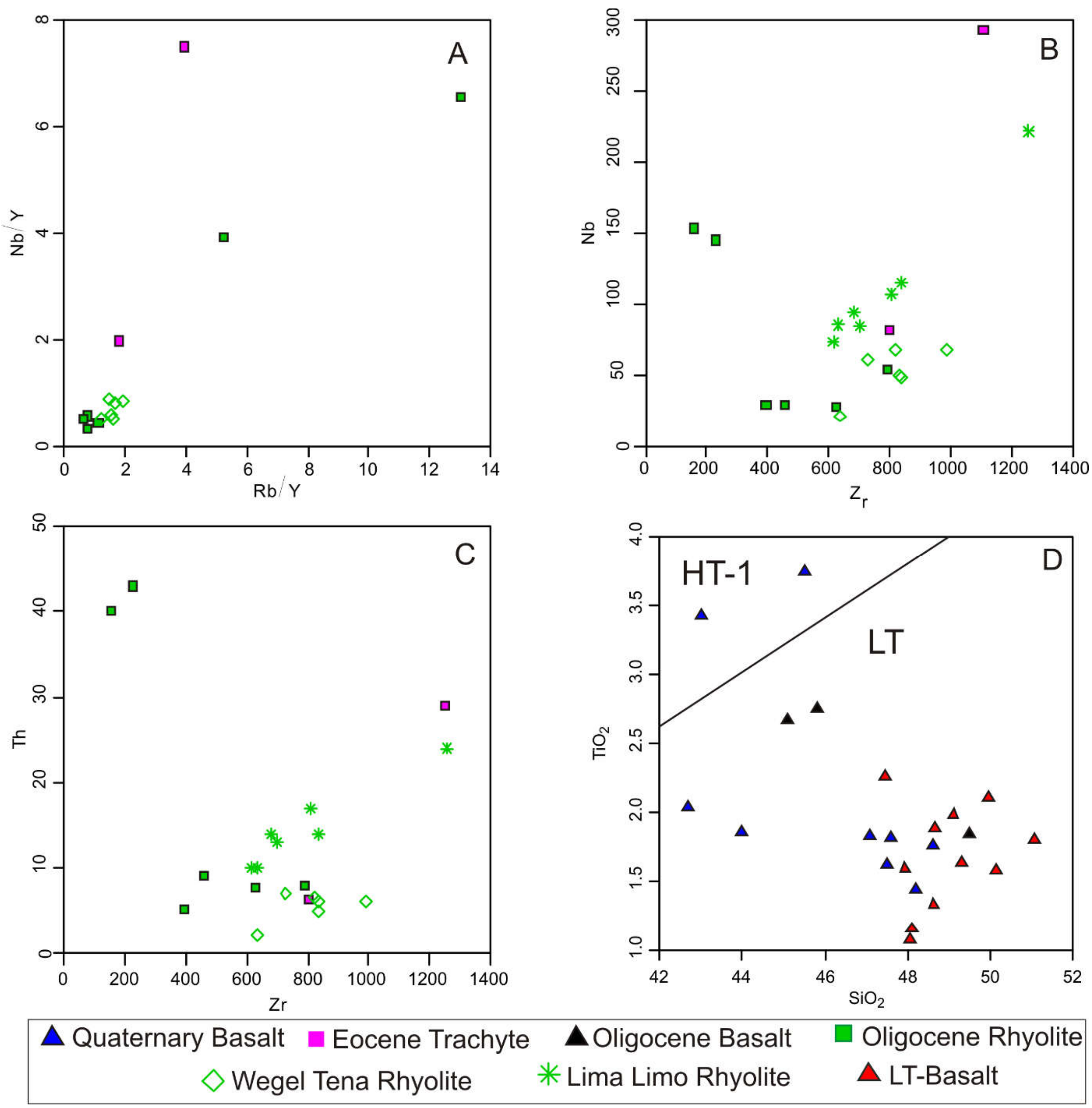

Figure 6.4: (A) Rb/Y vs. Nb/Y (B) Zr vs. Nb (C) Zr vs. Th and (D) SiO2 vs TiO2

The modern classifications of the Ethiopian plateau flood basalt were done based on the Ti (TiO_2) concentration. It is classified in to three magma types: two high-Ti groups (HT1 and HT2) and one low Ti group (LT). The transitional to tholeiitic LT suite exhibits low TiO2 (1-2.6 wt. %) and high SiO_2. In contrast, the HT2 suite exhibits high TiO_2, low SiO_2 content (Pik et al., 1998; 1999). Based on the above classification the Tana area Quaternary and Oligocene basalts are generally categorized under the transitional to tholeiitic low Ti (LT) and high Ti (HT1) group (Fig. 6.4.D) with a range of (1.44–3.74 wt. %) TiO_2.

As shown in figure 6.5 the southern and southeastern part of the Lake Tana areas are used as a boundary to separate the southwestern High Ti (HT1) sub-province from the northwestern low Ti (LT) sub-province (Pik et al., 1998). Physically, those highest TiO_2 samples are brought from the most marginal areas of the LT group basalts province (Fig.6.4.D). These LT and some HT1 Tana basalts are reliable to the Pik et al., (1998; 1999) standards, such as #Mg (26.7-51.07), low SiO_2 (42.7-49.5 wt. %), high Al_2O_3 (14.65-17.15 wt. %), high FeO (9.7-14.4 wt. %) and MgO (5.09-10.1 wt. %) with the variable amount of total alkali content (3.34-6.03 wt. %).

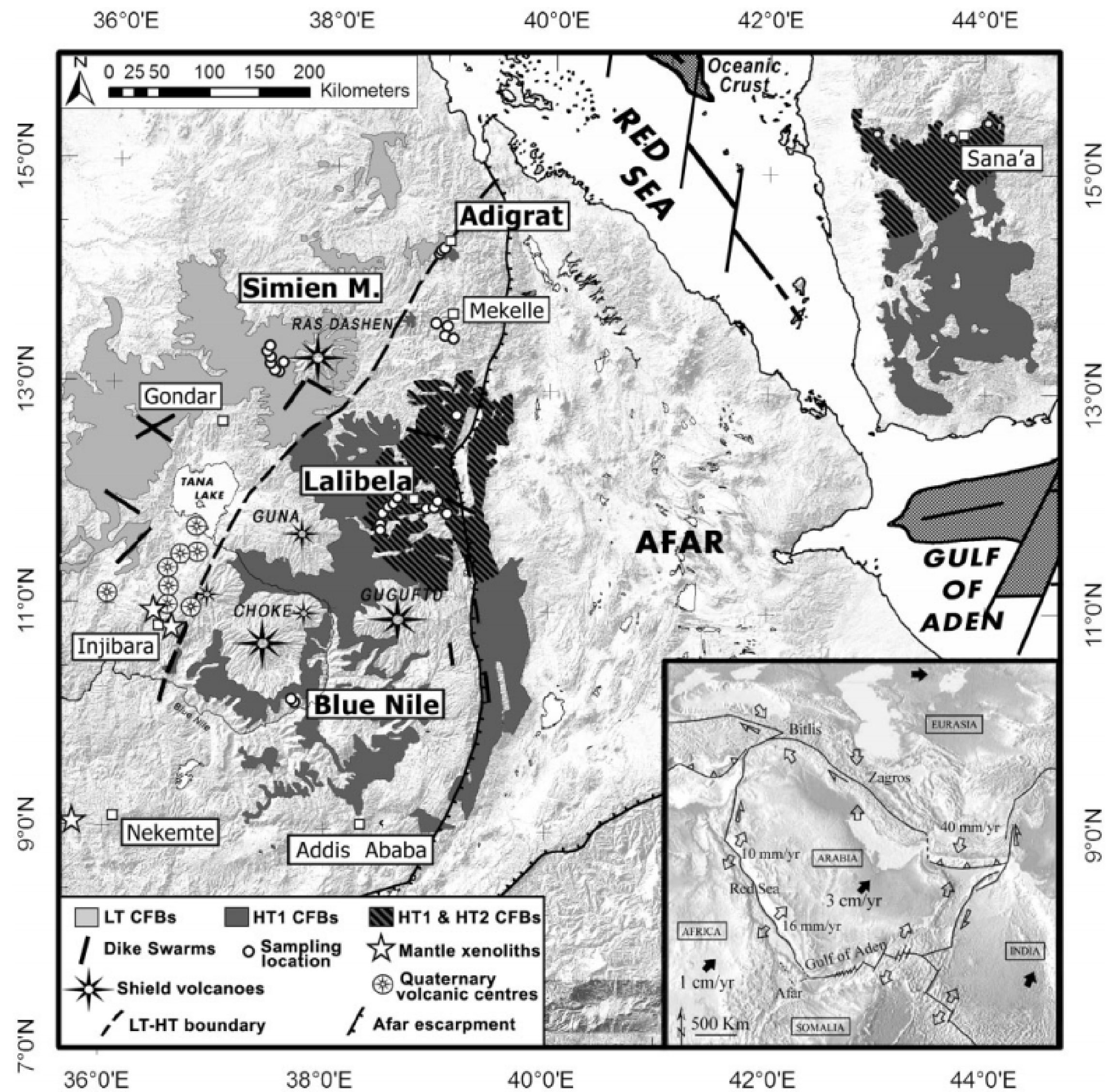

Figure 6.5: Sketch map of the Oligocene CFB of the Northern Ethiopia and the Yemen conjugate margins. Taken from Beccaluva et al., (2009): LT, Low-Ti tholeiitic basalts; HT1, High-Ti tholeiitic basalts; HT2, very High-Ti transitional basalts.

Table 6.1: Trace element characteristics of the Tana area rhyolite compared with other rhyolites of separate areas formed by partial melting of the crust. Data source: Ayalew and Yirgu, (2003) and references therein.

No.	Rhyolitic lava	Rb/Nb	La/Nb
1	Lima Limo rhyolite, Ethiopian plateau	1.17-3.0	1.4-2.9
2	Wegel Tena rhyolite, Ethiopian plateau	0.8-1.3	0.8-1.2
3	Macusani rhyolite, Peru	1.22-45	0.8-1.7
4	Loch Scridainrhyolite,UK	2.7 – 9.0	2.6-2.7
5	Yellow stone rhyolite, USA	3.2 – 5.0	0.8-2.3
6	Tana Rhyolite, the present study	0.53-2.63	0.12-1.79

Furthermore, Tana area rhyolites have higher Th (5.1–43 ppm) and Nb (27.2–153 ppm) concentrations, and lower Rb/Nb (0.53–2.63) and La/Nb (0.12–1.79) ratios, which suggest that only limited crustal material was involved in their genesis. On the other hand, Trace element ratio characteristics of Tana rhyolite are compared with rhyolite formed by partial melting of the crust (3, 4 and 5). Also, the Lima Limo rhyolite (1) and Wegel Tena rhyolite (2) which are mantle derived and they show a limited crustal contamination.

The comparison shows that the Tana Rhyolite incompatible trace element ratios are different from those of typical crustal melts and alike with the Lima Limo and Wegel Tena rhyolite, inferring that they did not originate by partial melting of the crustal rocks. Instead, the geochemical features are consistent with their derivation from mantle derived basaltic magma by low pressure fractionation. Trace elements compatible in alkali feldspar, such as Ba, Sr and Eu, are also variable, concentrations of Ba and Sr in the Tana area rhyolites (23.1-794 ppm Ba, 7.8-524 ppm Sr). These values are an indication for low-pressure fractional crystallization in crustal magma chambers, which probably causes crustal contamination (Ayalew and Yirgu, 2003 and references therein).

7. Conclusion and Recommendation

Conclusion

Based on the field observations, geological mapping, petrographic descriptions and whole rock geochemistry data collective approaches this study concluded that:

1. The major lithological units identified in the studied area include: Pliocene to Miocene ash tuff and associated basalt, Oligocene rhyolite and Oligocene basalt which are related to oldest NW Ethiopian plateau segments. Additionally, recent lacustrine sediments, southern Lake Tana Quaternary basalt and associated basanite intrusions and scoria cones are also related to the Quaternary volcanics periods.
2. The geological structures observed on the study area are flow banding, dikes, joints and NNE-SSW trending major faults that imitate the regional tectonic structure of the Lake Tana area Tectonics.
3. The geochemistry and petrographic studies suggest the rocks are a bimodal suite, with the absence of intermediate composition. The chemical compositions are mainly basaltic and silicic. The Oligocene basalts are tholeiitic to transitional whereas, the Quaternary basalts are alkaline affinity and the silicic rocks are dominantly sub alkaline rhyolite.
4. The overall major oxides variation in the Lake Tana area samples shows two significant fractionation trends. At first fractionation of Basaltic phases (olivine, pyroxene, plagioclase feldspar, Fe-Ti oxides and apatite) and later the felsic phase is controlled by a fractionation of alkali feldspar.
5. The major element Harker diagram, trace element modeling, REE variation diagram and multi element variation diagram of the felsic and mafic groups of the same age imply the rocks are linked by a fractional crystallization process with minimal contamination. Although, REE patterns of the Lake Tana area rhyolites are remarkably similar within each unit and are comparable for a given unit to those of associated basalts as an implication for the same magma source.
6. Comparing the Tana volcanics with other plateau formations, typically basaltic rocks are classified under LT basalt group and all of the Tana rhyolite petrological characteristics agree with plateau (Lima Limo and WegeleTena) rhyolites.

Recommendation

Moreover, isotope geochemistry works, age determinations, additional whole rock and mineral chemistry studies are much recommended to adequately understand the magma source characteristics, petrological and geochemical processes involved to produce the rock suites of the Lake Tana area.

References

Abate B., Koeberl, C., Buchanan, P.C. and Korner W. (1998). Petrography and geochemistry of basaltic and rhyiodacitic rocks from Lake Tana and Gimjabet-Kosober areas (north central Ethiopia). *Journal of African Earth Sciences* **26(**1),pp 119-134.

ALS, 2017. Analytical Testing Services Manual, 33p.

Asrat A., Barbey, P., Gleizes, G., 2001. The Precambrian Geology of Ethiopia: a review. Africa Geosciences Review, 8: 271-288.

Asrat A., Demissie, M., Mogessie, A., 2012. Geoheritage Conservation in Ethiopia: The case of the Simien Mountains. QuaestionesGeographicae, 31: 7-23.

Ayalew, D. (2011). The relations between felsic and mafic volcanic rocks in continental flood basalts of Ethiopia: implication for the thermal weakening of the crust. Geological Society, London, Special Publications, 357(1), 253–264.

Ayalew, D., & Gibson, S. A. (2009). Head-to-tail transition of the Afar mantle plume: Geochemical evidence from a Miocene bimodal basalt-rhyolite succession in the Ethiopian Large Igneous Province. Lithos, 112(3–4), 461–476.

Ayalew, D., Barbey, P., Marty, B., Reisberg, L., Yirgu, G., &Pik, R. (2002). Source, genesis, and timing of giant ignimbrite deposits associated with Ethiopian continental flood basalts. GeochimicaetCosmochimicaActa, 66(8), 1429–1448.

Ayalew, D., Yirgu, G., &Pik, R. (1999). Geochemical and isotopic (Sr, Nd and Pb) characteristics of volcanic rocks from southwestern Ethiopia. Journal of African Earth Sciences, 29(2), 381–391.

BCEOM (1998). Abbay River integrated development master plan project (phase 2), data collection-site investigation, survey and analysis, section IV, water resources, part

Beccaluva, L., Bianchini, G., Natali, C., & Siena, F. (2009). Continental flood basalts and mantle plumes: A case study of the Northern Ethiopian Plateau. Journal of Petrology, 50(7), 1377–1403.

Berhe, S. M., Desta, B., Nicoletti, M., &Teferra, M. (1987). Geology, geochronology and geodynamic implications of the Cenozoic magmatic province in W and SE Ethiopia. Journal of the Geological Society, 144, 213–226.

Beshawered E., Ashenafi S., Edris M.,Burusa G.,Zewede T., Tesfaye Y., Bekele H.,Tadesse M., Wendant M., (2010). Geology, geochemistry and gravity survey of the Bahir Dar area, memoir 30. Geolological Survey of Ethiopia.

Beyene, A., &Abdelsalam, M. G. (2005). Tectonics of the Afar Depression: A review and synthesis. Journal of African Earth Sciences, 41(1–2), 41–59. Birth and global change, Nature 389, pp338-341

Bonini, M., Corti, G., Innocenti, F., Manetti, P., Mazzarini, F., TsegayeAbebe and Pecskay, Z. (2005). Evolution of the Main Ethiopian Rift in the frame of Afar and Kenya rifts propagation. Tectonics 24(1).

Boynton, W.V., 1984. Geochemistry of rare earth elements: meteorite studies. In: Henderson, P. (Ed.), Rare Earth Element Geochemistry, pp. 63e114.

Chorowicz, J., Collet, B., Bonavia, F. F., Mohr, P., Parrot, J. F., & Korme, T. (1998). The Tana basin, Ethiopia : intra-plateau uplift, rifting and subsidence, 295(1998), 351–367.

Courtillot, V., Jaupart, C., Manighetti, I., Tapponnier, P., &Besse, J. (1999). On causal links between flood basalts and continental breakup. Earth and Planetary Science Letters, 166(3–4), 177–195.

Cox K.G., Bell, J.D. and Pankhurst, R.J. (1979). The Interpretation of Igneous Rocks. George Allen and Unwin, London, 450p.

Daniel Meshesha, &Shinjo R (2007) Rethinking geochemical feature of the Afar and Kenya mantle plumes and geodynamic implications. J Geophysics Res 113: B09209.

Davidson A. (Compiler), 1983. Reconnaissance geology and geochemistry of parts of Illubabor, Kefa, GemuGofa and Sidamo, Ethiopia. The Omo River Project. Ethiopian Institute of geological Surveys, Bulletin 2, Addis Ababa. Ethiopia, Scale 1:2,000,000, 2nd edition. Addis Ababa: Geological Survey of Ethiopia

Dercq, M., Arndt, N., Lapierre, H. and Gezahegn yirgu (2001). Les pitons trachytiques d'Ethiopienesont pas les conduits d'alimentation des trapps.C.R.Acad. Sci. paris 332:609-615.

Ewart, A. and Griffin, W. (1994). Application of proton-microprobe data to trace-element partitioning in volcanic rocks. *Chemical Geology* **117**(1):251-284.

Gani, N. D. S., Gani, M. R., &Abdelsalam, M. G. (2007). Blue Nile incision on the Ethiopian Plateau: Pulsed plateau growth, Pliocene uplift, and hominin evolution. GSA Today, 17(9), 4–11.

Gasparon, M., Innocenti, F., Manetti, P., Peccerillo, A. and TsegayeAbebe (1993). Genesis of the Pliocene to Recent bimodal mafic-felsic volcanism in the DebreZeyt area, central Ethiopia: volcanological and geochemical constraints. Journal of African Earth Sciences **17(2):**145-165.

Gichile S., 1991. Structures, Metamorphism and tectonic setting of a gneissic terrine, the Sagan-Aflata area, southern Ethiopia. MSc thesis, University of Ottawa, Canada. Possible manner of evolution, Geol. Rdsch. V.67, p.531-546.

Gill, R. (2010). Igneous rocks and processes: a practical guide.

Hanson, G. N. (1980). Rare Earth Elements in Petrogenetic Studies of Igneous Systems. *Annual Review of Earth and Planetary Sciences*, ***8*****(1)**, 371–406.

Hautot, S., Whaler, K., Gebru, W., &Desissa, M. (2006). The structure of a Mesozoic basin beneath the Lake Tana area, Ethiopia, revealed by magnetotelluric imaging. Journal of African Earth Sciences, 44(3), 331–338.

Haylemariam D.,Yismaw D.,Agonafir M., Zenebe B.,Sewnet M., Edris M., Burussa G., Yehualaeshet E., Ashenafi S., (2012). Geology, geochemistry and gravity survey of Yifag area (memoir no.32). Geological Survey of Ethiopia.

Hofmann, C., Courtillot, V., Feraud, G., Rochette, P., Yirgu, G., Ketefo, E. and Pik, R.

Irvine, T. and Baragar, W. (1971). A guide to the chemical classification of the common volcanic rocks. Canadian journal of earth sciences 8(5):523-548.

Jepsen, D.H., Athearn, M.J., 1961. A general geological map of the Blue Nile River basin, Ethiopia (1: 1,000,000). Dep. Water Resources, Addis Ababa.

Kabeto, K., 2010. Geological and geochemical variations in mid-tertiary Ethiopian flood basalt province, Maychew, tigray region, Ethiopia. Momona. Ethiop. J. Sci. 2 (1), 4e25.

Kazmin, V. (1972). The Geology of Ethiopia, E.I.G.S., Addis Ababa, Ethiopia

Kazmin. (1975). Explanation of the geological map of Ethiopia.

Kieffer, B., Arndt, N., Lapierre, H., Bastien, F., Bosch, D., Pecher, A., Meugniot, C. (2004). Flood and Shield Basalts from Ethiopia: Magmas from the African Superswell. Journal of Petrology, 45(4), 793–834.

Lamb, H.F., Bates, C.R., Coombes, P.V., Marshall, M.H., Mohammed Umer, Davies, S.J. and Eshete Dejen (2007). Late Pleistocene desiccation of Lake Tana, source of the Blue Nile. Quaternary Science Reviews 26, pp287-299, ELSEVIER.

Le Bas, M. J., Le Maitre, R., Streckeisen, A. and Zanettin, B. (1986). A chemical classification of volcanic rocks based on the total alkali-silica diagram. Journal of Petrology 27(3):745-750.

McDonough, W. F. and Sun, S.S. (1995). The composition of the Earth. *Chemical Geology* **120**(3):223-253.

Mège, D., &Korme, T. (2004). Fissure eruption of flood basalts from statistical analysis of dyke fracture length. Journal of Volcanology and Geothermal Research, 131(1–2), 77–92.

Merla G., Abbate E., Azzaroli A., Bruni P., Canuti P., Fazzuoli M., Sagri M., Tacconi P., 1979.

Merla, G., Abbate, E., Canuti, P., Sagri, M., &Tacconi, P. (1973). Geological map of Ethiopia and Somalia, 1: 2,000,000. ConsiglioNazionaleDelleRicerche Italy.

Mohr, P. (1962).The Geology of Ethiopia, Addis Ababa, Ethiopia, University CoIl. Of No. 29. Geological Survey of Ethiopia. 85p.

Mohr, P. (1971). Ethiopian Rift and plateaus: some volcanic petrochemical differences.

Mohr, P. (1983). Volcanotectonic aspects of Ethiopian rift evolution. Bulletin Centre Recherches Elf Aquitaine Exploration Production 7:175-189.

Mohr, P. (1983).The Ethiopian Flood Basalt Province, Nature, 303:577-584.

Mohr, P. and Zanettin, B. (1988). The Ethiopian flood basalt province. In: Continental

Pearce, J.A. and Cann, J.R. 1973. Tectonic setting of basic volcanic rocks determined using trace elements analyses. Earth and Planetary Science Letters, **19**, 290-300.

Peate, I. U., Baker, J. A., Al-Kadasi, M., Al-Subbary, A., Knight, K. B., Riisager, P., Menzies, M. A. (2005). Volcanic stratigraphy of large-volume silicic pyroclastic eruptions during Oligocene Afro-Arabian flood volcanism in Yeme. Bulletin of Volcanology, 68(2), 135–156.

Peccerillo, A., Barberio, M., GezahegnYirgu, DerejeAyalew, Barbieri, M. and Wu, T. (2003). Relationships between mafic and peralkaline silicic magmatism in continental rift settings: a petrological, geochemical and isotopic study of the Gedemsa volcano, central Ethiopian rift. Journal of Petrology 44(11).

Peccerillo, A., Donati, C., Santo, A., Orlando, A., GezahegnYirgu and DerejeAyalew (2007). Petrogenesis of silicic peralkaline rocks in the Ethiopian rift: geochemical evidence and volcanological implications. Journal of African Earth Sciences 48(2):161-173.

Pik, R., Deniel, C., Coulon, C., Yirgu, G., Hofmann, C., &Ayalew, D. (1998). The northwestern Ethiopian Plateau flood basalts: classification and spatial distribution of magma types. Journal of Volcanology and Geothermal Research, 81(1–2), 91–111.

Pik, R., Marty, B., Carignan, J., &Lavé, J. (2003). Stability of the Upper Nile drainage network (Ethiopia) deduced from (U–Th)/He thermos chronometry: implications for uplift and erosion of the Afar plume dome. Earth and Planetary Science Letters, 215(1), 73–88.

Poppe, L., Frankl, A., Poesen, J., Admasu, Teshager, Dessie, Mekete, Adgo, Enyew, Deckers, J., Nyssen, J. (2013). Geomorphology of the Lake Tana basin, Ethiopia. Journal of Maps, 9, 431–437.

Prave, A. R., Bates, C. R., Donaldson, C. H., Toland, H., Condon, D. J., Mark, D., &Raub, T. D. (2016). Geology and geochronology of the Tana Basin, Ethiopia : LIP volcanism, super eruptions and Eocene – Oligocene environmental change. Earth and Planetary Science Letters, 443, 1–8. Rechercheminieral Na 540, 2000, 3-10

Rochette, P., Tamrat, E., & Fe, G. (1998). Magnetostratigraphy and timing of the Oligocene Ethiopian traps, 164, 497–510.

Rollinson, H.R. (1993). Using geochemical data: evaluation, presentation, interpretation:

Rooney, T., Furman, T., Bastow, I., Ayalew, D. & Yirgu, G. (2007). Lithospheric modification during crustal extension in the Main Ethiopian Rift. Journal of Geophysical Research, 112: 1-21. B10201. Routledge.

Şengör, A.M.C. (2001). Elevation as indicator of mantle-plume activity. In: Mantle Plumes: Their identification through time (R.E., Ernst and K.L., Buchan, eds). Geological Society of America Special Paper, 352, 183–225.

Tefera M., Tadiwos C. &Workineh H. (1996). Explanation of the Geological Map of the northern Main Ethiopian Rift: birth of a triple junction. Earth and Planetary Science Letters, 224: 213–228.

Trua, T., Deniel, C. and Mazzuoli, R. (1999). Crustal control in the genesis of Plio Quaternary bimodal magmatism of the Main Ethiopian Rift (MER): geochemical and isotopic (Sr, Nd, Pb) evidence. Chemical Geology 155(3):201-231.

Ukstins, I., Baker, J. A., Kent, A. J. R., Al-kadasi, M., Al-subbary, A., Ayalew, D. (2003). Correlation of Indian Ocean tephra to individual Oligocene silicic eruptions from Afro-Arabian flood volcanism 1, 211, 311–327.

White, W. M. (2013). Geochemistry. John Wiley & Sons.

Wilson, B. (2007). Igneous petrogenesis a global tectonic approach.

Wilson, M. 1989. Igneous Petrogenesis. Unwin Hyman, London, 446 p.

Woldegabriel G., Aronson, J. L. and Walter, R. C. (1990). Geology, geochronology, and rift basin development in the central sector of the Main Ethiopia Rift. Geological Society of Americav Bulletin 102(4):439-458.

Wolfenden, E., Ebinger, C., GezahegnYirgu, Deino, A. and DerejeAyalew (2004). Evolution of the northern Main Ethiopian rift: birth of a triple junction. *Earth and Planetary Science Letters* **224**(1):213-228.

Appendix 1

Petrographic analysis

Sample Code: Tan 2					
Minerals	**Modal Proportion (%)**	**Phenocryst Maximum grain Size (mm)**	**Phenocryst Maximum grain Shape**	**Texture**	**Rock Name**
Olivine	8	0.4	Anhedral	Porphyritic	Porphyritic basanite
Clinopyroxene	10	0.4-0.5	Subhedral		
Plagioclase	38	0.6-1	Euhedral lath		
Nepheline	12	0.3-0.6	Euhedral		
Groundmass of:Plagioclase, olivine, clinopyroxene, and opaque minerals	30				

Sample Code: Tan 7 and 8					
Minerals	**Modal Proportion (%)**	**Phenocryst Maximum grain Size (mm)**	**Phenocryst grain Shape**	**Texture**	**Rock Name**
Microcline	5	0.3-0.5	Subhedral to euhedral	Porphyritic texture	Trachyte
Na-plagioclase	4	0.6	Subhedral to euhedral		
Sanidine	26	0.5-1	Euhedral		
Biotite	2	0.1-0.2			
Pyroxene	1	0.1			
Groundmass of:Quartz K-feldspar	61				
Opaque minerals	1				

Sample Code: Tan 10					
Minerals	**Modal Proportion (%)**	**Phenocryst Maximum grain Size (mm)**	**Phenocryst Maximum grain Shape**	**Texture**	**Rock Name**
Olivine	9	0.4	Euhedral	Intergranular , glomeroporphyritic and trachytic texture	Olivine pyric basalt
Ca-plagioclase	30	0.4	Subhedral to Anhedral		
Clinopyroxene	11	0.3-0.5	Anhedral		
Groundmass of plagioclase, pyroxene, and opaque minerals	50				

Sample Code: Tan 5					
Minerals	**Modal Proportion (%)**	**Phenocryst Maximum grain Size (mm)**	**Phenocryst Maximum grain Shape**	**Texture**	**Rock Name**
No Phenocryst	-	-	-	Aphanitic and Trachytic texture (flow texture)	Aphanitic basalt
Groundmass of Plagioclase&Clinopyroxene	90				
Opaque minerals	10				

Sample Code: Tan 11					
Minerals	**Modal Proportion (%)**	**Phenocryst Maximum grain Size (mm)**	**Phenocryst Maximum grain Shape**	**Texture**	**Rock Name**
Olivine	6	0.2-0.5	Subhedral to anhedral	Vesicular, Reaction (dissolution) texture, trachytic texture, and glomeroporphyritic texture	Olivine pyric vesicular basalt
Ca-plagioclase	34	0.1-2	Elongate and tabular		
Augite	15	0.4	Anhedral		
Groundmass of: Plagioclase and Ilmenite (Fe, Ti oxides)	45				

Sample Code: Tan 12					
Minerals	**Modal Proportion (%)**	**Phenocryst Maximum grain Size (mm)**	**Phenocryst Maximum grain Shape**	**Texture**	**Rock Name**
Olivine	6	0.5-1.2	Anhedral	Porphyritic texture	Porphyritic basanite
Clinopyroxene	14	1	Sub- anhedral		
Plagioclase	20	0.1-0.2	Sub- anhedral		
Opaque minerals (Fe, Ti oxides)	35	0.15			

Sample Code: Tan 15 and 21					
Minerals	**Modal Proportion (%)**	**Phenocryst Maximum grain Size (mm)**	**Phenocryst Maximum grain Shape**	**Texture**	**Rock Name**
Olivine	6	0.4-0.6		Vesicular texture	Vesicular(scoriaceous) basalt
Augite	8	0.4			
Groundmass of: Plagioclase Olivine and clinopyroxene	40				
Vesicles	45				
Opaque minerals	1				

Sample Code: Tan 18					
Minerals	**Modal Proportion (%)**	**Phenocryst Maximum grain Size (mm)**	**Phenocryst Maximum grain Shape**	**Texture**	**Rock Name**
Plagioclase	5	0.2-2	Subhedral-anhedral	Trachytic and dissolution texture	Pyroxene phyric basalt
Clinopyroxene	10	0.1-0.2			
Groundmass of plagioclase	65				
Olivine microphynocryst	6				
Opaque minerals (Fe, TI oxides)	14	0.1			

Sample Code: Tan 19,20					
Minerals	**Modal Proportion (%)**	**Phenocryst Maximum grain Size (mm)**	**Phenocryst Maximum grain Shape**	**Texture**	**Rock Name**
Olivine	5	0.3	Euhedral-Anhedral	Trachytic texture	Olivine phyric basalt
Augite	18	0.5	Anhedral		
Plagioclase	70	0.4	Elongate		
Opaque minerals of Magnetite (Fe oxide)	7				

Sample Code: Tan 22					
Minerals	**Modal Proportion (%)**	**Phenocrysts Maximum grain Size (mm)**	**Phenocrysts Maximum grain Shape**	**Texture**	**Rock Name**
Plagioclase	52	0.2-2	Elongate lath	Porphyritic texture	Plagioclase pyric basalt
Olivine	8	0.3-0.4	Euhedral to subhedral		
Clinopyroxene	10	0.4	subhedral		
Groundmass of plagioclase, olivine, pyroxene, and opaque minerals	30				

Appendix 2

1. CIPW norm for the Tana Volcanics

Rock Type	Basanite	Basalt	Rhyolite	Trachyte	Trachyte	Basalt	Basalt
Normative minerals	**Tan-2**	**Tan-5**	**Tan-6**	**Tan-7**	**Tan-8**	**Tan-9**	**Tan-10**
Quartz	0	0	39.33	13.89	1.52	0	0
Plagioclase	52.59	41.62	32.71	48.56	56.18	52.14	54.21
Orthoclase	7.18	11.41	24.6	25.37	34.1	5.25	7.34
Nepheline	3.94	3.94	0	0	0	0	2.53
Corundum	0	0	1.18	0	0	0	0
Diopside	13	14.22	0	0.78	1.3	11.8	15.09
Hypersthene	0	0	1.1	4.7	3.03	7.12	0
Olivine	11.56	15.48	0	0	0	6.05	9.6
Acmite	0	0	0	3.46	1.25	0	0
Ilmenite	2.04	3.18	0.05	0.38	0.39	4.25	1.96
Magnetite	8.79	8.57	0.92	2.79	2.05	12.64	8.67
Apatite	0.9	1.59	0.1	0.08	0.17	0.74	0.61
Total	100	100.01	99.99	100.01	99.99	99.99	100.01

Rock Type	Basalt	Basanite	Rhyolite	Rhyolite	Scoria	Rhyolite	Rhyolite	Basalt
Normative minerals	**Tan-11**	**Tan-12**	**Tan-13**	**Tan-14**	**Tan-15**	**Tan-16**	**Tan-17**	**Tan-18**
Quartz	0	0	34.28	33.43	0	30.33	32.42	2.92
Plagioclase	55.8	40	37.65	41.45	46.84	38	36.35	53.34
Orthoclase	5.88	7.77	23.63	20.54	7.25	28.01	25.79	9.41
Nepheline	0	6.93	0	0	5.27	0	0	0
Corundum	0	0	1.07	0.78	0	1.03	0.17	0
Diopside	11.57	13.33	0	0	17.27	0	0	7.65
Hypersthene	4.4	0	1.59	1.69	0	1.36	2.54	15.13
Olivine	10.41	15.13	0	0	11.33	0	0	0
Acmite	0	0	0	0	0	0	0	0
Ilmenite	1.82	3.87	0.2	0.27	2.04	0.07	0.27	2.08
Magnetite	9.51	11.87	1.52	1.74	9.19	1.16	2.41	8.6
Apatite	0.61	1.11	0.06	0.1	0.81	0.04	0.04	0.88
Total	100	100.01	100	100	100	100	99.99	100.01

Rock Type	Basalt	Basalt	Scoria	Basalt	Rhyolite
Normative minerals	Tan-19	Tan-20	Tan-21	Tan-22	Tan-24
Quartz	0	0	0	0	34.47
Plagioclase	54.73	53.08	35.52	52.59	36.4
Orthoclase	4.83	7.17	6.5	5.3	9.45
Nepheline	1.73	3.79	9.05	0	0
Corundum	0	0	0	0	2.55
Diopside	16.03	13.1	20.04	10.37	0
Hypersthene	0	0	0	9.15	8.84
Olivine	11.48	11.18	14.18	6.97	0
Acmite	0	0	0	0	0
Ilmenite	1.61	2.02	2.33	3.25	1.5
Magnetite	8.99	8.77	11.66	11.66	6.28
Apatite	0.59	0.89	0.73	0.72	0.51
Total	99.99	100	100.01	100.01	100

2. Ratio of Trace elements

Sample Code	La/Nb	Zr/Nb	Rb/Nb	Nb/Th	Th/La	Rb/Sr	Ba/Y	Rb/Zr
Tan-2	0.602041	3.290816	0.507653	15.37255	0.108051	0.037689	14.86239	0.154264
Tan-5	0.625592	2.969984	0.546603	14.78972	0.108081	0.042041	22.47748	0.184043
Tan-6	0.123529	1.026144	1.339869	3.825	2.116402	18.30357	0.590793	1.305732
Tan-7	0.655637	9.828431	0.914216	12.76995	0.119439	4.875817	10.12048	0.093017
Tan-8	0.482877	4.280822	0.52911	10.10381	0.204965	17.75862	1.497436	0.1236
Tan-9	1.055838	11.42132	0.604061	9.949495	0.095192	0.02931	5.153203	0.052889
Tan-10	0.682731	4.417671	0.795181	12.83505	0.114118	0.041772	15.39906	0.18
Tan-11	0.770925	4.361233	0.568282	12.33696	0.105143	0.036857	15.18349	0.130303
Tan-12	0.84	8.28	0.872	13.6612	0.087143	0.038929	9.207547	0.105314
Tan-13	1.560976	15.95819	2.634146	3.133188	0.204464	1.848411	11.85075	0.165066
Tan-14	1.786765	23.05147	2.323529	3.550914	0.157613	1.519231	8.331318	0.100797
Tan-15	0.624339	2.830688	0.566138	13.26316	0.120763	0.044864	14.0708	0.2
Tan-16	0.182007	1.577855	1.99308	3.360465	1.634981	36.92308	0.832579	1.263158
Tan-17	0.526217	14.81273	1.382022	6.78526	0.280071	6.473684	4.810526	0.0933
Tan-18	1.681818	14.92424	1.962121	4.615385	0.128829	0.058333	12.52396	0.131472
Tan-19	0.699115	3.716814	0.60177	15.06667	0.094937	0.031481	12.17391	0.161905
Tan-20	0.594872	3.25641	0.489744	15.6	0.107759	0.036243	14.0367	0.150394
Tan-21	0.641686	2.271663	0.622951	11.57182	0.134672	0.044781	17.94258	0.274227
Tan-22	1.126316	10.57895	0.668421	9.74359	0.091121	0.027974	8.064516	0.063184
Tan-24	1.342657	13.77622	1.248252	5.607843	0.132813	0.06813	8.87522	0.090609